T cell Reactivity and Regulation in Human Cancer

Andrew J.S. Furness

University College London
PhD Supervisor: Professor Sergio Quezada

A thesis submitted for the degree of
Doctor of Philosophy
University College London

August 2018

Declaration

I, Andrew J.S. Furness, confirm that the work presented in this thesis is my own. Where information has been derived from other sources, I confirm this has been indicated in the thesis.

Table of Contents

Abstract

Modulation of co-inhibitory and co-stimulatory immune checkpoint molecules with antibody-based therapies has emerged as a promising anti-cancer strategy, however response rates to such agents are modest. The discrepancy in activity observed between mouse models and human cancers is rarely acknowledged, but deciphering this might provide valuable insights into underlying mechanisms of response and resistance. Through parallel analysis of mouse models and human cancers, this study demonstrates the importance of the local microenvironment in determining the activity of immune modulatory antibodies (mAb), providing novel insights into the mechanism of anti-cytotoxic T-lymphocyte-associated antigen-4 (CTLA-4, CD152) and anti-interleukin-2 receptor alpha chain (IL-2Rα, CD25) antibodies.

A limitation of such approaches is the requirement for a pre-existing T cell infiltrate. In human tumours, paucity of immune infiltrate is well recognised, highlighting the need to identify relevant drivers of T cell infiltration. Complementary analysis of genomic and immunological landscapes in human tumours demonstrates that beyond total neoantigen burden, clonal architecture influences anti-tumour immunity, with prognostic implication and predictive value in the context of immune checkpoint modulation. Targeting clonal neoantigens, present on every tumour cell, might hold promise in overcoming the significant therapeutic challenge posed by tumour evolution and consequent intra-tumour heterogeneity.

Acknowledgment

I would like to thank Sergio Quezada for his enthusiasm, example, mentorship and generosity in rewarding hard work with opportunity. I genuinely could not have wished for a better supervisor. I am indebted to Professor Karl Peggs, Dr James Larkin and Professor Martin Gore for giving me, an unknown quantity, the opportunity to step directly out of clinical training and embark on this research fellowship.

I am hugely grateful to all past and present members of the Peggs/Quezada laboratory, particularly Andy Georgiou for his endless patience and support. I would like to thank all those with whom I have been fortunate enough to collaborate, including Nicholas McGranahan, Rachel Rosenthal, Yinyin Yuan and Charles Swanton. I would particularly like to thank Frederick Arce Vargas and Teresa Marafioti for their friendship and productive collaboration.

It is difficult to express the extent of my gratitude to my wife Sukhera. This fellowship has coincided with the arrival of two children, two house moves and countless hospital rotations. Thank you for your perspective, love, sacrifice and support.

As a father, I cannot begin to fathom the impact of losing a child; this study has been inspired by and is dedicated to the memory of Sam Keen, the tireless efforts of the foundation established in his name and my two children, Benjamin and Sophie.

Table of Figures

List of Tables

Abbreviations:

ADCC – antibody-dependent cell-mediated cytotoxicity

ADCP – antibody-dependent cell-mediated phagocytosis

APC – antigen-presenting cell

CD – cluster of differentiation

CTLA-4 – cytotoxic T-lymphocyte-associated antigen-4

DC – dendritic cell

DR4 – death receptor 4

DR5 – death receptor 5

EGFR – epidermal growth factor receptor

Fc – fragment crystallisable

FcγR – fragment crystallisable gamma receptor

FDA – Food and Drug Administration

GITR – glucocorticoid-induced TNFR-related protein

GzmB – granzyme B

h - human

HER-2 – human epidermal growth factor receptor-2

HLA – human leucocyte antigen

IC – immune complex

IHC - immunohistochemistry

ICOS – inducible T cell co-stimulator

IgG – immunoglobulin G

IL2Rα– interleukin-2 receptor alpha chain

IRAE – immune-related adverse event

ITAM – immunoreceptor tyrosine-based activation motif

ITIM – immunoreceptor tyrosine-based inhibitory motif

LAG-3 – lymphocyte-activation gene 3

m - murine

mAb – monoclonal antibody

MFI – mean fluorescent intensity

MMR – mismatch repair

NART – neoantigen reactive T cell

NSCLC – non-small cell lung cancer

MHC – major histocompatibility complex

NK – natural killer

PBMC – peripheral blood mononuclear cells

PD-1 – programmed cell death receptor 1

RCC – renal cell carcinoma

RNA – ribonucleic acid

SEM – standard error of the mean

Teff – effector T cell

TCGA – The Cancer Genome Atlas

TGFβ – transforming growth factor beta

TIL – tumour-infiltrating lymphocyte

TNFR – tumour necrosis factor receptor

Treg – regulatory T cell

U.S. – United States

WES – whole exome sequencing

1. Introduction

1.1 Mechanisms of therapeutic anti-CTLA-4 antibodies in cancer

In contrast to monoclonal antibodies (mAbs) which specifically bind and destroy tumour cells, immune modulatory mAbs serve to engage or block the function of cell surface signalling molecules on host immune cells, influencing the direction and magnitude of the immune response (Yao et al., 2013). Immune modulatory mAbs targeting co-inhibitory and co-stimulatory immune checkpoint molecules were initially thought to act solely via regulation of effector T (Teff) cell responses. CTLA-4 was the first so-called 'immune checkpoint' molecule subject to therapeutic targeting in pre-clinical models and more recently clinical trials (Hodi et al., 2010; Robert et al., 2011).

CTLA-4 and CD28 are homologous receptors expressed on both $CD4^+$ and $CD8^+$ T cells. They share a pair of ligands expressed on the surface of antigen-presenting cells (APCs) and mediate opposing functions in T cell activation. CD28 interacts with the CD80 dimer with relatively high affinity and the CD86 monomer with lower affinity, mediating T cell co-stimulation in the context of T cell receptor (TCR) signalling. CTLA-4 also interacts with both ligands, but does so with higher affinity and avidity than CD28 (Collins et al., 2002; Schwartz et al., 2001; Stamper et al., 2001), serving to inhibit T cell responses. CTLA-4-CD80 binding represents the highest avidity interaction and CD28-CD86 the weakest, raising the possibility that CTLA-4 competes with CD28 for ligand binding and acts as an antagonist of CD28-mediated co-stimulation (Thompson and Allison, 1997; Walker and Sansom, 2011). Such interaction occurs at the immune synapse between T cells and APCs, where CTLA-4 has been demonstrated to recruit CD80, limiting its interaction with CD28 (Pentcheva-Hoang et al., 2004; Yokosuka et al., 2010).

Therapeutic anti-CTLA-4 mAbs were therefore initially proposed to exert anti-tumour activity through competitive blockade of an inhibitory signal, promoting the expansion of Teff cells (Krummel and Allison, 1996; Leach et al., 1996). In support of this as a primary mechanism, in pre-clinical models, enhanced anti-

tumour responses following CTLA-4 ‘blockade’ have been associated with CD8 T-cell-mediated autoimmunity, including depigmentation in melanoma models (van Elsas et al., 2001), prostatitis following vaccination against prostate cancer-specific antigens (Hurwitz et al., 2000) and the generation of anti-double-stranded DNA antibodies (Lute et al., 2005). However, CTLA-4 was subsequently demonstrated to be constitutively expressed on regulatory T cells (Treg), raising the possibility of an additional impact of these mAbs on the Treg cell compartment (Read et al., 2000, 2006; Sakaguchi et al., 2001; Wing et al., 2008).

Pre-clinical studies in mouse models of cancer demonstrated that targeting CTLA-4 on both Teff and Treg cell compartments was required for maximal anti-tumour activity, supporting the concept of an additional impact of anti-CTLA-4 mAbs on Treg cells (Peggs et al., 2009). However, it was challenging to envisage a mechanism by which anti-CTLA-4 mAbs would differentially impact upon each compartment. Indeed, expansion of Teff and Treg cells in secondary lymphoid organs and blood of mice and humans had been demonstrated by multiple groups (Kavanagh et al., 2008; Quezada et al., 2006; Schmidt et al., 2009), lending support to the existing concept that anti-CTLA-4 mAbs act principally by promoting T cell expansion.

A consistent observation associated with anti-CTLA-4-mediated tumour rejection had been an increase in the ratio of Teff to Treg cells within the tumour microenvironment (Chen et al., 2009; Curran and Allison, 2009; Kavanagh et al., 2008; Liakou et al., 2008; Quezada et al., 2006; Shrikant et al., 1999; Waitz et al., 2012). This was thought to occur secondary to preferential expansion of Teff over Treg, however it remained unclear why this was restricted to the tumour microenvironment and why a mAb simultaneously targeting two cellular populations with opposing activities favoured Teff cell function and promoted tumour rejection.

More recent pre-clinical data in mouse models of cancer demonstrates that anti-CTLA-4 mAbs act to promote expansion of Teff and Treg cells in secondary lymphoid organs, whilst promoting Teff cell expansion and

concomitant depletion of Treg cells within the tumour (Bulliard et al., 2013; Selby et al., 2013; Simpson et al., 2013). Depletion of tumour-infiltrating Treg cells results in an increase in the ratio of Teff to Treg cells and tumour rejection (Figure 2).

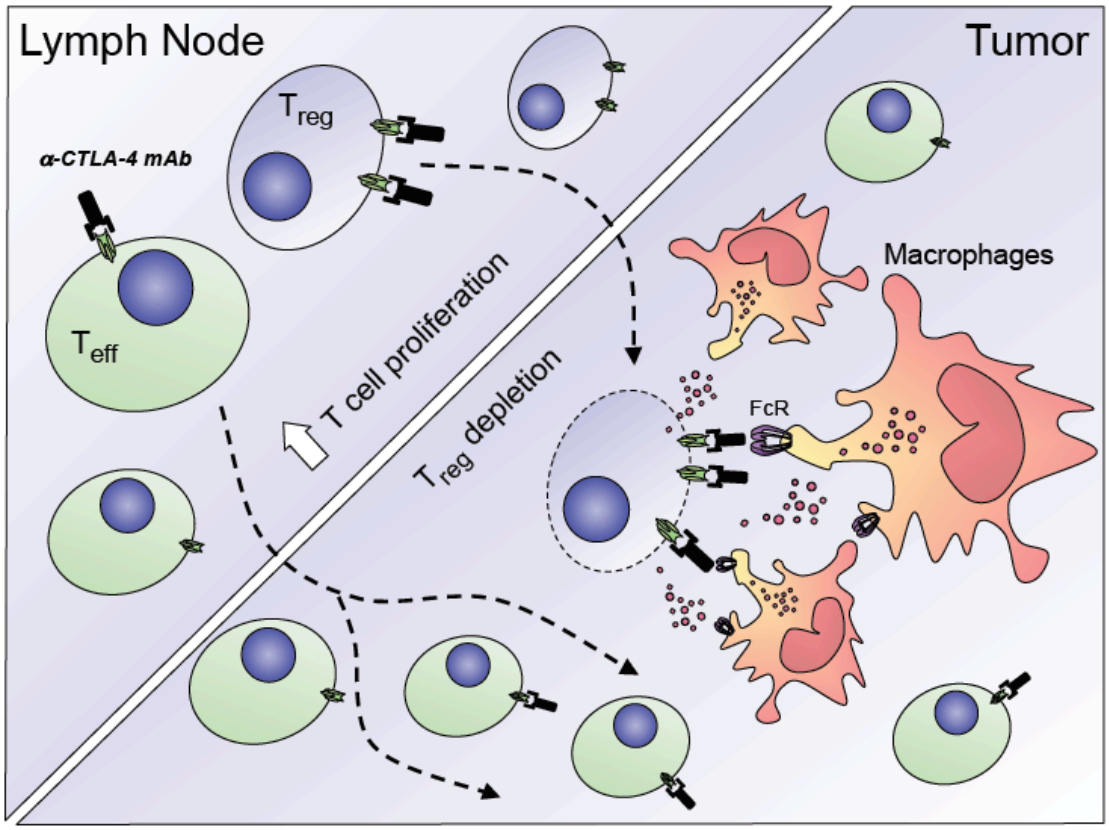

Figure 1: Activity of anti-murine CTLA-4 antibodies depends upon local microenvironment

Reproduced with permission from (Furness et al., 2014). In lymph node (LN) anti-CTLA-4 antibodies expand both Teff and Treg cell populations. In contrast, the tumour microenvironment is enriched with FcγR-expressing cell subsets and CTLA-4 upregulated on Treg relative to Teff cells. As a consequence, preferential elimination of Treg cells occurs via ADCC. This activity is restricted to the tumour microenvironment and mediates a shift in the intra-tumoural CD8/Treg cell ratio resulting in tumour rejection.

Depletion of tumour-infiltrating CTLA-4^{+} Treg cells occurs via antibody-dependent cell-mediated cytotoxicity/phagocytosis (ADCC/P), mediated by tumour-infiltrating CD11b^{+} macrophages expressing the activatory fragment crystallisable gamma receptor IV (FcγRIV). Macrophages appeared enriched in tumour relative to lymph node (>50-fold), where they were observed express higher relative levels of FcγRIV, explaining the paradoxical impact of

anti-CTLA-4 mAbs on Teff and Treg cell accumulation in secondary lymphoid organs versus the tumour (Bulliard et al., 2013; Simpson et al., 2013). Preferential depletion of Treg over Teff cells results from higher relative expression (based on mean fluorescence intensity (MFI)) of CTLA-4 on Treg cells. In keeping with this, a small population of Teff cells expressing high levels of CTLA-4 was also eliminated, highlighting the relevance of density of target molecule expression in the context of mAbs with depleting activity (Simpson et al., 2013).

Taken together, these data demonstrated a previously unappreciated dual activity of murine anti-CTLA-4 mAbs. Without blocking activity, Teff cells would not expand, infiltrate and accumulate; without depleting activity, Treg cells would not be eliminated and the intra-tumoural balance would continue to favour tumour progression.

1.2 A common mechanism for anti-GITR and anti-OX40 antibodies

A similar requirement for activating FcγRs in the activity of anti-glucocorticoid-induced tumour necrosis factor (TNF)-related protein (GITR) and anti-OX40 antibodies was recently demonstrated (Bulliard et al., 2013, 2014). Surface expression of GITR and OX40 appeared significantly higher on tumour-infiltrating Treg cells relative to Teff cells. Myeloid cells expressing activating FcγRs were enriched in the tumour microenvironment and under-represented in tumour-draining lymph nodes. Similar to observations with anti-murine CTLA-4 mAbs, following the administration of therapeutic mAbs, rapid depletion of tumour-infiltrating Treg cells was observed, mediating a shift in the intra-tumoural Teff/Treg cell ratio and tumour rejection, supporting a common mechanism shared between mAbs targeting B7 and TNFR molecules.

1.3 Fc gamma receptors as regulators of immune response

The capacity of an individual mAb to mediate ADCC/P depends on the expression profile of the target molecule, antibody isotype and the local abundance of FcγR-expressing innate effector cells (Bulliard et al., 2013, 2014; Furness et al., 2014; Simpson et al., 2013). FcγRs are broadly

expressed on cells of haematopoetic lineage including B cells, dendritic cells, macrophages, mast cells, natural killer (NK) cells and neutrophils (Nimmerjahn and Ravetch, 2007). They are divided functionally into two classes: activating and inhibitory receptors. Activating receptors comprise human (h) FcγRI, FcγRIIa, FcγRIIIa/b and mouse (m) orthologues FcγRIa, FcγRIII and FcγRIV (Figure 1).

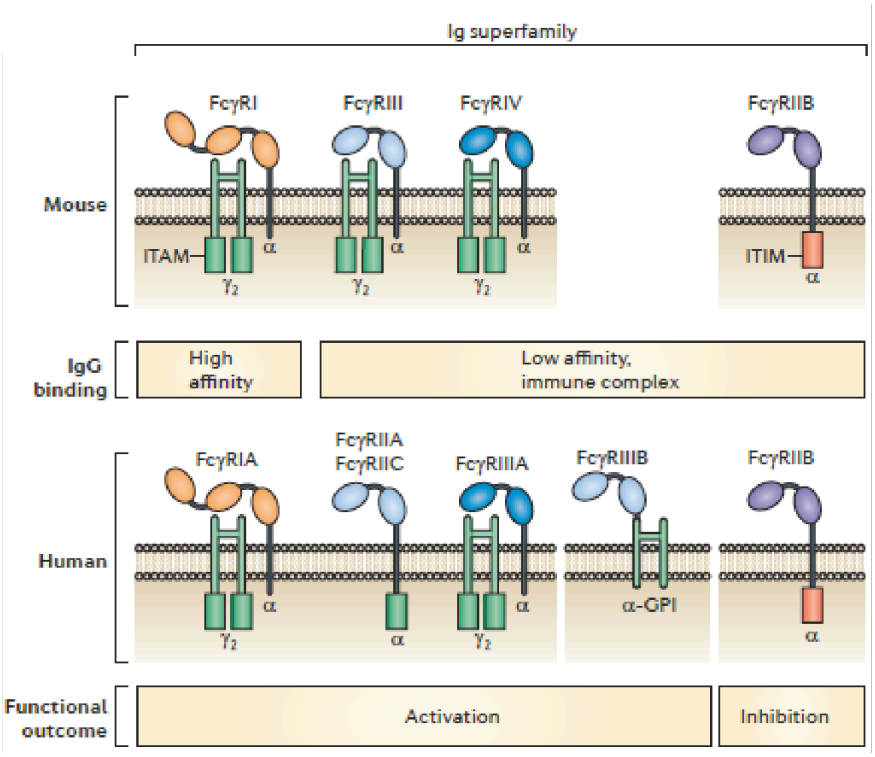

Figure 2: Structure and function of human and mouse Fc gamma receptors. Reproduced with permission from (Schwab and Nimmerjahn, 2013)**.** Schematic representation of Fc gamma receptors at the cell membrane and their association with the FcRγ-chain dimer in mice (upper panel) and humans (lower panel). Green boxes represent immunoreceptor tyrosine-based activation motifs (ITAMs) and red boxes immunoreceptor tyrosine-based inhibitory motifs (ITIMs). Predicted binding of IgG subclasses is displayed between upper and lower panels and functional outcome at bottom of figure.

Activating FcγRs possess an immunoreceptor tyrosine-based activation motif (ITAM) within their intra-cytoplasmic domain, or, in the case of hFcγRI and IIIa, associate with the ITAM-containing signalling subunit Fc receptor (FcR) common gamma chain (Guilliams et al., 2014). FcγRIIb is the only inhibitory receptor in mice and humans, consisting of an immunoreceptor tyrosine-

based inhibition motif (ITIM) in its intra-cytoplasmic domain (Ravetch and Lanier, 2000). A key feature of the FcγR system is co-expression of activating and inhibitory receptors on the same cell. This serves to set thresholds for activation, with potentially important implications for mAb selection and/or design. The exception to this is B cells, which exclusively express inhibitory FcγRIIb, and human natural killer (NK) cells, which express activating FcγRIIIa alone.

The molecular mechanisms by which clustering of FcγRs trigger or suppress cell activation are crucial in mediating appropriate responses to IgG-complexed antigens. Clustering of activating FcγRs leads to activation of intracellular SRC-family protein kinases (including SRC, FYN, FGR, HCK and LYN) and phosphorylation of tyrosine residues in the ITAM. The phosphorylated ITAM then serves as a docking site for the SRC-homology 2 (SH2) domain of the cytosolic protein SYK (Ghazizadeh et al., 1994; Wang et al., 1994). Activating signalling through ITAM-containing FcγRs leads to an oxidative burst, cytokine release and phagocytosis by macrophages, ADCC by NK cells or degranulation of mast cells (Takai, 2002).

The activation pathway can be inhibited by co-aggregation of FcγRIIb, which acts physiologically as a negative regulator of immune complex-triggered activation. Its function is best described within B cells, in which the initial event in inhibitory signalling is phosphorylation by the SRC-family kinase LYN of the ITIM tyrosine found in the FcγRIIb cytoplasmic tail (Muta et al., 1994). This results in recruitment of SH2-domain-containing phosphatases, principally the SH2-domain-containing protein tyrosine phosphatase 1 (SHP1), SHP2 and SH2-domain-containing inositol polyphosphate ‘5 phosphatase (SHIP) (D’Ambrosio et al., 1995; Damen et al., 1996; Muta et al., 1994; Ono et al., 1996). SHIP is the primary effector of FcγRIIb-mediated inhibition, acting to dephosphorylate phosphoinositides and inositol polyphosphates. Its main in vivo substrate is phosphatidylinositol-3,4,5-triphosphate (PtdIns(3,4,5)P_3) which is formed by the action of phosphatidylinositol 3-kinase (PI3K). Thereafter, the proposed signalling cascade of inhibition occurs via three distinct, but interacting pathways: (i) SHIP-mediated hydrolysis of

PtdIns(3,4,5)P_3, which leads to impaired membrane translocation of signal-transducing molecules (Bolland et al., 1998; Fluckiger et al., 1998; Scharenberg et al., 1998) (ii) suppression of the activation of mitogen-activated protein (MAP) kinases and recruitment of the anti-apoptotic kinase AKT (Liu et al., 1998) and (iii) inhibition of RAS activation through SHIP binding to FcγRIIb (Tamir et al., 2000; Tridandapani et al., 1997a, 1997b).

The fate of immune complexes (ICs) will therefore vary, depending on the encountered cell subset and FcγR expression profile. Under steady state conditions, the inhibitory receptor dominates, secondary either to higher expression, or a greater affinity for abundant antibody isotypes (Kalergis and Ravetch, 2002). In health, this is critical in order to avoid non-specific immune activation, however, in the context of disease, this balance may impact significantly upon outcome.

1.4 Fc gamma receptors and antibody isotype

The efficacy of mAb-mediated ADCC depends upon the relative affinity of individual immunoglobulin G (IgG) subclasses for activating and inhibitory FcγRs. Recent studies have determined the affinity of monomeric antibody isotypes for their respective activating and inhibitory FcγR pairs, allowing generation of an activating to inhibitory FcγR binding ratio (A:I) (Bruhns et al., 2009; Nimmerjahn et al., 2005). Assigned A:I ratios for individual antibody isotypes correlate with therapeutic activity in-vivo. In mice, mIgG1 antibodies have an A:I ratio of less than 1; the depleting activity of this isotype is therefore strongly governed by the inhibitory FcγRIIb. In contrast, mIgG2a and mIgG2b have A:I ratios of up to 70, and are therefore less regulated by FcγRIIb. It follows that mIgG2a and mIgG2b isotypes are recognised to be more efficient in target cell depletion than mIgG1 and mIgG3 (Hamaguchi et al., 2006) and that in models of tumour cell killing and platelet depletion by IgG Fc variants, deletion of FcγRIIb was found to impact most strongly on mIgG1 activity (Nimmerjahn and Ravetch, 2005). In the humans, the affinity of IgG subclasses differs, such that hIgG1 and hIgG3 have a higher affinity for both activating and inhibitory FcγRs than their hIgG2 and hIgG4 counterparts,

with hIgG1 typically selected for clinical reagents where ADCC activity is desirable (Bruhns et al., 2009).

1.5 Fc gamma receptor polymorphisms and response to monoclonal antibodies in cancer

Monoclonal antibodies have been used extensively against cancer. In this setting they act to block the interaction of soluble ligands with target receptors, bind to cell surface antigens on tumour cells, modulating signal transduction (Li et al., 2005), or, deplete/phagocytose antigen-expressing target cells by ADCC or ADCP (Johnson and Glennie, 2003). In this regard there is strong evidence from pre-clinical models that ADCC and ADCP effector function is critical to the therapeutic activity of hIgG1 mAbs targeting CD20 (de Haij et al., 2010), human epidermal growth factor receptor 2 (HER-2) (Barok et al., 2007) (Clynes et al., 2000) (Musolino et al., 2008), epidermal growth factor receptor 2 (EGFR) (Hara et al., 2008), fibroblast growth factor receptor 3 (Li et al., 2005) and CD52 (Golay et al., 2006).

Demonstrating this in vivo has proved more challenging, perhaps the strongest evidence for a role of FcγR-mediated effector function in antibody-based cancer therapies derives from clinical studies demonstrating an association between clinical responses and specific alloforms of activating hFcγRs (Cartron et al., 2002; Musolino et al., 2008; Weng and Levy, 2003; Zhang et al., 2007).

A non-synonymous polymorphism (519G>A, rs1801274) in exon 4, encoding the membrane proximal Ig-like domain of FCGR2A, leads to an arginine (R) to histidine (H) change at position 131, altering receptor affinity for ligand. In contrast to the R131 allele, the FcRIIa-H131 allele readily binds to human IgG2 (Parren et al., 1992; Salmon et al., 1992). Given that hFcγRIIa is the most broadly expressed hFcγR across a range of cell subsets, this has significant implications for human disease beyond the setting of malignancy (Li et al., 2014). In the second extracellular domain of FCGR3A, a point substitution of T to G at nucleotide 559 (rs396991) changes the phenylalanine (F) at amino acid position 158 to valine (V). The FcγRIIIa-158V allele displays higher affinity for IgG1 and IgG3 relative to the 158F allele and is also capable

of binding IgG4. Similar to the FcRIIa-H131, beyond the context of human cancer, the FcγRIIIa-158V polymorphism has been associated with pathogenesis, including a predisposition to the development of autoimmune disease (Koene et al., 1997; Wu et al., 1997).

However, whilst multiple clinical studies have identified a relationship between hFcγR polymorphism status and response to cancer cell targeting mAbs such as Rituximab (reviewed in Mellor et al., 2013), there has been no formal assessment of the impact of such polymorphisms on response to anti-CTLA-4 or other immune modulatory mAbs. Where ADCC may be relevant to the activity of immune modulatory mAbs, both antibody isotype and hFcγR polymorphism status are potentially highly relevant. This is further apparent when considering the current pipeline of U.S. Food and Drug Association-approved immuno-oncology (I-O) mAbs (Table 1).

Target	Company	Drug	First approved	Approved indications	Isotype	Predicted ADCC activity
CTLA-4	BMS	Ipilimumab	2011	Melanoma	IgG1	Yes
PD-1	Merck	Pembrolizumab	2014	Melanoma, NSCLC, HNK Bladder, HD	IgG4	No
PD-1	BMS	Nivolumab	2014	Melanoma, NSCLC, RCC, bladder, HD	IgG4	No
PD-L1	Roche	Atezolizumab	2016	Bladder	IgG1 N298A	No
PD-L1	Merck	Avelumab	2017	Merkel cell	IgG1	Yes
PD-L1	AZ	Durvalumab	Submitted 2017	Bladder, NSCLC	IgG1*	No

Table 1: FDA-approved immune modulatory antibodies

AZ, AstraZeneca, BMS, Bristol-Myers Squibb, HD, Hodgkin disease, HNK, head and neck carcinoma, NSCLC, non-small cell lung cancer and RCC, renal cell carcinoma. *glycoengineered to abrogate Fc function.

Three anti-PD-L1 mAbs are FDA-approved, of these, only Avelumab has predicted ADCC activity. In pre-clinical models, anti-PD-L1 mAbs with capacity for ADCC displayed augmented anti-tumour activity relative to those without (Dahan et al., 2015). Although these mAbs will almost certainly never undergo head-to-head evaluation in clinical trials, it is paramount moving forward that such pre-clinical studies inform the design of the next generation of therapeutic mAbs for clinical application.

1.6 Barriers to clinical translation

Ipilimumab, a human IgG1 mAb directed against CTLA-4, mediates durable remissions in patients with advanced melanoma, although such responses are limited to a small subset (Hodi et al., 2010; Robert et al., 2011; Schadendorf et al., 2015). Despite its potentially depleting isotype, the contribution of ADCC and role of FcγRs in the activity of ipilimumab in vivo remains controversial. Two recent clinical studies have identified a reduction in tumour-infiltrating Treg cells post ipilimumab therapy (Romano et al., 2015; Tarhini et al., 2014). Moreover, in vitro studies demonstrate that ipilimumab depletes CTLA-4-expressing Treg cells in the presence of FcγR-expressing monocytes and NK cells, consistent with predicted binding affinity for activatory FcγRs (Jie et al., 2015; Romano et al., 2015). A second anti-CTLA-4 mAb, tremelimumab, has also displayed activity in early phase studies (Comin-Anduix et al., 2016). In contrast to ipilimumab, a human IgG2 isotype was selected during pre-clinical design to minimize potential ADCC/ADCP activity (Hanson et al., 2004), thus arguing against a role for Treg cell depletion in the activity of anti-CTLA-4 mAbs in humans.

Deciphering the contribution of Fc-FcγR interaction to the activity of immune modulatory antibodies is likely to significantly inform the optimal design of the next generation of therapeutics. The biological activity of specific IgG Fc subclasses depends upon their relative affinity for activatory and inhibitory FcγRs (Bruhns et al., 2009; Nimmerjahn and Ravetch, 2005). Mutagenesis and glycoform engineering of mAbs has been demonstrated to modulate the affinity of Fc-FcγR interaction, with impact upon cytotoxicity in cell-based assays (Duncan et al., 1988; Redpath et al., 1998; Sarmay et al., 1992; Shields et al., 2001, 2002). Such findings have informed the development of mAbs engineered to display superior activatory to inhibitory FcγR binding profiles and improved ADCC activity (Lazar et al., 2006).

In this context, efficacy studies in mouse models represent an important step in the pre-clinical development of antibody-based therapies. However, reliable translation of such findings across species is often problematic owing to variation in FcγR subtypes, their distribution and the affinity of individual IgG

subclasses in each species. In addition, the previously described polymorphisms in human FcγRs may further influence the binding and biological effects of different IgG subtypes (Koene et al., 1997; Warmerdam et al., 1991; Wu et al., 1997).

The first objective of this study was to bridge this translational void in attempt to better inform the design of the next generation of immune modulatory mAbs optimised appropriately for agonistic, blocking or depleting activity according to the expression profile of relevant target molecules, desired effector function and features of the local microenvironment.

1.7 Towards the identification of selective targets for T cell modulation

Beyond CTLA-4 and PD-1, monoclonal antibodies targeting further co-inhibitory and co-stimulatory immune checkpoint molecules are currently under evaluation in clinical trials (Furness et al., 2014). Increasingly, combination strategies are employed, in this setting toxicity is common, grade III/IV adverse events were observed in 55% of study participants with advanced melanoma treated combination anti-CTLA-4/PD-1 antibodies within a recent phase III study (Larkin et al., 2015).

Characterisation of the immune landscape in sites commonly associated with immune-related adverse events (IRAE) including skin, colon and pituitary is paramount in order to inform the design of mAbs displaying optimal activity but with greater restriction to the tumour microenvironment. A recent translational study demonstrated ‘ectopic’ expression of CTLA-4 on human pituitary endocrine cells at both ribonucleic acid (RNA) and protein levels, providing insights into the possible aetiology of ipilimumab-mediated hypophysitis (Iwama et al., 2014).

Whilst many of these adverse events appear to be reversible with early recognition and prompt administration of high dose steroid therapy, devastating outcomes have been reported in the literature (Johnson et al., 2016). This has prompted modification of dosage and scheduling within

clinical trials (Long et al., 2017), however this is no substitute for translational studies dissecting the mechanisms underlying such off target toxicity. Another method by which toxicity might also be reduced is through the identification and in vivo evaluation of targets with a more restricted expression profile (relative to CTLA-4 or PD-1), allowing more selective targeting of T cell populations.

1.8 CD25 as a selective target for regulatory T cells

CD25, the interleukin-2 high affinity receptor alpha chain (IL-2Rα), was first identified by Sakaguchi and colleagues (Sakaguchi et al., 1995) and used as a surface marker for the identification and isolation of Treg cells prior to the discovery of their master regulator, transcription factor forkhead box P3 (FoxP3) (Fontenot et al., 2005).

$CD4^+FoxP3^+CD25^+$ regulatory T cells play a key role in the maintenance of peripheral self-tolerance. Characterisation of the mechanisms underlying this remains an area of scientific enquiry, however they act, at least in part, to regulate $CD4^+$ and $CD8^+$ T cell activity in a cell extrinsic manner, and their depletion leads to enhanced T cell responses to pathogens (Mendez et al., 2004), self-antigens (Kim et al., 2007) and tumours (Onizuka et al., 1999; Turk et al., 2004). Sakaguchi and colleagues demonstrated that Treg cells with strong suppressive capacity are defined by the expression of CD25 (Sakaguchi et al., 1995). Elimination of $CD25^+$ Treg cells results in the development of autoimmunity in rodents, whilst adoptive transfer of Treg cells prevents the onset of autoimmune diseases (Salomon et al., 2000; Stephens and Mason, 2000; Suri-Payer et al., 1998). It follows that CD25 has been extensively studied as a target for therapeutic Treg cell depletion.

1.9 Therapeutic targeting of CD25 in pre-clinical and clinical studies

Pre-clinical studies in mouse models of cancer have principally evaluated the anti-CD25 antibody clone PC61 (rat IgG1, λ). This has been demonstrated to partially deplete Treg cells in the blood and peripheral lymphoid organs of mice via murine FcγRIII (Setiady et al., 2010). Consistently within these studies, CD25-directed Treg cell depletion has been observed to synergise

with a variety of immunotherapeutic approaches, although this only occurs when it is administered either prior to or soon after tumour challenge. In this context, depletion of circulating or LN-resident Treg cells with anti-CD25 mAb appears to augment or induce anti-tumour immunity. However this approach lacks translational value, reflected in the observation that the use of anti-CD25 mAbs as a therapeutic intervention against established tumours has consistently failed to delay tumour growth and/or prolong survival (Golgher et al., 2002; Jones et al., 2002; Onizuka et al., 1999; Shimizu et al., 1999).

Quezada and colleagues sought to shed light on this, evaluating the impact of therapeutic CD25 depletion on established tumours, with use of an anti-CD25 mAb (PC61 clone) or administration of diphtheria toxin (DT) in FoxP3-DTR transgenic mice. It had previously been demonstrated that the anti-tumour activity of GVAX (a whole tumour cell vaccine expressing human GM-CSF) in combination with anti-CTLA-4 mAbs (9H10 clone) varied depending on timing of administration, such that efficacy was reduced when used more than four days after implantation of the B16/BL6 cell line (van Elsas et al., 1999). They hypothesised that Treg cells might be contributing to the observed lack of activity and therefore CD25-directed depletion of Treg cells might effectively synergise with GVAX/anti-CTLA-4 (anti-CTLA-4 mAbs had not been demonstrated to deplete Treg cells at this time).

Combination vaccination therapy (GVAX/anti-CTLA-4) was delayed until 8 days after tumour implantation, a time point at which GVAX/anti-CTLA-4 is incapable of rejecting established tumours. ‘Prophylactic’ CD25 depletion (administered on day -4) and GVAX/anti-CTLA-4 synergised to reject established tumours, however therapeutic CD25 depletion failed to impact on tumour growth or rejection. This was found to relate to a lack of target, with evidence of poor intra-tumoural T cell infiltration, likely related to the model (B16/BL6) and timing of GVAX/anti-CTLA-4 rather than either CD25-directed therapy. Whilst this is of potential relevance to non-inflamed human tumours, the study failed to provide any additional insights into the intra-tumoural activity of anti-CD25 mAbs.

Despite a lack of promising pre-clinical activity, CD25-directed approaches have undergone evaluation within small, predominantly early-phase clinical studies in the form of daclizumab (a humanised IgG1 murine anti-human CD25 antibody) or denileukin difitox (a recombinant fusion protein combining human IL-2 and a fragment of diptheria toxin) (Table 2) (Attia et al., 2005; Dannull, 2005; Jacobs et al., 2010; Janik et al., 2015; Luke et al., 2016; Mahnke et al., 2007; Rasku et al., 2008; Rech et al., 2012; Sampson et al., 2012; Telang et al., 2011).

Study	Disease setting	Therapy	Dose and scheduling	Observations	Response assessment
Attia et al. (J. Immunother. 2005)	Advanced Melanoma RCC (n=13)	Denileukin Diftitox (DAB_{389}IL-2) monotherapy	9 or 18μg/kg OD for 5 days q. 21 days	No observed depletion of circulating Treg cells	No objective responses
Dannull et al. (J. Clin. Invest. 2005)	Advanced RCC & ovarian (n=11)	Denileukin Diftitox (DAB_{389}IL-2) & DC vaccine	Single dose at 18μg/kg	Selective elimination of circulating $CD25^{hi}$ Treg cells Improved generation of vaccine-specific effector T cells, only if Denileukin Diftitox (DAB_{389}IL-2) omitted during priming	Not assessed
Mahnke et al. (Int J Cancer 2007)	Advanced melanoma (n=7)	Denileukin Diftitox (DAB_{389}IL-2) & MelanA/MART-1 vaccine	5 or 18μg/kg OD for 3 days prior to vaccination	Selective depletion of circulating Treg cells Increase in melanoma antigen-specific CD8's.	No objective responses 1 stable disease
Rasku et al. (J. Transl. Med. 2008)	Advanced melanoma (n=16)	Denileukin Diftitox (DAB_{389}IL-2) monotherapy	12μg/kg OD for 4 days q. 21 days	Transient depletion of all circulating T cell subsets De novo appearance of melanoma-antigen specific CD8's	6 partial responses.
Jacobs et al. (Clin. Cancer Res. 2010)	Advanced melanoma (n=30)	Daclizumab & DC vaccination	Daclizumab 0.5mg/kg 4 or 8 days prior to DC vaccination	Depletion of all circulating $CD25^{hi}$ T cell subsets Reduction in vaccine-specific effector T cells	No impact on progression free survival
Telang et al. (BMC Cancer 2011)	Advanced melanoma (n=60)	Denileukin Diftitox (DAB_{389}IL-2) monotherapy	12μg/kg OD for 4 days q. 21 days	Not assessed	16.7% partial responses 5% stable disease 15% mixed response
Rech et al. (Sci. Transl. Med. 2012)	Advanced breast cancer (n=10)	Daclizumab + hTERT peptide vaccine	Daclizumab 1mg/kg single infusion, 7 days prior to vaccination	Marked reduction in circulating Treg cells Robust CD8/CD4 T cell priming and boosting to all vaccine antigens	Not assessed
Sampson et al. (PloS ONE 2012)	Glioblastoma multiforme (n=3)	Daclizumab, EGFRvIII vaccine & Temozolamide	Single infusion of daclizumab at time of vaccination	Reduction in frequency of circulating Treg cells Inverse relationship between Treg cell frequency and level of EGFRvIII-specific humoral responses	Not assessed
Janik et al. (Proc Natl Acad Sci U S A 2015)	Relapsed/refractory HL (n=46)	^{90}Y-daclizumab	10-15mCi ^{90}Y-daclizumab with 5mg unlabeled daclizumab ≤ 7 infusions	Significant reduction in circulating Treg cells	14 complete responses 9 partial responses 14 stable disease
Luke et al. (J. Immunother. Cancer 2016)	Advanced melanoma (n=17)	Denileukin Diftitox (DAB_{389}IL-2) & 4-peptide vaccine	Single dose at 18μg/kg prior to vaccination	No change in circulating Treg cells No change in FoxP3 transcripts in one tumour biopsy No increase in antigen-specific T cells	One partial response 8 stable disease

Table 2: Clinical studies of CD25-directed therapies in human cancer

HL = Hodgkin lymphoma; OD = once daily and RCC = renal cell carcinoma

The setting of these studies was consistently either in advanced solid cancer or refractory lymphoma. Direct comparison is challenging owing to varied dosing and scheduling of drug, particularly when given in combination with vaccination approaches. In the majority of studies, both Denileukin Diftitox (DAB_{389}IL-2) and daclizumab effectively depleted circulating Treg cells and this was associated with either de novo or enhanced generation of antigen-specific effector T cells. However, clinical responses were rare, raising the possibility that observations in blood may not be reflective of activity in the

tumour microenvironment. Similar to pre-clinical studies, limited evaluation of the tumour microenvironment was performed. On review of all studies, only one tumour biopsy was obtained following a single infusion of DAB_{389}IL-2 (Luke et al., 2016), analysis of this demonstrated no change in FoxP3 transcripts relative to baseline, highlighting the importance of further study of the impact of such therapies on all compartments (blood, LN and tumour).

Another potential explanation offered for the observed lack of activity against established tumours in mouse models and human tumours is that anti-CD25 mAbs might also deplete CD25-expressing Teff cells generated upon antigen encounter with tumour, however such observations derive largely from in vitro studies, with little in vivo data to support this in pre-clinical or clinical studies (Boyman and Sprent, 2012).

1.10 Re-evaluating CD25 as a therapeutic target

Given the relevance of the antibody isotype, target molecule density and intra-tumoural FcγR expression in the depleting activity of immune modulatory antibodies in mouse models (Bulliard et al., 2013, 2014; Dahan et al., 2015; Selby et al., 2013; Simpson et al., 2013), the second objective of this thesis was to dissect the in vivo activity of anti-CD25 mAbs (PC61 clone) through comprehensive analysis of blood, LN and tumour in mouse models of cancer with validation of the translational relevance of any findings in human tumour samples.

1.11 Identification of drivers of T cell reactivity in human cancer

The majority of current immunotherapeutic approaches against human cancer rely upon the presence of an existing immune infiltrate. To those studying the immune tumour microenvironment of human tumours, heterogeneity in immune infiltrate is well recognised and paucity or indeed complete absence of T cell infiltration is not an infrequent finding; although this is rarely acknowledged in the literature (Melero et al., 2014). Identification of the most relevant antigenic stimuli or drivers of T cell infiltrate therefore remains an area of high scientific priority.

1.12 Lessons from adoptive T cell therapy

In humans, adoptive transfer of TILs with concomitant administration of interleukin-2 (IL-2) mediates tumour regression in 34-40% of patients with advanced melanoma (Rosenberg et al., 1988). This setting has provided a useful platform for characterisation of antigens eliciting T cell reactivity associated with clinical response (Gros et al., 2014; Tran et al., 2016). Early studies demonstrated melanoma TILs were able to recognise shared antigens on melanoma cell lines established from different patients, in a class I major-histocompatibility complex (MHC)-restricted manner in vitro (Hom et al., 1993; Kawakami et al., 1992). The first gene identified to code for an antigen recognised on human tumours by autologous TILs was MAGE-1, silent in normal tissues except in testis, and expressed by a number of other solid tumour subtypes (van der Bruggen et al., 1991). Subsequently, three further self-proteins, all melanoma/melanocyte lineage-specific, encoded by MART-1, tyrosinase and gp100, were identified (Brichard et al., 1993; Coulie et al., 1994; Kawakami et al., 1994). Although these 'public' tumour-associated antigens appeared attractive targets for both adoptive cell-based and vaccination strategies, neither approach has been observed to yield particularly promising activity in the clinical setting (June, 2007).

The identification of CTLA-4, followed by the demonstration of efficient rejection of established murine tumours with CTLA-4 'blockade', highlighted immune regulation as a potential contributor to the limited clinical activity of therapeutic strategies directed against these tumour-associated antigens (Brunet et al., 1987; Leach et al., 1996). In a pooled analysis of patients with advanced melanoma treated with ipilimumab, an antibody directed against CTLA-4, three-year survival was found to range between 20 and 26% (Schadendorf et al., 2015). Amongst a cohort of 107 patients with advanced melanoma, one of the earliest to be treated with nivolumab, an anti-PD-1 antibody, 5-year survival was recently reported as 34% (Hodi S., AACR, 2016). This is remarkable in a solid tumour subtype in which no therapy had prolonged survival prior to ipilimumab, however, it is important to acknowledge that the majority of patients do not respond to these forms of immune checkpoint blockade, at least as monotherapy. This has engendered

significant efforts to dissect underlying mechanisms of response within translational studies, with focus on tumours derived from patients responding to such therapies.

1.13 Tumour-specific mutations serve as neoantigens

A hallmark of tumours in patients that appear to derive benefit from checkpoint blockade with therapeutic CTLA-4 or PD-1 antibodies is pre-existing T cell infiltration or an 'inflamed' tumour microenvironment (Huang et al., 2017; Ji et al., 2012; Tumeh et al., 2014). Tumour exome analysis in mice has revealed specific missense mutations that encode MHC class I presented mutational epitopes, capable of eliciting T cell-mediated tumour rejection (Castle et al., 2012; Matsushita et al., 2012). Tumour-specific mutations may therefore serve as 'private' neoantigens, eliciting anti-tumour T cell responses (Castle et al., 2012; Lu et al., 2013; Robbins et al., 2013; Segal et al., 2008). In contrast to non-mutated self antigens, these are thought to be of particular relevance in tumour control, since the quality of the T cell pool available for these antigens is not affected by central T cell tolerance (Gilboa, 1999).

Brown and colleagues studied tumours from 515 patients, including 6 tumour subtypes, using RNA sequencing data derived from the The Cancer Genome Atlas (TCGA) (Brown et al., 2014). Mutations predicted to be immunogenic were identified based on their potential to give rise to mutational epitopes presented by MHC proteins encoded by each patient's autologous HLA-A alleles. Mutational epitope burden demonstrated a positive association with survival. Tumours with a high burden of predicted mutational epitopes were observed to display a higher cytotoxic T lymphocyte content (based on CD8A gene expression) and elevated expression of co-inhibitory immune checkpoint molecules including PD-1 and CTLA-4. These findings were supported by even larger, elegant studies, confirming an inextricable relationship between the genomic landscape of tumours and anti-tumour immunity (Rooney et al., 2015).

It follows that response to immune checkpoint modulation might also depend upon mutational epitope burden. Two pivotal studies subsequently

demonstrated that patients with advanced melanoma and non-small cell lung cancer (NSCLC), deriving benefit from CTLA-4 and PD-1 blockade respectively, appeared to have tumours enriched with putative neoantigens (Rizvi et al., 2015; van Rooij et al., 2013; Snyder et al., 2014). However, in contrast to tumour-associated antigens, tumour-specific mutations appear unique to individual tumours. Analysis of 110 patients with advanced melanoma undergoing CTLA-4 blockade demonstrated an association between predicted neoantigen burden and clinical benefit, however no recurrent neoantigen peptide sequences were identified amongst responding patients (Van Allen et al., 2015).

1.14 Identification and characterisation of neoantigen-reactive T cells

Prediction of tumour-specific neoepitopes on an individual patient basis remains, at present, an unrealistic prospect for the majority of healthcare systems across the globe. However, whilst tumour-specific mutations vary between patients, the regulatory mechanisms underlying T cell activity are common to all. Circulating T cells have been demonstrated to recognise tumour-specific neoantigens in vitro (Rizvi et al., 2015; Snyder et al., 2014), however tumour-infiltrating neoantigen-reactive T cells are poorly described. The final objective of this study was to attempt to identify such cell subsets, determine phenotypic and functional markers by which they might be identified and characterise any regulatory mechanisms serving to limit their activity.

1.15 Aims

- **Characterisation of in vivo determinants of response to anti-CTLA-4 antibodies in mouse and man**

- **Re-evaiuation of CD25 as a therapeutic target for the selective depletion of Treg cells in mouse models and human cancers**

- **Identification of novel drivers of T cell reactivity in human cancers**

2 Materials and Methods

2.1 Mice

C57BL/6 and BALB/c mice were purchased from Charles River Laboratories. FcγRα null and human FcγR transgenic of C57BL/6 background (Smith et al., 2012) mice were a kind gift from J.V. Ravetch (The Rockefeller University, New York, USA), housed and bred in Charles River Laboratories, U.K.. Experiments were typically performed with 6-10 week old females.

Fcer1g$^{-/-}$ and *Fcgr3*$^{-/-}$ mice were kindly provided by S. Beers (University of Southampton, UK). *Fcgr4*$^{-/-}$ and *Fcgr2b*$^{-/-}$ mice were a kind gift from J.V. Ravetch (The Rockefeller University, New York, USA). All knockout mice were of C57BL/6 background and bred in University College London. All animal studies were performed under University College London and UK Home Office ethical approval and regulations.

2.2 Cell lines and tissue culture

MCA205 cells were cultured in Dulbecco's modified Eagle medium (DMEM, Sigma) supplemented with 10% foetal calf serum (FCS, Sigma), 100U/mL penicillin, 100μg/mL streptomycin and 2mM L-glutamine (all from Gibco). MC38, CT26, B16 and SupT1 cells were cultured in Roswell Park Memorial Institute (RPMI) media supplemented as above. K562 cells used for antibody production were cultured in phenol red-free Iscove's Modified Dulbecco's medium (IMDM) supplemented with 10% IgG-depleted FCS (Life Technologies).

2.2.1 Generation of CTLA-4-expressing target cells

A cell line with stable membrane-bound expression of murine CTLA-4 was generated by transduction of SupT1 cells with a retroviral vector (a kind gift from Claire Roddie, University College London). CTLA-4 expression was confirmed prior to assays by flow cytometry.

2.2.2 Generation of monocyte-derived human macrophages

Monocytes were isolated from healthy donor PBMCs with use of anti-CD14 microbeads (Miltenyi Biotec) and cultured for 7 days in RPMI supplemented with 10% FCS and recombinant human macrophage colony-stimulating factor (M-CSF, CELL guidance systems) at 40ng/mL. Additional media was added every 48 hours as required. The final phenotype and Fc gamma receptor expression profile of macrophages was determined by flow cytometry on day 7.

2.2.3 Carboxyfluorescein succinimidyl ester (CFSE) labelling

CFSE was used to label target cells employed within ADCC assays. Cells were resuspended at $5x10^6$/mL in PBS/0.1% bovine serum albumin (BSA) and labeled with 5μM CFSE (CellTrace CFSE Cell Proliferation Kit, Life Technologies). To obtain a 5μM solution of CFSE, 2μL CFSE was resuspended in 1mL of warm PBS/BSA 0.1%. 1mL of diluted CFSE was added to target cells and mixed thoroughly to obtain homogeneous staining prior to incubation at 37°C for 10 minutes. The reaction was then immediately quenched, by adding 5 volumes of cold RPMI and incubating for 5 minutes on ice. In order to minimise cell toxicity and to obtain clean labeling, 4 wash steps were then performed prior to use.

2.2.4 Antibody production

2.2.4.1 Anti-CTLA-4

Antibody production was outsourced to Evitria AG (Switzerland). The sequence of the variable regions of the heavy and light chains of anti-mouse CTLA-4, clone 4F10, was kindly provided by J.A. Bluestone and used to generate chimeric antibodies with the constant regions of human IgG1 and IgG2 heavy chains and κ light chain, as well as the mutated IgG1 variants N297A and S239D/A330L/I332E (SDALIE) (Lazar et al., 2006).

2.2.4.2 Anti-CD25

The sequence of the variable regions of the heavy and light chains of anti-CD25 were resolved from the PC-61.5.3 hybridoma by rapid amplification of

cDNA ends (RACE) and then cloned into the constant regions of murine IgG2a and κ chains sourced from the pFUSEss-CHIg-mG2A and pFUSE2ss-CLIg-mk plasmids (Invivogen). Each antibody chain was then sub-cloned into a murine leukaemia virus (MLV)-derived retroviral vectors used to generate K562 stable cell lines. For preliminary experiments, antibody was purified from supernatants with a protein G HiTrap MabSelect column (GE Healthcare), dialysed in phosphate-buffered saline (PBS), concentrated and filter-sterilised. For subsequent experiments, antibody production was outsourced to Evitria AG (Switzerland).

2.2.5 In vitro ADCC assay

SupT1 cells expressing murine CTLA-4 were labelled with 10μM CFSE (CellTrace CFSE Cell Proliferation Kit, Life Technologies) and co-cultured overnight with human macrophages at the indicated ratios in the presence of the indicated mAbs (50μg/mL) (Figure 3). The absolute number of CFSE-labelled cells in each condition was then quantified by flow cytometry using a defined number of fluorescent beads (Cell Sorting Set-up Beads for UV Lasers, ThermoFisher) as reference. The percentage of killing was determined as: 100-(number $CFSE^+$ targets treated/number $CFSE^+$ targets untreated).

	$IgG1_{N297A}$			IgG1			IgG2			$IgG1_{SDALIE}$		
Control	A/1	2	3	4	5	6	7	8	9	10	11	12
10:1	B											
5:1	C											
2.5:1	D											
1:1	E											
	F											
	G											
	H											

Figure 3: 96 well plate design of in vitro ADCC assay

Therapeutic antibodies are displayed above. Each condition was performed in triplicate. Control wells consisted of CTLA-4-expressing SupT1 target cells and therapeutic mAbs alone. Depicted ratios are of effector (macrophages) to target cell (SupT1s).

2.3 Mouse tumour experiments

Cultured tumour cells were trypsinised, washed, re-suspended in 100uL of PBS and injected subcutaneously (s.c.) in the flank. Therapeutic antibodies were injected intra-peritoneally at the time points and doses detailed in the figure legends. Tumours were measured twice weekly and volumes calculated as the product of three orthogonal diameters. Mice were euthanized when any diameter reached 150mm.

2.3.1 Processing of mouse tissue for immunological analyses

Mice were sacrificed at specified time points with CO_2. Lymph nodes (inguinal, axillary and brachial) and tumours were dissected into RPMI. Lymph nodes were dispersed through a 70μm filter, whereas tumours were mechanically disrupted using scissors, digested with a mixture of 0.33 mg/ml DNase (Sigma) and 0.27mg/ml Liberase TL (Roche) in serum free RPMI for 25 minutes, and dispersed through a 70μm filter.

2.3.2 Therapeutic antibodies

Commercial anti-CD25 (clone PC-61.5.3) and anti-CTLA-4 (clone 9H10) mAbs used for in vivo experiments were purchased from BioXcell (USA). The binding affinity of different isotype variants to FcγRs was measured by surface plasmon resonance in the Ravetch laboratory as described previously (Nimmerjahn and Ravetch, 2005).

2.4 Human tumour experiments

2.4.1 Study oversight

Presented human data derives from three translational studies, each approved by local institutional review board and Research Ethics Committee (Melanoma - REC no. 11/LO/0003, NSCLC – REC no.13/LO/1546, RCC – REC no. 11/LO/1996). All were conducted in accordance with the provisions of the Declaration of Helsinki and with Good Clinical Practice guidelines as defined by the International Conference on Harmonization. All patients (or their legal representatives) provided written informed consent before enrolment.

2.4.2 Patient identification and tumour sampling

Patients were identified in the clinic and consented to relevant studies. Tumour samples and peripheral blood were obtained directly from the operating theatre. Sampling of tumour representative and normal tissue areas was performed under the supervision of a Consultant Pathologist. Fresh tissue was placed in RPMI supplemented with 10% FCS and transported at room temperature to the wet laboratory.

2.4.3 Patient selection and demographics

The human data presented in this study derives from distinct patient cohorts identified to address specific scientific questions.

2.4.3.1 Cohort 1 – T cell profiling

Numerous patient samples were evaluated over the course of this study. For T cell analyses, data is presented from an experiment including patients with advanced melanoma (Table 3), early NSCLC (Table 4) and varied-stage RCC (Table 5). This was performed to allow direct comparison between tumour subtypes.

Melanoma samples derived from patients with stage III/IV disease undergoing palliative resections. Patients were either treatment naïve or had progressed through varied systemic therapies. In contrast, non-small cell lung cancer samples derived from patients undergoing resection of primary lung cancers; no patient had received any form of neoadjuvant therapy. Renal cell carcinoma samples derived predominantly from patients with clear cell histology undergoing cytoreductive surgery. All were treatment naive and most commonly of advanced stage.

Identifier	Age	Sex	Subtype	Stage	Biopsy site	Mutational status	Current therapy	Previous therapy
MM1	53	M	Cutaneous	IIIc	LN	BRAF WT NRAS mutant	Nil	Adjuvant ipilimumab/ nivolumab
MM2	52	M	Cutaneous	IV – M1c	Small bowel	BRAF mutant	Pembrolizumab	Ipilimumab
MM3	76	F	Cutaneous	IV – M1c	Small bowel	BRAF WT NRAS mutant	Nil	Nil
MM4	76	M	Cutaneous	IIIc	LN	BRAF mutant	Nil	Nil
MM5	74	F	Cutaneous	IV – M1a	LN	BRAF WT	Nil	Nil
MM6	61	M	Cutaneous	IV – M1a	LN	BRAF WT	Nil	Ipilimumab
MM7	42	M	Cutaneous	IIIc	LN	BRAF mutant	Nil	Nil
MM8	49	M	Cutaneous	IV – M1c	LN	BRAF WT NRAS mutant	Nil	Paclitaxel Trametinib Ipilimumab Pembrolizumab

Table 3: Demographics and baseline characteristics of patients with advanced melanoma (M, male; F, female; LN, lymph node)

Identifier	Age	Sex	Subtype	Stage	Resection site(s)	Current therapy	Previous therapy
NSCLC1	74	M	Adenocarcinoma	IIa	Right lower lobe	Nil	Nil
NSCLC2	76	M	Squamous	IIIa	Right upper lobe	Nil	Nil
NSCLC3	53	F	Squamous	IIa	Left upper lobe	Nil	Nil
NSCLC4	90	M	Squamous	IIa	Left lower lobe	Nil	Nil
NSCLC5	60	M	Adenocarcinoma	IIa	Left upper lobe	Nil	Nil
NSCLC6	57	M	Adenocarcinoma	IIb	Left lower Lobe	Nil	Nil
NSCLC7	54	F	Adenocarcinoma	IIa	Right upper lobe	Nil	Nil
NSCLC8	69	M	Adenocarcinoma	Ia	Left lower lobe	Nil	Nil

Table 4: Demographics and baseline characteristics of patients with early-stage NSCLC (M, male; F, female)

Identifier	Age	Sex	Subtype	Stage	Current therapy	Previous therapy
RCC1	44	M	Clear cell	III	Nil	Nil
RCC2	69	M	Clear cell	IIa	Nil	Nil
RCC3	78	F	Mixed - clear cell/ tubulo-papillary	Ia	Nil	Nil
RCC4	65	F	Clear cell	IV	Nil	Nil
RCC5	50	F	Clear cell	IV	Nil	Nil
RCC6	60	F	Clear cell	IV	Nil	Nil
RCC7	19	F	Clear cell	IV	Nil	Nil
RCC8	59	M	Clear cell	IV	Nil	Nil

Table 5: Demographics and baseline characteristics of patients with varied stage renal cell carcinoma (M, male; F, female)

2.4.3.2 Cohort 2 – myeloid cell profiling

Preliminary data demonstrated that cryopreservation impacted negatively upon a number of FcγR-expressing cell subsets particularly granulocytes. FcγR profiling therefore required a separate cohort of patients. Analyses were performed exclusively on freshly isolated resection specimens of advanced melanoma derived from multiple anatomical sites including subcutaneous, small bowel, lymph node and splenic metastases (Table 6). Pathology guidance was particularly important in this setting to ensure sampling of bona fide tumour-representative areas.

Identifier	Age	Sex	Subtype	Stage	Biopsy site	Mutational status	Current therapy	Previous therapy
Myeloid 1	66	M	Cutaneous	IV M1c	LN	BRAF WT	Pembrolizumab	Ipilimumab
Myeloid 2	60	M	Ocular	IV M1c	Splenic metastasis	BRAF WT	Nil	Nil
Myeloid 3	76	M	Cutaneous	IV M1c	SC	BRAF mutant	Nil	Nil
Myeloid 4	86	F	Cutaneous	IV M1c	SC	BRAF WT	Nil	Nil
					LN			
Myeloid 5	46	F	Cutaneous	IV M1c	SC	BRAF mutant	Nil	Dabrafenib/ Trametinib
Myeloid 6	50	M	Cutaneous	IV M1c	Small bowel	BRAF mutant	Pembrolizumab	Ipilimumab
Myeloid 7	69	M	Cutaneous	IV M1c	SC	BRAF WT	Pembrolizumab	Ipilimumab
Myeloid 8	76	F	Cutaneous	IV M1c	Small bowel	BRAF WT	Nil	Nil
Myeloid 9	53	M	Cutaneous	IIIc	LN	BRAF WT	Nil	Adjuvant ipilimumab/ nivolumab

Table 6: Demographics and baseline characteristics of patients with advanced melanoma undergoing FcγR profiling (M, male; F, female; LN, lymph node; SC, subcutaneous)

2.4.3.3 Cohort 3 - longitudinal analyses

Longitudinal assessment of the tumour microenvironment was performed via image-guided core biopsy of the same primary or metastatic site following 4 cycles of either nivolumab (3mg/kg Q2W) in advanced RCC, or 2 cycles of pembrolizumab (200mg Q3W) in patients with advanced melanoma (Table 7). Samples were obtained by the interventional radiology team and underwent formalin fixation and paraffin embedding. Cut slides were analysed by multiplex immunohistochemistry (IHC).

Patient	Age	Sex	Subtype	Stage	Biopsy site	Mutational status	Current therapy	Previous therapy
CB1	64	M	Cutaneous melanoma	IV – M1c	SC	BRAF WT	Pembrolizumab	Ipilimumab
CB2	54	M	Cutaneous melanoma	IV – M1c	SC	BRAF mutant	Pembrolizumab	Ipilimumab
CB3	32	F	Cutaneous melanoma	IV – M1c	SC	BRAF WT NRAS WT	Pembrolizumab	Ipilimumab
CB4	69	F	Cutaneous melanoma	IV – M1c	LN	BRAF mutant NRAS WT	Ipilimumab + Nivolumab	Nil
CB5	62	M	Clear cell RCC	IV	Adrenal metastasis	-	Nivolumab	Nil
CB6	53	M	Clear cell RCC	IV	Primary renal mass	-	Nivolumab	Nil

Table 7: Demographics and baseline characteristics of patients with advanced melanoma and RCC undergoing PD-1 blockade (M, male; F, female; LN, lymph node; SC, subcutaneous)

2.4.3.4 Cohort 4 – identification of neoantigen-reactive T cells

Two patients undergoing resection of primary lung tumours were studied; L011 and L012. Demographics and baseline characteristics are displayed in Figure 23. Resection specimens were subjected to multi-regional sampling by the Swanton laboratory team under the supervision of a Consultant Pathologist as described previously (de Bruin et al., 2014; Jamal-Hanjani et al., 2017).

2.4.4 Preparation of human samples for immunological analyses

Peripheral blood mononuclear cells (PBMCs) were isolated from whole blood obtained at venesection following gradient centrifugation with Ficoll-paque (GE Healthcare). Tumour samples were digested with Liberase TL (0.3mg/mL, Roche) and DNAse I (0.2 mg/mL, Roche) at 37°C for 30 minutes, homogenised using gentleMACS (Miltenyi Biotech) and filtered through a 0.7μm cell mesh. Leukocytes were enriched by gradient centrifugation with Ficoll-paque (GE Healthcare). Isolated live cells were analysed immediately for FcγR profiling or frozen at -80°C and stored in liquid nitrogen until analysis.

2.4.5 In-vitro expansion of tumour-infiltrating lymphocytes

For high-throughput screening with MHC multimers, human TILs were expanded with use of a rapid expansion protocol (REP) in T25 flasks containing EX-VIVO media (Lonza) supplemented with 10% human AB serum (Sigma), soluble anti-CD3 (OKT3, BioXCell), 6000IU/mL recombinant human (rhIL-2, PeproTech) and $2x10^7$ irradiated PBMCs (30Gy) pooled from 3 allogeneic healthy donors. Fresh media containing rhIL-2 at 6000IU/mL was added every three days as required. Following 2 weeks of expansion, TILs were counted, phenotyped by flow cytometry and frozen in human AB serum (Sigma) at -80°C before use in relevant assays or long-term storage in liquid nitrogen.

2.4.6 Preparation of human samples for genomic analyses

Multi-regional sampling, DNA extraction and whole exome sequencing was led and performed by the Swanton laboratory. Relevant methodology has been previously described in full (de Bruin et al., 2014; Jamal-Hanjani et al., 2017).

2.5 Flow cytometry analyses

Cell surface staining was performed in round-bottomed 96 well plates. Surface antibodies were applied for 30 minutes in the dark, on ice, using cold buffers and reagents, followed by a double wash in staining buffer (PBS, 2% FCS and 0.1% sodium azide) supplemented with 10% superblock (500uL rat serum, 500uL mouse serum +/- mouse/human FcγR block). Intracellular staining was performed using the FoxP3 Transcription Factor Staining Buffer Set (eBioscience). For quantification of absolute number of cells, a defined number of fluorescent beads (Cell Sorting Set-up Beads for UV Lasers, ThermoFisher) was added to each sample before acquisition and used as a counting reference. Antibodies used for staining of mouse and human cells are displayed in Table 8 and Table 9 respectively.

Antibody	Clone	Supplier
CD4-V500	RM4-5	BD Biosciences
CD25-FITC	7D4	BD Biosciences
CD4-BrilliantViolet785	RM4-5	BioLegend
CD8-BrilliantViolet650	53-6.7	BioLegend
CD19-BrilliantViolet605	6D5	BioLegend
CD3-BrilliantViolet785	17A2	BioLegend
CD64-APC	X54-5/7.1	BioLegend
OX40-biotin	OX86	BioLegend
Streptavidin-BrilliantViolet605	-	BioLegend
Streptavidin-BrilliantViolet705	-	BioLegend
Anti-CD16/32-AlexaFluor488	2.4G2	BioXcell
CD3-PE.Cy7	145-2C11	eBioscience
CD5-PerCP.Cy5.5	53-7.3	eBioscience
FoxP3-FITC	FJK-16s	eBioscience
I-Ab-eFluor450	AF6-210.1	eBioscience
NK1.1-AlexaFluor700	PK136	eBioscience
NK1.1-BrilliantViolet650	PK136	eBioscience
Ki67-eFluor450	SolA15	eBioscience
GITR-eFluor450	DTA-1	eBioscience
4-1BB-biotin	17B-5	eBioscience
PD-1-eFluor450	RMP1-30	eBioscience
TIM-3-PE	8B.2C12	eBioscience
PD-1-PERCP.Cy5.5	J43	eBioscience
FoxP3-PE	FJK-16s	eBioscience
CD5-eFluor450	53-7.3	eBioscience
CD11b-PERCP-Cy5.5	M1/70	eBioscience
FcγRIV- AlexaFluor488	9E9.27	Ravetch laboratory
CD32b- AlexaFluor647	K9.361	Ravetch laboratory

Table 8: Antibodies used for staining of mouse cells

Antibody	Clone	Supplier
Ki67-FITC	B56	BD Biosciences
CD8-V500	SK1	BD Biosciences
CD64-AF700	10.1	BD Biosciences
CD16a/b-V500	3G8	BD Biosciences
Granzyme B-V450	GB11	BD Biosciences
TIM-3-Q650	7D3	BD Biosciences
CD14-PE-Cy7	M5E2	BD Biosciences
CD32b-APC	6-G11	BioInvent
CD11c-V450	3.9	BioLegend
CD45-Q655	HI30	BioLegend
CD56-BV711	HCD56	BioLegend
CD19-BV785	HIB19	BioLegend
CD11b-PerCP-Cy5.5	ICRF44	BioLegend
CD15-PE	HI98	BioLegend
PD-1-Q605	EH12.2H7	BioLegend
CD25-BV711	BC96	BioLegend
CD3-BV785	OKT3	BioLegend
BTLA-PerCP-Cy5.5	MIH26	BioLegend
CTLA-4-APC	L3D10	BioLegend
Streptavidin-Q650	-	BioLegend
OX40-PE-Cy7	ACT35	BioLegend
ICOS-APC	C398.4A	BioLegend
4-1BB-PE	4B4-1	BioLegend
CD3-BrilliantViolet785	OKT3	BioLegend
CD25-BrilliantViolet650	BC96	BioLegend
LAG-3-PE-Cy7	3DS223H	eBioscience
TIGIT-FITC	MBSA43	eBioscience
CD3-e605	OKT3	eBioscience
Anti-CD4-AlexaFluor700	OKT4	eBioscience
Anti-FoxP3-PerCP-Cy5.5	PCH101	eBioscience
HLA-DR-PE	L243	eBioscience
Fixable viability dye-e780	-	eBioscience
GITR-Biotinylated	DT5D3	Miltenyi
CD32a-FITC	IV.3	StemCell

Table 9: Antibodies used for staining of human cells

2.6 MHC multimer generation and combinatorial encoding-flow cytometry analysis

MHC multimers holding the predicted neoepitopes were produced in-house at Technical University of Denmark, Hadrup laboratory. Synthetic peptides were purchased at Pepscan Presto, NL. HLA molecules matching the HLA-expression of L011 (HLA-A1101, A2402, and B3501) and L012 (HLA-A1101, A2402, and B0702) were refolded with a UV-sensitive peptide, and exchanged to peptides of interest following UV exposure (Bakker et al., 2008; Chang et al., 2013; Frøsig et al., 2015; Toebes et al., 2006). HLA complexes loaded with UV-sensitive peptide were subjected to 366-nm UV light (CAMAG) for one hour at 4°C in the presence of candidate neoantigen peptides in a 384-well plate. Peptide-MHC multimers were generated using a total of 9 different fluorescent streptavidin (SA) conjugates: PE, APC, PE-Cy7, PE-CF594, Brilliant Violet (BV)421, BV510, BV605, BV650, Brilliant Ultraviolet (BUV)395 (BioLegend). MHC multimers were generated with two different streptavidin-conjugates for each peptide-specificity to allow a combinatorial encoding of each antigen responsive T cell, enabling analyses for reactivity against up to 36 different peptides in parallel (Andersen et al., 2012; Hadrup et al., 2009).

2.6.1 Screening of in-vitro-expanded tumour-infiltrating $CD8^+$ T cells

In-vitro expanded $CD8^+$ T lymphocytes isolated from region-specific lung cancer samples and adjacent normal lung tissue were screened with MHC multimers bearing mutant peptides (with predicted HLA binding affinity <500nM, including multiple potential peptide variations from the same missense mutation) in patient L011 and L012 respectively. Simultaneously, TIL responses to HLA-matched viral peptides were assessed, demonstrating functionality of the employed MHC-multimer technology. Viral peptides screened for L011 and L012 are displayed (Table 10). Reactivity of healthy donor $CD8^+$ PBMC's against the same peptides was also assessed, in order to demonstrate a lack of background/non-specific staining.

L011	L012
A11 EBV-EBNA4 (AVFDRKSDAK)	A11 EBV EBNA4 (AVFDRKSDAK)
A11 HCMV pp65 (GPISGHVLK)	A11 HCMV pp65 (GPISGHVLK)
A24 EBV LMP-2 419-427 (TYGPVMCL)	A24 EBV EBNA-3 114-121 (RYSIFFDY)
A3 EBV EBNA 3A RLR (RLRAEAQVK)	A24 EBV LMP-2 419-427 (TYGPVFMCL)
A24 HCMV 248-256 (AYAQKIFKIL)	A24 EBV RTA 28-37 (DYCNVLNKEF)
B35 Flu Matrix (ASCMGLIY)	A24 HCMV 248-256 (AYAQKIFKIL)
B35 ENV EBNA 3B (AVLLHEESM)	B7 CMV pp65 RPH-L (RPHERNGFTV)
EBV EBNA-3 114-121 (RYSIFFDY)	B7 CMV pp65 TPR (TPRVTGGGAM)
EBV BZLF1 (APENAYQAY)	B7 EBV EBNA RPP (RPPIFIRLL)

Table 10: Control HLA-matched viral peptides

For staining of in-vitro expanded $CD8^+$ T lymphocytes, samples were thawed, treated with DNAse for 10 minutes, washed and stained with MHC multimer panels for 15 minutes at 37°C. Subsequently, cells were stained with LIVE/DEAD® Fixable Near-IR Dead Cell Stain Kit for 633 or 635 nm excitation (Invitrogen, Life Technologies), CD8-PerCP (Invitrogen, Life Technologies) and FITC coupled antibodies to a panel of CD4, CD14, CD16, CD19 (all from BD Pharmingen) and CD40 (AbD Serotec) for an additional 20 minutes at 4°C. Cut off values for the definition of positive responses were ≥0.005% of total CD8+ cells and ≥10 events.

2.6.2 Screening and characterisation of non-expanded tumour-infiltrating T cells

Tumour samples were thawed, washed and first stained with custom-made MHC multimers for 10-15 minutes at 37°C. Cells were thereafter transferred onto wet ice and stained for 30 minutes with a panel of surface antibodies used at the manufacturer's recommended dilution: CD8-V500, SK1 clone (BD Biosciences), PD-1-BV605, EH12.2H7 clone (Biolegend), CD3-BV785, OKT3 clone (Biolegend), LAG-3-PE, 3DS223H clone (eBioscience). A fixable viability dye (eFlour780, eBioscience) was included in the surface mastermix.

Cells were permeabilised for 20 minutes with use of an intracellular fixation and permeabilisation buffer set from eBioscience. An intracellular staining panel was applied for 30 minutes and consisted of the following antibodies used at the manufacturer's recommended dilution: granzyme B-V450, GB11 clone (BD Biosciences), FoxP3-PerCP-Cy5.5, PCH101 clone (eBioscience), Ki67-FITC, clone B56 (BD Biosciences) and CTLA-4 – APC, L3D10 clone (Biolegend).

2.7 Data acquisition

All flow cytometry data acquisition was performed with use of a BD LSR II Fortessa (BD Biosciences).

2.8 Multiplex immunohistochemistry (IHC)

2-5μm tissue sections of formalin-fixed and paraffin-embedded tumour samples were cut and stained with the following antibodies: anti-CD8 (SP239), anti-FoxP3 (236A/E7) (a gift from Dr. G. Roncador CNIO, Madrid, Spain) and anti-CD25 (4C9) (Leica Biosystems). Dilutions were optimised with single conventional immunostaining of human tonsil sections. For multiple staining, tissue sections were incubated with the primary antibodies for 30 minutes after antigen retrieval by heating and endogenous peroxidase blocking (DakoCytomation). Detection was performed using the peroxidase-based detection reagent conjugate (OptiView DAB IHC Detection Kit) followed by the alkaline phosphatase detection kit (UltraView Universal Alkaline Phosphatase Red Detection Kit), both from Ventana Medical Systems, Inc.. The immuno-complexes were visualized with either Fast Red or Fast Blue if used previously, or vice versa. Cell counting was performed with use of ImageJ (1.48v).

2.9 Bioinformatics analyses

Bioinformatics analyses were performed by the Swanton laboratory, detail on relevant methodology is provided below courtesy of Nicholas McGranahan and Rachel Rosenthal, this has also been described elsewhere (McGranahan et al., 2016).

2.9.1 Variant calling

Analysis of germline, primary tumour regions and variant calling from previously published cohorts was performed by the Swanton laboratory and has previously been described in full (de Bruin et al., 2014; Jamal-Hanjani et al., 2017; McGranahan et al., 2016).

2.9.2 Clonal architecture analysis

The clonal status of each mutation was estimated based on multi-region sequencing calls. In brief, each mutation was classified as clonal if identified and present in each and every tumour region sequenced within the tumour. Conversely, any mutations not ubiquitously present in every tumour region were classified as subclonal. For single sample sequenced tumours, a modified version of PyClone was used. This modification was implemented to allow clustering on mutations occurring in regions of subclonal copy number.

2.9.3 HLA typing of patient samples

For all TCGA patients, the 4-digit HLA type was determined using POLYSOLVER (POLYmorphic loci reSOLVER) (Shukla et al., 2015). Patients L011 and L012 were serotyped (outsourced to Anthony Nolan, London) and simultaneously genotyped using Optitype (Szolek et al., 2014), which produced concordant results.

2.9.4 Identification of putative neoantigens

Identified non-silent mutations were used to generate a comprehensive list of peptides 9-11 amino acids in length with the mutated amino acid represented in each possible position. The binding affinity of every mutant peptide and its corresponding wild-type peptide to the patient's germline HLA alleles was predicted using netMHCpan-2.8 (Hoof et al., 2009; Nielsen et al., 2007). Candidate neo-antigens were identified as those with a predicted binding strength of <500 nM.

2.9.5 TCGA exome datasets

Tumour samples, with mutation calls and HLA typing described below, were obtained from the Cancer Genome Atlas (TCGA) for a cohort of lung adenocarcinoma patients (LUAD, n=150). SNV data was obtained from TumorPortal (Lawrence et al., 2014) for the LUAD. One LUAD patient, TCGA-05-4396, was excluded for having over 7000 low quality mutations called, mostly in a C[C>G]G context.

2.9.6 TCGA survival analysis

Clinical data for the TCGA patients was accessed through the TCGA data portal. Patients were first grouped according to quartile of the variable being considered. Survival analyses were then performed in R using the survival package. Complete survival data was available for 139/150 LUAD patients.

2.9.7 Differential gene expression analysis

RNA-sequencing data was downloaded from the TCGA data portal. For each LUAD sample, all available 'Level_3' gene-level data was obtained. The raw read counts were used as input into the R package DESeq2 for analysis. Transcriptome-wide differential gene expression analyses were performed between all TCGA LUAD tumours and between high and low clonal neoantigen TCGA LUAD groups. Significantly differentially expressed immune-related genes were identified. These genes were clustered on their co-expression using the metric 1-r2.

2.10 Statistical analyses

Flow cytometry data analysis was performed in FlowJo version 10.0.8 (Tree Star Inc.). Statistical analyses were performed in Prism 6 (GraphPad Software, Inc.); *p* values were calculated using Kruskall-Wallis analysis of variance and Dunn's *post-hoc* test, unless otherwise indicated in the figure legends (ns = $p > 0.05$; * = $p < 0.05$; ** = $p < 0.01$; *** = $p < 0.001$; **** = $p < 0.0001$). Analysis of the significance of differentially expressed immune-related genes was performed with use of Wald's test. Analysis of Kaplan-Meier survival curves was performed with use of the log-rank test.

3 Results 1: Dissecting the in vivo activity of anti-CTLA-4 antibodies

3.1 Introduction

Pre-clinical data in mouse models of cancer clearly demonstrate that in addition to blockade of a co-inhibitory molecule, anti-CTLA-4 mAbs act to deplete intra-tumoural Treg cells expressing high levels of surface CTLA-4 via ADCC (Bulliard et al., 2013; Selby et al., 2013; Simpson et al., 2013). In mouse models, this activity is required for maximal efficacy, however demonstrating a common mechanism in human cancers has proved challenging. The first objective of this thesis was to attempt evaluate this further through:

(i) comprehensive evaluation of CTLA-4 expression in circulating and tumour-infiltrating T cell subsets in mouse models and human cancers

(ii) profiling of activatory and inhibitory FcγRs on circulating and tumour-infiltrating lymphocyte and innate effector cell subsets in mouse models and human cancers

(iii) attempting to bridge the translational void with use of chimeric anti-mouse CTLA-4 mAbs with human Fc variants within a transgenic mouse model bearing human FcγRs

(iv) confirm the translational relevance of in vivo findings through in silico analysis of tumour exomes in patients treated with anti-CTLA-4 mAb

In vivo mouse work was performed by Fred Arce Vargas. Ex vivo work was performed together with Andrew Furness. Study of human samples was performed independently by Andrew Furness. Bioinformatics analyses were led and interpreted by Andrew Furness; data was generated by Rachel Rosenthal.

3.2 Identification of circulating and tumour-infiltrating T cell subsets in human cancers

Analysis of immune checkpoint molecule expression in human tumour samples is often largely focused on $CD8^+$ T cells (Gros et al., 2014). Given the differential expression of CTLA-4, OX40 and GITR observed in mouse models of cancer (Bulliard et al., 2013, 2014; Selby et al., 2013; Simpson et al., 2013), the prevalence of individual T cell subsets within the peripheral blood and tumours of patients with solid tumours was studied.

Isolated peripheral blood mononuclear cells (PBMCs) and tumour digests were analysed by multi-parametric flow cytometry (Figure 4). Single, live, $CD3^+$ T cells were identified before application of further gating to distinguish between $CD4^+FoxP3^+$ regulatory T cells (Treg), $CD4^+FoxP3^-$ and $CD8^+$ effector T cells (Teff) (Figure 4A). Relative frequencies of both circulating and tumour-infiltrating T cell subsets were compared across a cohort of patients with advanced melanoma, early-stage NSCLC and RCC of varied stage (Figure 4B, Chapter 2.4.3.1, Materials and Methods).

A.

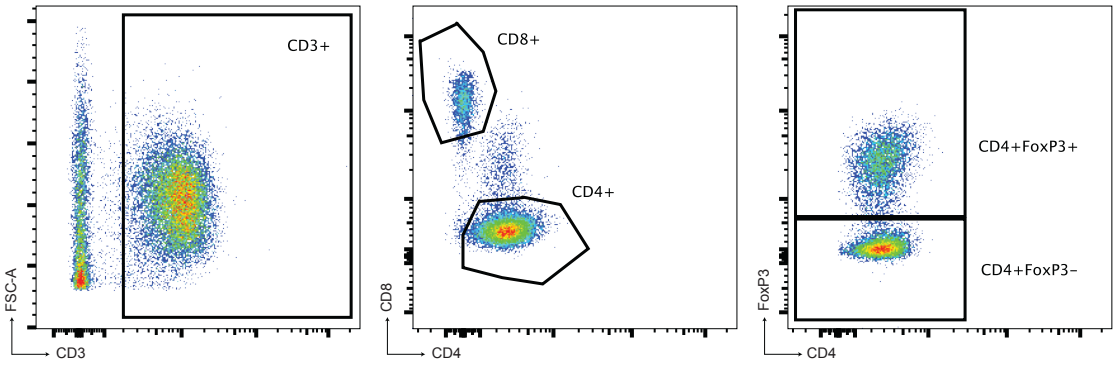

B.

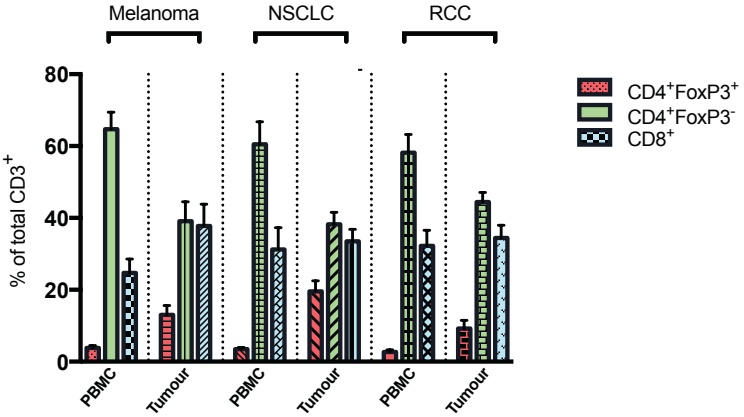

Figure 4: Identification of circulating and tumour-infiltrating T cell subsets in human cancers

Matched peripheral blood mononuclear cells (PBMC) and tumour digests were analysed by multi-parametric flow cytometry. (A) Gating strategy for identification of $CD8^+$ and $CD4+FoxP3^-$ effector T cells (Teff) and $CD4+FoxP3^+$ regulatory T cells (Treg). (B) The relative frequency of T cell subsets in blood (PBMC) and tumour in patients with advanced melanoma (n=8), NSCLC, (n=8) and renal cell carcinoma (n=8).

In tumours, the frequency of $CD4^+FoxP3^-$ T cells was consistently lower than in blood (mean % $CD4^{eff}$ of total $CD3^+$ cells in PBMC: melanoma=64.7%, NSCLC=60.5% and RCC=58.1% vs. tumour: melanoma=39.1%, NSCLC=38.2% and RCC=44.4%). In contrast, the frequency of $CD8^+$ T cells in tumours was either higher or comparable to blood (mean % $CD8^+$ of total $CD3^+$ cells in PBMC: melanoma=24.4%, NSCLC=33.6% and RCC=32.2% vs. tumour: melanoma=38.7%, NSCLC=33.4% and RCC=34.5%). Notably, across all three tumour subtypes, an increase in frequency of tumour-infiltrating Treg was observed relative to blood (mean % Treg of total $CD3^+$ cells in blood: melanoma=3.8%, NSCLC=3.5% and RCC=2.7% vs. tumour:

melanoma=13%, NSCLC=19.6% and RCC=9.2%), suggesting that these cells are enriched in the tumour microenvironment and may represent an attractive target for therapeutic intervention.

3.3 CTLA-4 is expressed at high levels on tumour-infiltrating Treg cells in mouse and man

CTLA-4 has been described to be constitutively expressed on Treg cells (Read et al., 2000, 2006; Wing et al., 2008) and emerging data suggest this may also be relevant to Treg cells infiltrating human tumours (De Simone et al., 2016; Plitas et al., 2016).

Given the relevance of target molecule density to the activity of immune modulatory antibodies in mouse models (Bulliard et al., 2013, 2014; Selby et al., 2013; Simpson et al., 2013), the relative expression of CTLA-4 on circulating and tumour-infiltrating $CD4^{+}FoxP3^{+}$, $CD4^{+}FoxP3^{-}$ and $CD8^{+}$ T lymphocytes was evaluated via multi-parametric flow cytometry. Preliminary analysis of human melanoma demonstrated an expression profile consistent with mouse models (Figure 5)

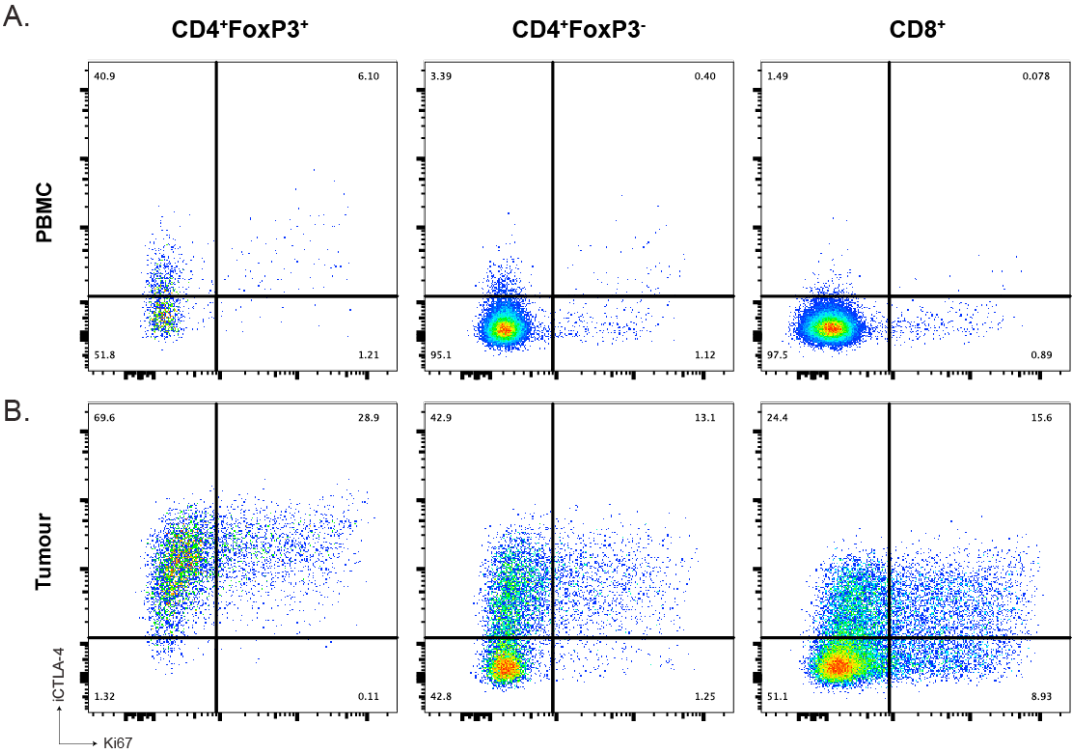

Figure 5: Preliminary analysis of CTLA-4 expression in human melanoma

Intracellular (i) CTLA-4 expression was evaluated on (A) circulating and (B) tumour-infiltrating $CD4^+FoxP3^+$, $CD4^+FoxP3^-$ and $CD8^+$ T cell subsets in patients with advanced melanoma. A representative example is displayed in which CTLA-4 is plotted against Ki67. CTLA-4 appeared upregulated within the tumour microenvironment and expressed at highest levels (based on MFI) in $CD4^+FoxP3^+$ Treg. No consistent relationship between Ki67 and CTLA-4 expression was observed.

Based on these data, analysis of CTLA-4 expression was expanded into multiple murine models of transplantable tumour cell lines of variable immunogenicity including B16 melanoma, CT26 colorectal carcinoma, MCA205 sarcoma, MC38 colonic adenocarcinoma and additional human solid tumour subtypes including early-stage NSCLC and varied stage RCC (Figures 6 and 7).

In mice, CTLA-4 expression was evaluated in tumour-infiltrating lymphocytes (TIL), draining lymph nodes (LN) and PBMCs by flow cytometry 10 days after tumour challenge. In humans, TILs were isolated from resection specimens and PBMCs from peripheral blood sampled at matched time points and

evaluated similarly (Chapter 2.3.1 and 2.4.4, Materials and Methods). Across all studied mouse models, CTLA-4 expression appeared higher in the tumour and was largely restricted to $CD4^+FoxP3^+$ Treg cells (mean expression 68.3%), relative to $CD4^+FoxP3^-$ effector ($CD4^+$eff) T cells (10.2%, $p<0.0001$) and $CD8^+$ T cells (5.4%, $p<0.0001$) (Figure 6A-B). Where CTLA-4 expression was observed in TIL subsets other than Treg cells, this was at significantly lower levels based on mean fluorescent intensity (MFI). Mean MFI of Treg cells 2271.8 relative to $CD4^+$eff cells 498.6 ($p<0.0001$) and $CD8^+$ T cells 701.0 ($p<0.0001$) (Figure 6C).

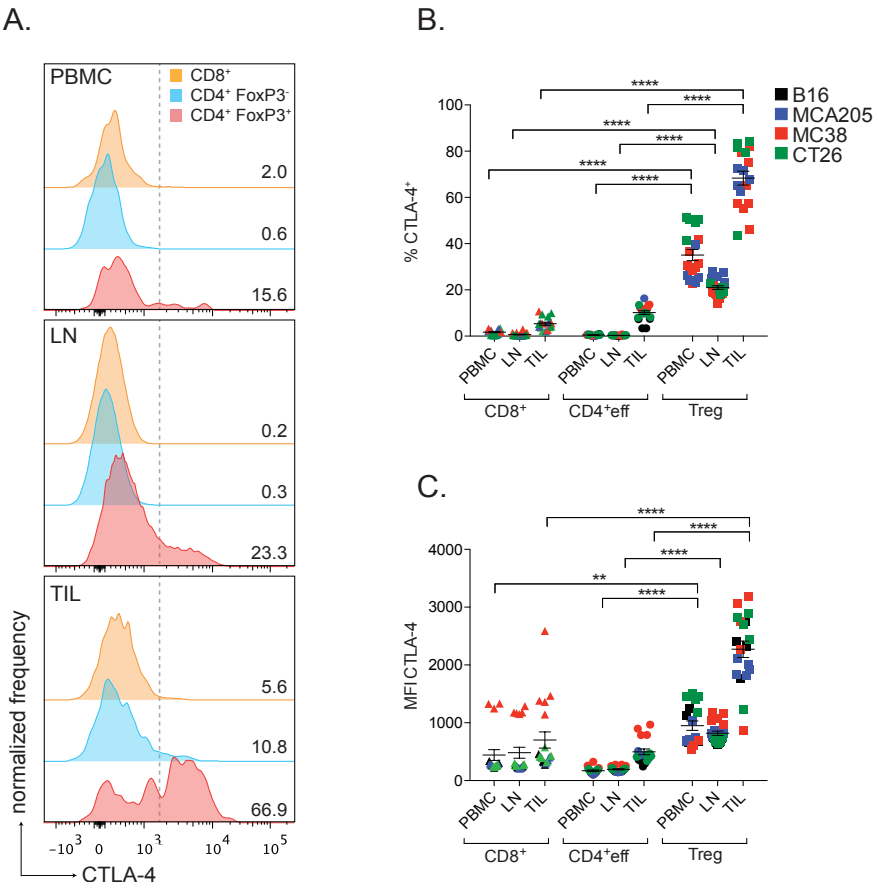

Figure 6: CTLA-4 is highly expressed by tumour-infiltrating Treg cells across multiple mouse models of cancer. (A) Representative histograms of CTLA-4 expression detected by intracellular staining of individual T cell subsets from mice with MCA205 tumours. Grey dotted lines represent the gating, numbers indicate percentage of $CTLA\text{-}4^+$ cells in each subset. (B) Percentage and (C) MFI of CTLA-4-expressing cells in murine tumour models. Data shown

correspond to one of two separate experiments (n=5). Error bars represent standard error of the mean (SEM).

In human tumours, the CTLA-4 expression profile initially observed in melanoma appeared consistent across all evaluated tumour subtypes (Figure 7). Similar to mouse models, higher expression was observed in tumour relative to blood and the expression profile amongst individual T cell subsets was comparable (mean % CTLA-4$^+$ Treg cells=82.1%, relative to CD4$^+$eff T cells=26.5% ($p<0.0001$) and CD8$^+$ T cells=17.4% ($p<0.0001$) (Figure 7A-B). Although CTLA-4 expression was also observed in a proportion of human CD4$^+$eff and CD8$^+$ TILs, this was again at significantly lower levels based on MFI (MFI Treg cells=1349.6, relative to CD4$^+$eff T cells=385.9 ($p<0.0001$) and CD8$^+$ T cells=239.4 ($p<0.0001$) (Figure 7C).

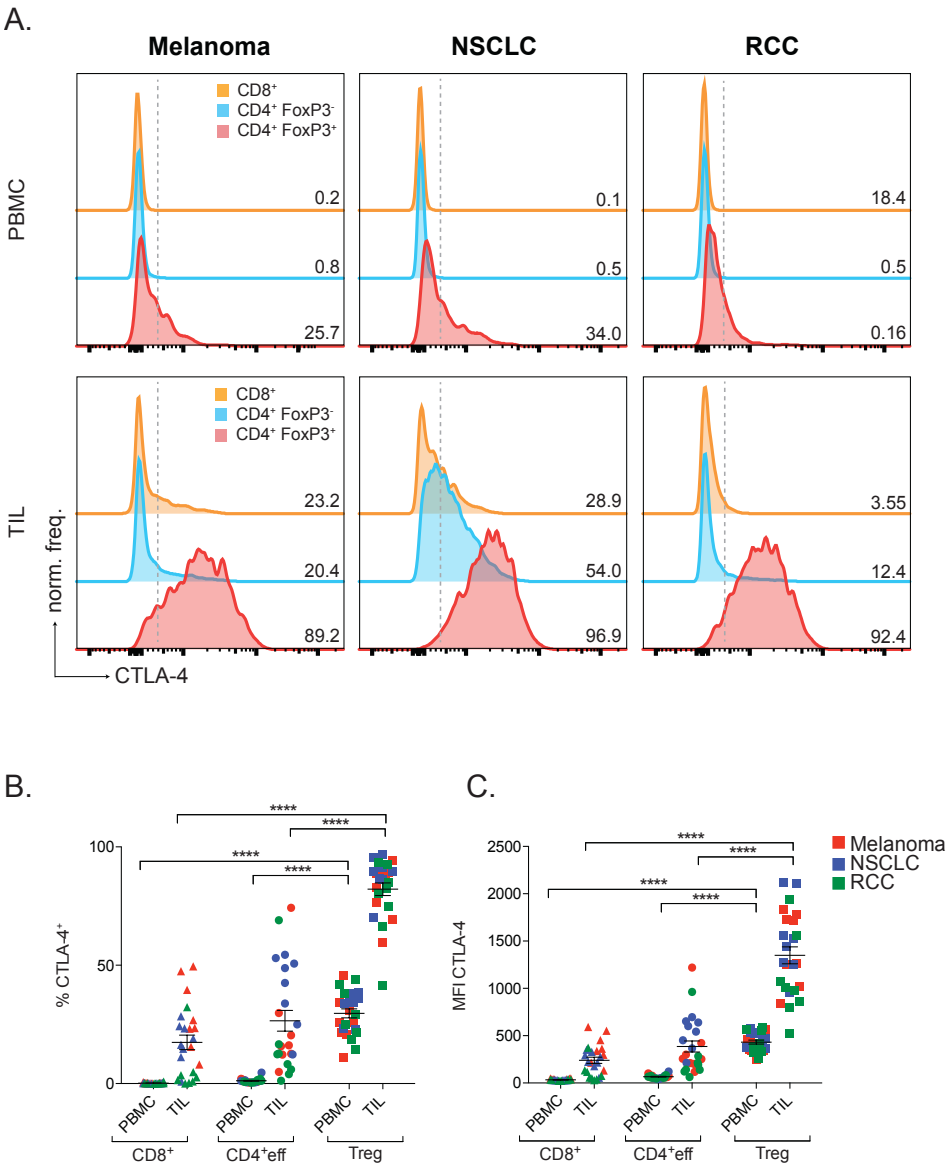

Figure 7: CTLA-4 is highly expressed by tumour-infiltrating Treg cells in human melanoma, NSCLC and RCC (A) Representative histograms of CTLA-4 expression detected by intracellular staining of circulating (PBMC) and tumour-infiltrating (TIL) T cell subsets in a patient with advanced melanoma. Grey dotted lines indicate the gating, numbers indicate percentage of CTLA-4$^+$ cells in each subset. (B) Percentage and (C) MFI of CTLA-4 expression on circulating and tumour-infiltrating T cells in patients with the indicated tumour subtypes. Error bars represent standard error of the mean (SEM).

The observed expression profile of CTLA-4 in human tumours raised the possibility that anti-human CTLA-4 mAbs might impact on the Treg cell compartment in a similar manner to that observed in pre-clinical models. However, convincingly demonstrating ADCC or indeed dynamic changes

amongst individual T cell subsets within the solid tumour microenvironment (relative to blood or bone marrow) is particularly challenging. In attempt to overcome this and more effectively mirror the clinical setting, the potential utility of a mouse model described to effectively recapitulate human FcγR structural and functional diversity was determined through comparison of FcγR expression profiles in this model to human melanoma (Smith et al., 2012).

3.4 FcγR expression in human tumours is recapitulated in a transgenic mouse model bearing human FcγRs

Despite the recognised contributory role of Fc-FcγR interaction to the activity of antibody-based therapies, limited data exists regarding FcγR expression in human tumours (Furness et al., 2014; Grugan et al., 2012). Translation of findings from animal models is complicated by interspecies variation in FcγR subtypes, FcγR expression patterns and affinity to IgG subclasses. Moreover, therapeutic mAbs are most often evaluated in vitro with use of effector cell subsets derived from peripheral blood, on which FcγR expression may not be reflective of the tumour microenvironment.

Analysis of human melanoma metastases including subcutaneous, LN and colonic resection specimens demonstrated consistent FcγR expression profiles on individual cell subsets, but important differences were observed in tumour relative to blood (Figure 8).

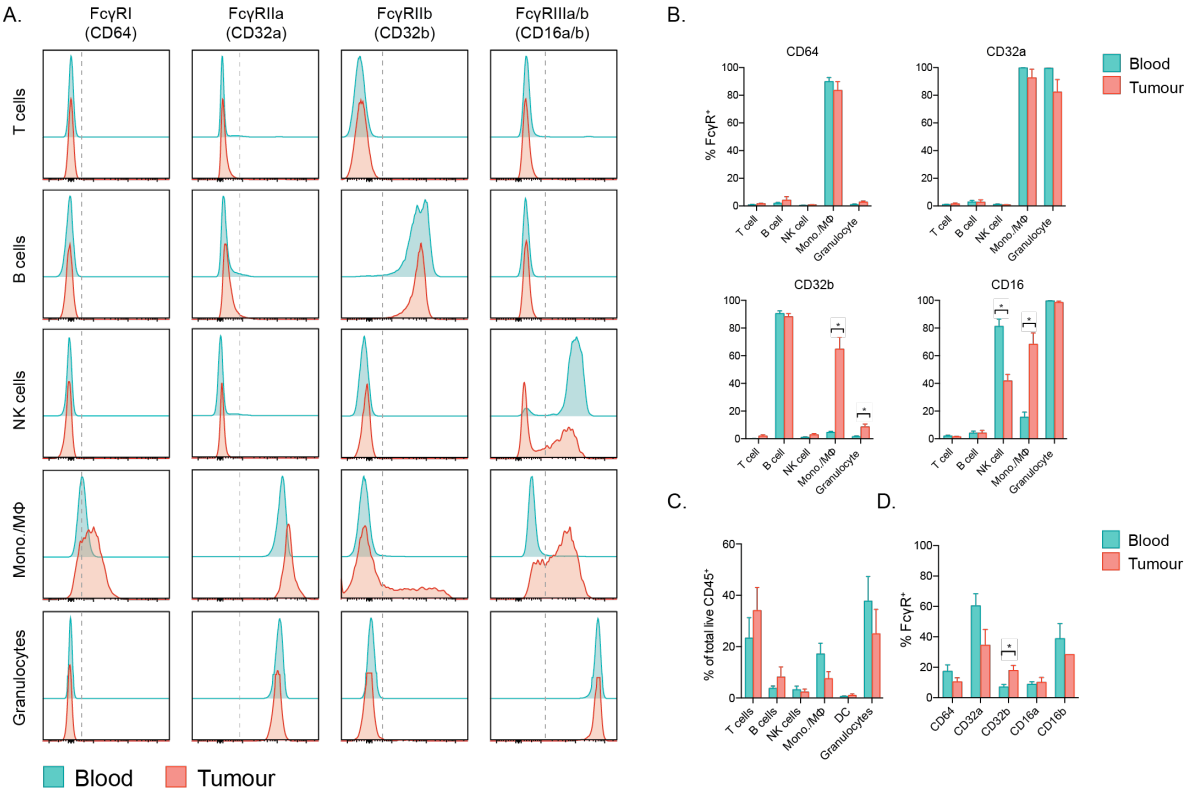

Figure 8: Expression profile of human FcγRs on circulating and tumour-infiltrating cell subsets in advanced melanoma

(A) Representative histograms demonstrating FcγR expression on $CD3^+CD56^-$ T cells, $CD19^+CD3^-$ B cells, $CD56^+CD3^-$ NK cells, $CD11b^+CD14^+HLA\text{-}DR^+$ monocytes/macrophages (Mono./Mϕ) and $CD11b^+CD15^+CD14^-$ granulocytes isolated from human blood (PBMC) and tumour samples. Grey dotted lines indicate gating. (B) Expression profile of FcγRs on leukocyte subsets across cohort of studied melanoma lesions (n=10). C) Frequency of circulating and tumour-infiltrating cell subsets as percentage of total $CD45^+$ cells and (D) expression of individual FcγRs as a percentage of total $CD45^+$ cells. Error bars represent SEM.

FcγR expression on lymphocytes in blood and tumour was confined to $CD19^+CD3^-$ B cells, which expressed the inhibitory receptor CD32b. Activatory FcγR expression was observed on tumour-infiltrating $CD11b^+CD15^+CD14^-$ granulocytes, $CD56^+CD3^-$ NK cells and $CD11b^+CD14^+HLA\text{-}DR^+$ macrophages (MΦ's). Where NK cells were identified, the fraction of $CD16a^+$ cells was consistently lower on tumour-infiltrating subsets (mean % $CD16^+$ in tumour=41.6% vs. blood=81.1%, $p<0.05$) (Figure 8A and B).

Circulating monocytes and tumour-associated MΦ's expressed all three activating FcγRs (CD64, CD32a and CD16a) as well as the inhibitory receptor CD32b. Although FcγR distribution remained similar between circulating monocytes and tumour-associated MΦ's, activating FcγRs CD64, CD32a, CD16a and the inhibitory FcγR CD32b, were consistently expressed at higher levels (based on MFI) on tumour-infiltrating MΦ's (Figure 8A). Further, CD16a and CD32b were consistently expressed by a greater fraction of tumour-associated MΦ's than circulating monocytes (mean fraction of $CD16^+$ tumour-associated MΦ's=68.1% vs. $CD16^+$ circulating monocytes=15.5% ($p < 0.05$), mean fraction $CD32b^+$ tumour-associated MΦ's=64.7% vs. $CD32b^+$ circulating monocytes=4.6% ($p<0.05$)) (Figure 8B).

In contrast, FcγR expression on circulating and tumour-infiltrating granulocytes appeared similar, with constitutive expression of the activatory receptors CD32a and CD16b (Figure 8A and B). NK cells and dendritic cells (DCs) accounted for a very small fraction of $CD45^+$ tumour-infiltrating cell subsets (Figure 8C) (mean % of NK cells=2.26% and DCs=0.95% of total $CD45^+$ cells). Dendritic cells were present at too low a frequency for accurate profiling of FcγRs. Overall, amongst all tumour-infiltrating leukocyte subsets; CD32a was the most abundantly expressed FcγR in human tumours (Figure 8D).

Analysis of cell subsets in draining LNs, tumour and spleen of hFcγR transgenic mice, 10 days after inoculation with MCA205 tumours (Figure 9), demonstrated an expression pattern consistent with previous descriptions (Smith et al., 2012). Expression of activating FcγRI (CD64), IIa (CD32a) and IIIa/b (CD16a/b) was observed on monocytic and granulocytic myeloid cells and a small fraction of natural killer (NK) cells (Figure 9A and B). Expression of the inhibitory FcγRIIb (CD32b) was observed on B cells and myeloid cell subpopulations (Figure 9A and B). Although this expression pattern was maintained on tumour-infiltrating leukocytes, similar to human melanoma, the expression levels of all receptors appeared higher in the tumour relative to LN or spleen, reflected in a higher MFI, particularly on myeloid cells (Figure 9A). Also similar to human tumours, amongst all tumour-infiltrating leukocyte

subsets, CD32a appeared the most abundantly expressed FcγR in murine tumours (Fig. 9C).

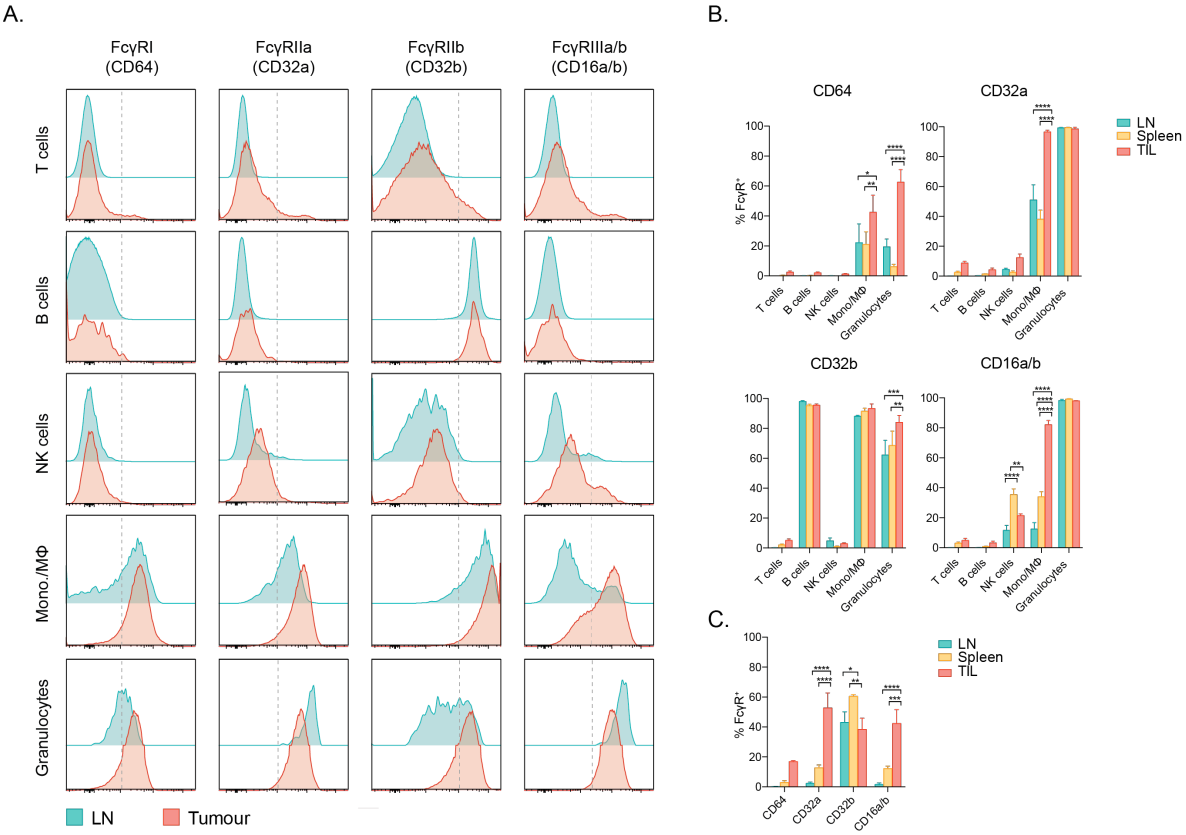

Figure 9: Expression profile of human FcγRs in transgenic mice bearing MCA205 tumours

(A) Representative histograms demonstrating FcγR expression on $CD5^{+}CD19^{-}$ T cells, $CD5^{-}CD19^{+}$ B cells, $CD5^{-}NK1.1^{+}$ NK cells, $CD11b^{+}NK1.1^{-}Ly6G^{+}SSC^{low}$ monocyte/macrophages (Mono./Mϕ) and $CD11b^{+}Ly6G^{+}$ granulocytes isolated from LN and tumour in hFcγR mice. Grey dotted lines indicate gating. (B) Expression of individual hFcγRs on leukocyte subsets in LN, spleen and TILs in hFcγR mice (n=5) and (C) Expression of individual hFcγRs in human FcγR mice as a percentage of total live cells. Error bars represent SEM.

Intra-tumoural FcγR expression profiles were largely comparable between MCA205 tumours in hFcγR mice and human melanoma. However, expression of the inhibitory CD32b in mouse LN and spleen varied relative to blood in human melanoma. In the mouse model, in addition to circulating B cells, this appeared highly expressed on myeloid cells, whereas in humans expression in blood was largely confined to B cells. This could result in a less favourable A:I FcγR ratio in secondary lymphoid organs in the mouse model relative to

human blood and tumours, thus a lack of ADCC activity in these organ sites might not necessarily be reflective of the periphery (blood) in humans.

Based on the comparable expression profile of CTLA-4 on T lymphocytes and FcγRs on tumour-infiltrating innate effector cell subsets in human melanoma and hFcγR mice, the ability of anti-CTLA-4 antibodies of a human isotype to promote depletion of intra-tumoural Treg cells in a similar manner to that mediated by murine FcγRs was determined (Bulliard et al., 2013; Selby et al., 2013; Simpson et al., 2013).

3.5 Human IgG1 and IgG2 anti-CTLA-4 antibodies efficiently deplete CTLA-4-expressing target cells in vitro

Chimeric anti-murine CTLA-4 (mCTLA-4) antibodies (based on clone 4F10) with the human IgG variants employed in ipilimumab (IgG1) and tremelimumab (IgG2) were constructed (performed by Fred Arce-Vargas) and their activity compared to mutated IgG1 isotypes with either enhanced binding affinity to activatory CD16a ($IgG1_{SDALIE}$) or no binding to hFcγRs ($IgG1_{N297A}$).

The capacity of individual mAbs to deplete murine CTLA-4-expressing target cells was first assessed in vitro. In attempt to recapitulate the tumour microenvironment, monocyte-derived human macrophages with an FcγR expression profile reflective of tumour-associated macrophages, were used as effector cells at varying effector to target (E:T) cell ratios (Figure 10A). In keeping with predicted binding affinity for FcγRs (Figure 10B), IgG1 and IgG2 mAbs demonstrated superior ADCC activity relative to $IgG1_{N297A}$. However, the $IgG1_{SDALIE}$ mAb promoted enhanced ADCC activity relative to all evaluated isoforms at E:T ratios of 2.5:1 and above (Figure 10C).

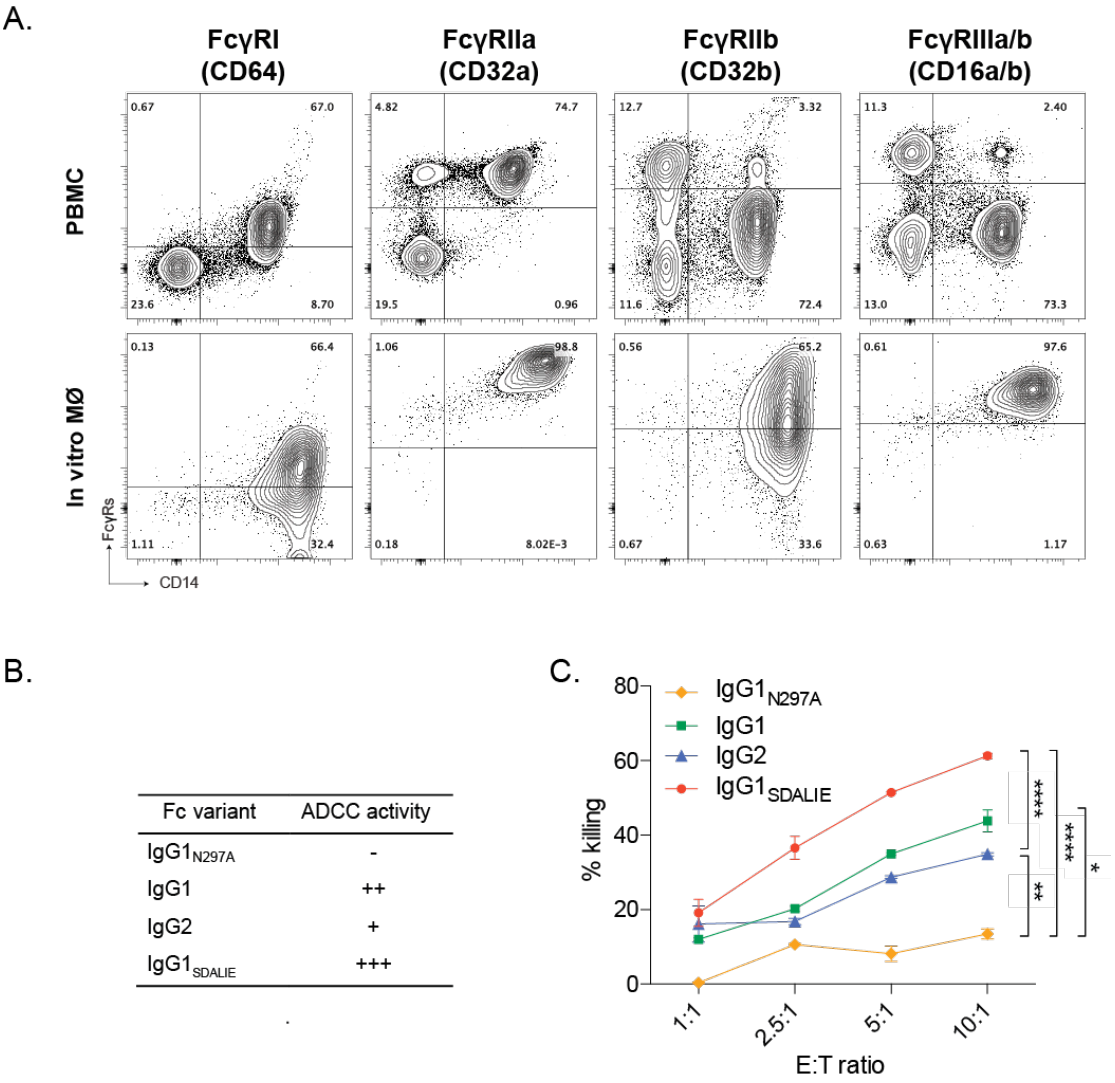

Figure 10: Anti-murine CTLA-4 antibodies of hIgG1 and hIgG2 isotype mediate depletion of mCTLA-4-expressing target cells in vitro (A) FcγR expression on $CD45^{+}CD14^{+}$ subsets in peripheral blood (upper panel) and on the same donor cells following 7 days of in-vitro differentiation with human recombinant M-CSF (lower panel). (B) Predicted ADCC activity of human IgG Fc variants. (C) In-vitro killing of mCTLA-4-expressing target cells by human monocyte-derived macrophages at varied effector/target (E:T) ratios, in the presence of anti-mCTLA-4 human IgG Fc variants.

3.6 Human IgG1 and IgG2 anti-murine CTLA-4 antibodies efficiently deplete intra-tumoural Treg cells in vivo

The impact of chimeric anti-mCTLA-4 hIgG variants was thereafter determined in vivo with use of hFcγR mice. Mice were treated with human anti-mCTLA-4 on days 7 and 9 after subcutaneous inoculation with MCA205

tumours. On day 11, the frequency of T cell subpopulations was analysed in tumour, draining LNs and blood (Figure 11).

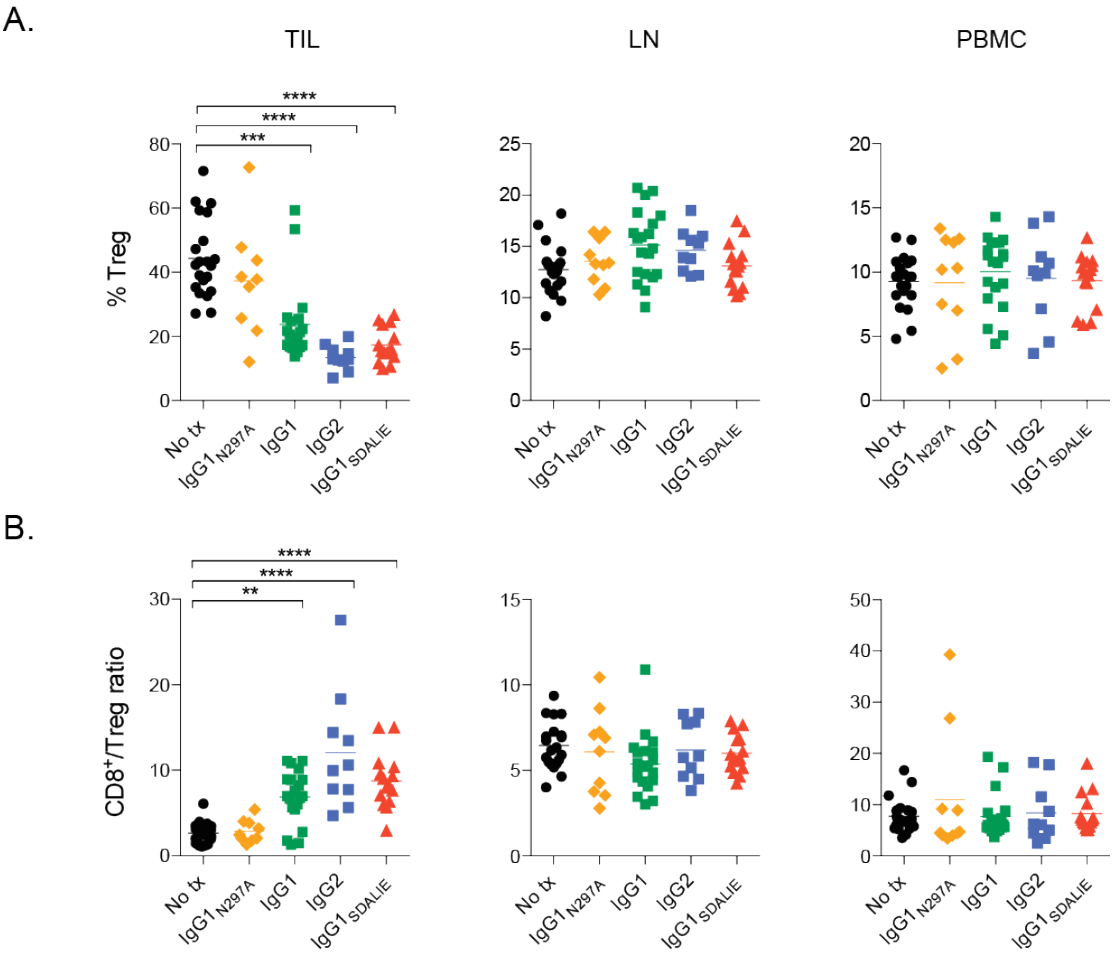

Figure 11: Anti-murine CTLA-4 antibodies of hIgG1 and hIgG2 isotype mediate depletion of intra-tumoural Treg cells in vivo

Mice were treated with 200µg of anti-CTLA-4 mAb on days 6 and 9 after s.c. inoculation with MCA205 tumour cells (n=9-21). TILs, LNs and PBMCs were processed on day 11 and stained for flow cytometry analysis. (A) Percentage of $FoxP3^+CD4^+$ Treg cells of total $CD4^+$ T cells in TIL, LN and PBMC compartments and (B) $CD8^+$/Treg cell ratio in the indicated anatomical sites.

Consistent with in vitro data, there was a reduction in the proportion of tumour-infiltrating Treg cells in mice treated with the IgG1 mAb (mean percentage of Treg cells of total $CD4^+$ T cells 24%) compared to those treated with the $IgG1_{N297A}$ variant (37%) or to control mice (44%, $p<0.001$). The depleting activity of the $IgG1_{SDALIE}$ isotype appeared superior to the wild-type

IgG1 mAb (mean percentage of Treg cells of total $CD4^+$ T cells 17% vs. 24%, respectively), but this did not meet statistical significance. An unexpected finding was the observation of efficient IgG2-mediated depletion of tumour-infiltrating Treg cells in vivo (13% of total $CD4^+$ T cells). The IgG2 isotype is often described as a poor mediator of ADCC since it only binds to activatory CD32a (Schneider-Merck et al., 2010). However, given the abundance of CD32a in the tumour microenvironment, this bears potential relevance to the mechanism of action of tremelimumab and other therapeutic human IgG2 mAbs.

As previously described in wild-type mice (Simpson et al., 2013), the depleting activity of all human IgG antibody variants in this new model was restricted to the tumour microenvironment, a consequence of the density of target molecule expression, with no impact on Treg cells in LNs or blood in hFcγR mice (Figure 11A). As a result, anti-CTLA-4 mAb of human IgG1, $IgG1_{SDALIE}$, IgG2 but not $IgG1_{N297A}$ isotypes, led to a selective increase in the intra-tumoural ratio of $CD8^+$ to Treg cells (Figure 11B). This was only observed within the tumour microenvironment demonstrating that in the context of human FcγR-IgG interactions in vivo, depletion of tumour-infiltrating Treg cells is a major contributor to the shift in this ratio, which has previously been associated with therapeutic responses in mouse and man (Hodi et al., 2008; Quezada et al., 2006).

In summary, using a model that allows evaluation of human FcγR-IgG interactions in vivo, this data supports a unifying hypothesis in which both of the anti-CTLA-4 mAbs employed in the clinic (ipilimumab, IgG1 and tremelimumab, IgG2) are likely to promote preferential depletion of tumour-infiltrating Treg cells and increase the intra-tumoural ratio of Teff to Treg cells. Further, these data also suggest that high intra-tumoural expression of CD32b may impact on the ADCC activity of human IgG1 anti-CTLA-4 mAbs and this may be overcome, at least in part, by engineering of the constant region of the antibody to optimise the A:I FcγR binding ratio.

3.7 Anti-CTLA-4-mediated intra-tumoural Treg cell depletion underlies tumour response and influences long-term survival

In order to determine the impact of intra-tumoural Treg cell depletion on anti-tumour activity and survival, hFcγR mice were challenged with subcutaneous MCA205 tumours on day 0 and treated with 50μg of chimeric anti-mCTLA-4 mAb IgG variants on days 6, 9 and 12 (Figure 12A).

Tumour growth was equivalent in untreated mice and those treated with the Fc-silent $IgG1_{N297A}$ anti-mCTLA-4 mAb, demonstrating that CTLA-4 blockade alone is insufficient to promote tumour rejection in the context of human FcγR-IgG interactions (Figure 12B). In contrast, the majority of mice treated with either IgG1 or IgG2 anti-CTLA-4 mAb rejected tumours completely (66.67% and 80%, respectively). $IgG1_{SDALIE}$ anti-CTLA-4 mAb, with enhanced affinity for activating FcγRs, resulted in eradication of established tumours in all treated mice, although there was no statistical significance compared to IgG1 and IgG2 mAbs (Figure 12B). Importantly, responses appeared durable, with responding mice from all treatment groups alive for more than 80 days (Figure 12C). These data suggest that in a mouse system that models human FcγR-IgG interactions in vivo, anti-CTLA-4 mAbs with enhanced capacity to deplete Treg cells have a favourable impact on tumour response and survival.

A.

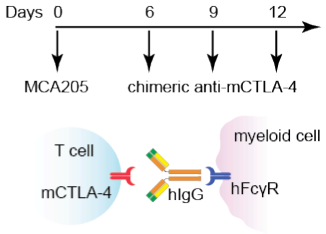

B.

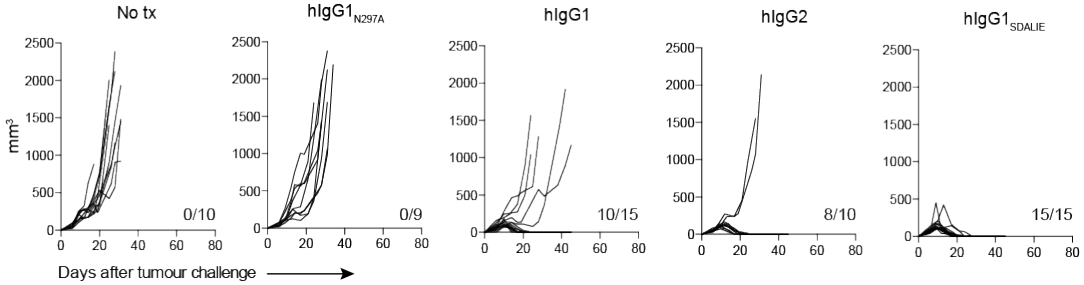

C.

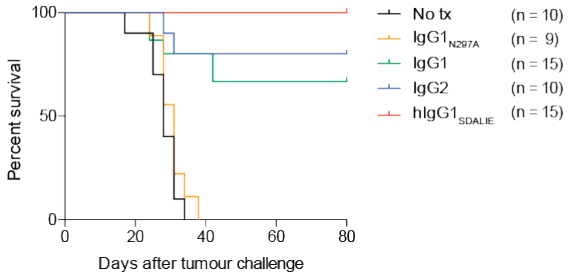

Figure 12: Anti-CTLA-4-mediated intra-tumoural Treg cell depletion is required for tumour response and long term survival

Human FcγR mice were treated with 50µg of anti-CTLA-4 on days 6, 9 and 12 after s.c. inoculation of MCA205 tumour cells. (A) Diagrammatic representation of the experimental protocol. (B) Tumour growth in individual hFcγR mice with each treatment. The tumour volume was calculated as the product of three orthogonal diameters. Numbers represent the proportion of mice with complete long-term tumour rejection. (C) Kaplan-Meier curve of accumulated data from mice in (B) (log rank $p<0.0001$). Cumulative data of two separate experiments for each condition.

3.8 Human FcγR polymorphisms impact upon response to ipilimumab in patients with advanced melanoma

Determining the relevance of Treg cell depletion to the activity of anti-CTLA-4 antibodies in the clinical setting has proved challenging. In humans, the strongest evidence for a role of FcγR-mediated effector function in tumour-targeting antibody-based cancer therapies (e.g. Trastuzumab) derives from clinical studies demonstrating an association between clinical responses and specific alloforms of activating FcγRs inferring higher binding affinity to IgG1, particularly the CD16a-V158F and CD32a-H131R single nucleotide polymorphisms (SNPs) (Cartron et al., 2002; Musolino et al., 2008; Weng and Levy, 2003; Zhang et al., 2007). However, no association between FcγR polymorphisms and clinical outcome has yet been described in the context of anti-CTLA-4 or other immune checkpoint modulators.

Mutational burden and putative neoantigen burden have been demonstrated to influence response to ipilimumab in patients with advanced melanoma (Nathanson et al., 2016; Snyder et al., 2014; Van Allen et al., 2015). These data point to mutations as a potential substrate for tumour recognition by the T cell compartment. Given the biological relevance of CTLA-4 in the context of T cell receptor engagement (Leach et al., 1996), the impact of FcγR polymorphism status, obtained from sequencing of germline DNA, on response to ipilimumab was determined in the same cohort of patients, with a working hypothesis that response would be associated with higher mutational or putative neoantigen burden (i.e. a substrate T cell response that could be amplified by ipilimumab) and the presence of the CD16a-V158F SNP (since ipilimumab is an IgG1 antibody).

In patients with low mutational or low predicted neoantigen burden (defined as below the median of the cohort) (Figure 13A and B), neither CD32a-H131R nor CD16a-V158F SNPs impacted on outcome. Further, amongst patients with high mutational or high predicted neoantigen burden (defined as above the median of the cohort), the CD32a-H131 SNP had no additional impact on outcome. However, as predicted based on the binding affinity of ipilimumab (IgG1) for CD16a, the CD16a-V158F SNP was enriched in patients with high

mutational (Figure 13A) or high predicted neoantigen burden (Figure 13B) deriving benefit from ipilimumab. Combination of these two metrics appeared to better identify long-term responders than considering mutational or predicted neoantigen burden alone.

A.

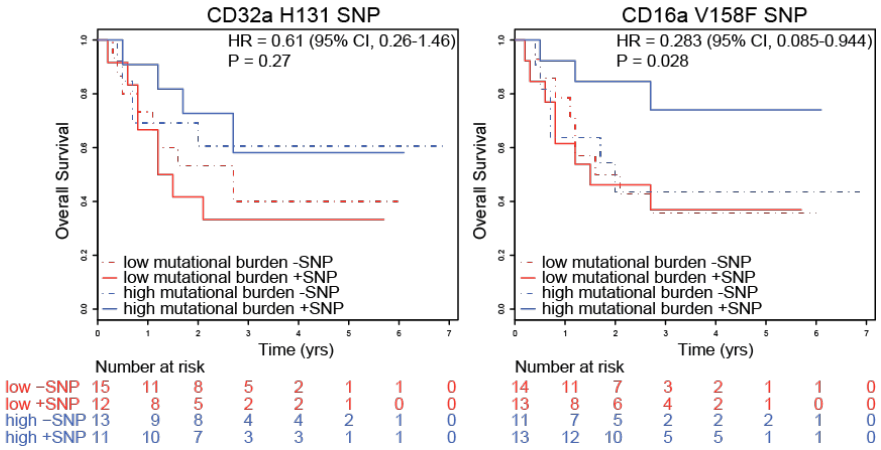

B.

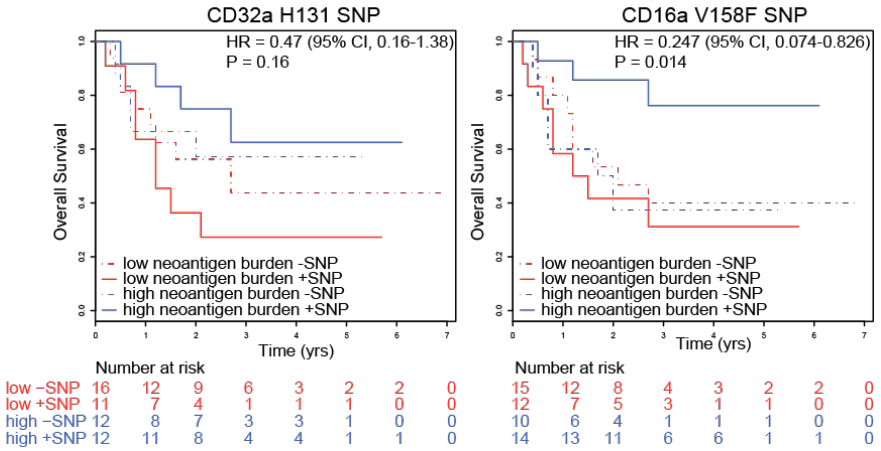

Figure 13: Human FcγR polymorphisms impact upon response to ipilimumab in patients with advanced melanoma

Overall survival analysis of patients with advanced melanoma treated with ipilimumab with (A) low mutational burden (below the median of the cohort) or high mutational burden (above the median of the cohort) and (B) low predicted neoantigen burden (below the median of the cohort) or high predicted neoantigen burden (above the median of the cohort) with or without germline CD32a-H131R or CD16a-V158F polymorphisms. (Key (lower left) in each plot depicts mutational or predicted neoantigen burden and polymorphism status. Log rank p values are displayed in individual plots. HR, hazard ratio; CI, confidence interval.

Pembrolizumab is an IgG4 mAb directed against PD-1, with low predicted binding affinity to hFcγRs and consequent ADCC activity. In pre-clinical studies, anti-PD-1 mAbs were demonstrated to be FcγR independent in vivo, the presence of FcγR binding capacity was observed to compromise anti-tumour activity (Dahan et al., 2015). In attempt to confirm this in human dataset, tumour exomes derived from of a cohort of patients with advanced non-small cell lung cancer treated with pembrolizumab were analysed (Figure 14) (Rizvi et al., 2015).

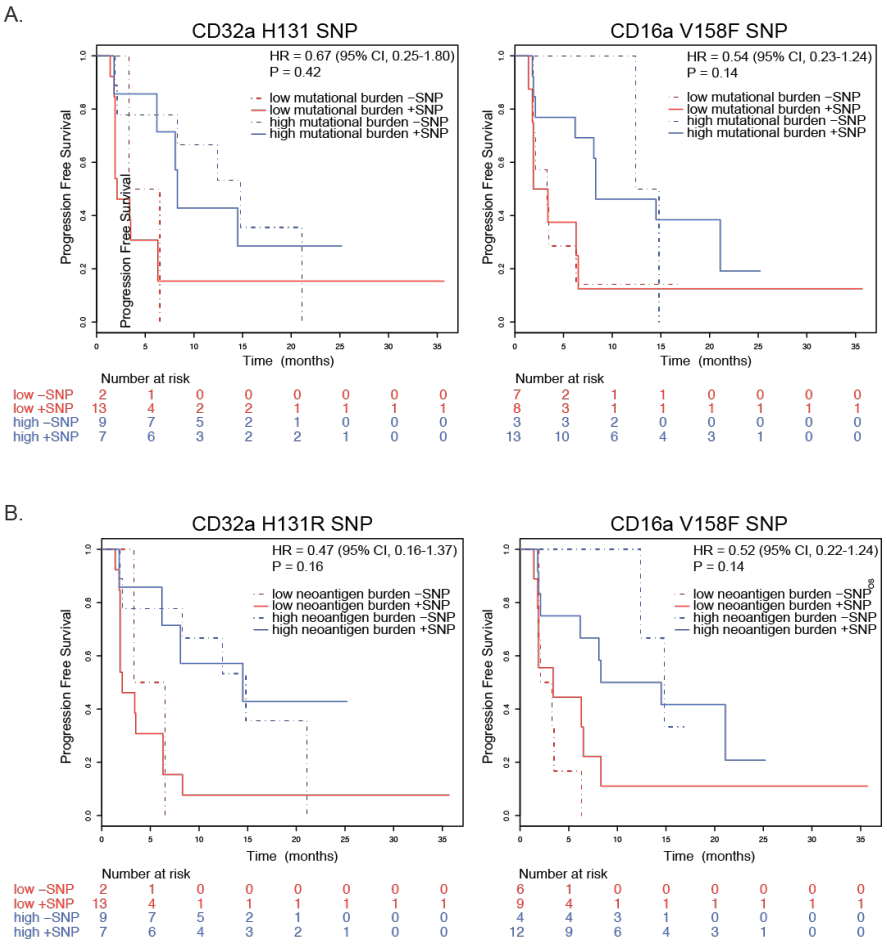

Figure 14: Human FcγR polymorphisms impact negatively upon response to pembrolizumab in patients with advanced NSCLC

Progression free survival (PFS) analysis of patients with NSCLC treated with pembrolizumab with (A) low mutational burden (below the median) or high mutational burden (above the median) and (B) low predicted neoantigen burden (below the median) or high predicted neoantigen burden (above the median) with or without the germline polymorphisms CD32a-H131R or CD16a-V158F. Log rank p values are displayed in individual plots. HR, hazard ratio; CI, confidence interval.

Within this cohort, FcγR polymorphism status was not associated with any additional benefit in progression free survival (PFS) in patients with high mutational burden (above the median of the cohort) (Figure 14A) or high predicted neoantigen burden (above the median of the cohort) (Figure 14B), supporting 'blockade' as the primary mechanism of activity of this mAb.

However, although overall numbers were small, consistent with pre-clinical data and the reported influence of the CD16a-V158F on FcγR binding to IgG4 (Koene et al., 1997), the presence of high mutational or neoantigen burden plus the CD16a-V158F SNP appeared to impact negatively on PFS, relative to those with high mutational or neoantigen burden and wild type for CD16, although this did not meet significance.

3.9 Discussion and Conclusions

Pre-clinical studies in mouse models of cancer have demonstrated that the activity of certain immune modulatory antibodies may extend beyond receptor stimulation or blockade of Teff cells, relying upon concomitant depletion of Treg cells for maximal anti-tumour activity (Bulliard et al., 2013, 2014; Selby et al., 2013; Simpson et al., 2013). Preferential depletion of tumour-infiltrating Treg cells by antibodies targeting CTLA-4, GITR and OX40 depends upon both a higher density of the target molecule on intra-tumoural Treg cells compared to Teff cells and the presence of an appropriate population of effector cells to mediate ADCC. Despite the growing body of evidence supporting the premise that immune modulatory antibodies can bear dual (immune modulatory and Treg cell depleting) activity, less evidence exists to support that this mechanism of action is as important in the clinical context.

In attempt bridge this translational gap, hFcγR mice and chimeric anti-mCTLA-4 mAbs with human IgG variants were used to model the rules of engagement for human FcγRs and human IgGs in the context of immune modulatory mAbs, demonstrating that anti-human CTLA-4 mAbs work, at least in part, through depletion of tumour-infiltrating Treg cells. Anti-CTLA-4 mAbs with the same Fc variants as ipilimumab (IgG1) and tremelimumab (IgG2) both induced in vivo depletion of tumour-infiltrating Treg cells in the

context of human FcγRs. Antibodies engineered to enhance this activity displayed improved anti-tumour activity, whilst those engineered to lack ADCC capacity demonstrated poor anti-tumour activity. The high expression of CTLA-4 in tumour-infiltrating Treg cells and the presence of innate effector cells expressing high levels of CD16 and CD32a activatory FcγRs both in mouse and man likely explain the preferential local depletion in the tumour by both antibody isotypes.

These findings are further supported by the demonstration of an association between the germline CD16a-V158F polymorphism and improved survival in patients with advanced melanoma and high mutational or predicted neoantigen burden treated with ipilimumab. The requirement for high mutational/neoantigen burden raises the possibility that ADCC activity may only be relevant in the context of an inflamed tumour microenvironment. This is consistent with previous reports and may explain the modest response rates observed in the clinic relative to pre-clinical models (Hodi et al., 2010; Ji et al., 2012; Ribas et al., 2013; Robert et al., 2011).

Whilst the extent of the contribution of ADCC to the activity of ipilimumab and tremelimumab has not been formally tested, the presented data suggest that it is potentially highly relevant, and that further enhancement of ADCC may improve anti-tumour activity and survival. Where ADCC activity is desirable, the IgG1 isotype is most commonly selected owing to its predicted binding affinity for activating FcγRs. However, the intra-tumoural composition of FcγR-expressing cell subsets is rarely considered, both in terms of the expression of individual FcγRs and their relative abundance. In both murine and human tumours the activatory FcγR CD16a and the inhibitory receptor CD32b appeared upregulated on tumour-associated macrophages relative to LN and blood. In keeping with this, $IgG1_{SDALIE}$ mAb, with an optimised A:I (CD16:CD32b) binding profile (Lazar et al., 2006), demonstrated superior anti-tumour activity relative to all evaluated chimeric anti-CTLA-4 Fc variants. Although not meeting significance, this is likely to be the result of the improved efficacy of intra-tumoural Treg cell depletion observed for $IgG1_{SDALIE}$ relative to wild type IgG1.

In contrast to the IgG1 isotype, IgG2 is generally regarded as a poor mediator of ADCC owing to its relatively low affinity for activatory FcγRs, particularly CD16 (Bruhns et al., 2009). However, the Fc effector functions of IgG2 are mediated by CD32a, and in vitro data demonstrate that IgG2 mAbs mediate effective ADCC via CD32a-expressing mononuclear and PMN cells (Schneider-Merck et al., 2010). In further support of these findings, chimeric anti-mCTLA-4 IgG2 mAb were observed to deplete intra-tumoural Treg cells in vivo with similar efficacy to IgG1 mAb. These results may be explained by the relative abundance of CD32a-expressing tumour-infiltrating myeloid cells, observed both in murine tumours and human melanoma samples. Further, the binding of IgG2 to inhibitory CD32b is minimal, resulting in a high A:I (CD32a:CD32b) ratio that favours Fc effector functions. These results raise the possibility that Treg depletion is also involved in the mechanism of action of tremelimumab and that polymorphisms might also contribute to its activity, since the CD32a-H131R polymorphism confers high binding affinity to IgG2 (Bruhns et al., 2009; Sanders et al., 1995; Schneider-Merck et al., 2010).

Target molecule density, antibody isotype and the intra-tumoural composition of FcγR-expressing cell subsets must all be considered in the design of immune modulatory mAbs. Optimal intra-tumoural ADCC activity may depend on CD16a or CD32a binding, according to which innate effector cells are enriched within the tumour microenvironment. Prospective clinical studies should consider exploring the use of polymorphism status and mutational burden to better identify those patients likely to respond to immune modulatory antibodies armed with dual activity.

4 Results 2: CD25 as a selective target for regulatory T cells

4.1 Introduction

Based on the observed determinants of the in vivo activity of anti-CTLA-4 mAbs, candidate target molecules require comprehensive profiling in order to more accurately inform the design of next generation of immune modulatory antibodies optimised appropriately for agonistic, blocking or depleting activity. Mapping the expression of co-inhibitory and co-stimulatory molecules formed an initial second objective of this thesis. However, whilst this identified a number of additional target molecules suitable for immune modulation, these data also highlighted significant overlap in the expression of target molecules between T lymphocyte subsets, prompting a search for more selective targets restricted to individual T cell subsets. Flow-based screening of candidate molecules identified CD25 as a more restricted target to Treg cells and prompted further evaluation of the in vivo activity of anti-CD25 mAbs in mouse models of cancer and validation of CD25 as a therapeutic target in human cancers.

Specific objectives were to:

(i) Map the expression of co-inhibitory and co-stimulatory immune checkpoint molecules in mouse models and human cancers

(ii) Re-evaluate CD25 as a selective target for Treg cells

(iii) Determine the in vivo activity of anti-CD25 mAbs

(iv) Validate CD25 as a therapeutic target in human cancers

In vivo mouse work was performed by Fred Arce Vargas. Ex vivo work was performed together with Andrew Furness. Study of human samples was performed independently by Andrew Furness. Surface plasmon resonance analyses were performed by the Ravetch laboratory.

4.2 Distinct expression profiles of co-inhibitory and co-stimulatory immune checkpoint molecules in mouse models and human cancers

Beyond CTLA-4 and PD-1, multiple co-inhibitory and co-stimulatory immune checkpoint molecules are expressed on TILs and represent potential targets for immune modulation with antibody-based therapies. Flow cytometry analysis of single cell suspensions generated from murine (subcutaneous B16, CT26, MCA205 and MC38) and human (melanoma, NSCLC and RCC) tumours demonstrated significant heterogeneity in expression profiles between tumour subtypes, particularly in molecules typically described on effector T cells, including 4-1BB, PD-1 and TIM-3 (Figure 15A). The percentage of cells expressing these molecules appeared higher amongst $CD8^+$ T cells in the more immunogenic MCA205, MC38 and CT26 mouse tumours relative to the poorly immunogenic mouse B16 melanoma and also higher in human melanoma relative to NSCLC and RCC, possibly related to the immunogenic burden of somatic mutations typically associated with these tumour subtypes (Alexandrov et al., 2013).

Despite this, a number of potentially exploitable patterns were observed. Similar to CTLA-4, the co-stimulatory receptors GITR, ICOS and OX40 were consistently expressed on tumour-infiltrating Treg cells in mouse and human tumours. Although expression of these molecules was also observed on $CD4^+FoxP3^-$ and $CD8^+$ T cell subsets, the level of expression, based on MFI, was significantly lower than on the Treg cell compartment (Figure 15B). Thus GITR, ICOS and OX40 appeared attractive targets in all three human tumour subtypes for dual activity antibodies with capacity for ADCC of intra-tumoural Treg cells. These findings are consistent with pre-clinical mouse studies, in which depleting isotypes of anti-GITR and anti-OX40 demonstrated maximal anti-tumour activity in vivo, associated with their ability to enhance effector function whilst simultaneously depleting tumour-infiltrating Treg cells (Bulliard et al., 2014; Coe et al., 2010).

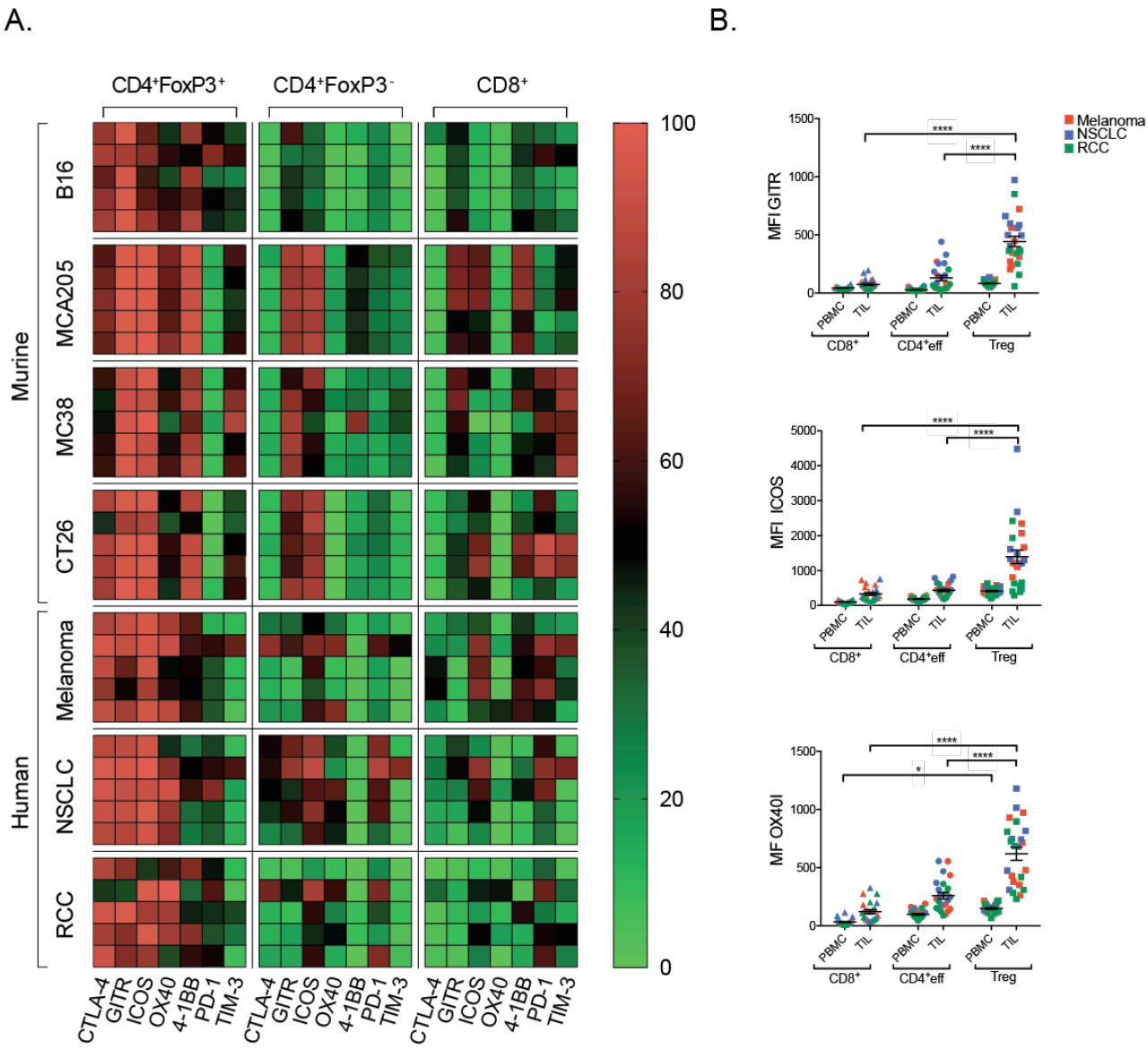

Figure 15: Expression of co-inhibitory and co-stimulatory immune checkpoint molecules on tumour-infiltrating T cell subsets in mouse models and human cancers

(A) Heatmap demonstrating the relative expression of co-inhibitory and co-stimulatory molecules quantified by flow cytometry based on the percentage of positive cells within the indicated T cell subsets in murine and human tumour subtypes. Data derived from 5 representative mice and human tumours of each subtype. (B) MFI of the indicated co-inhibitory and co-stimulatory molecules in blood (PBMC) and tumour (TIL) in patients with human melanoma, NSCLC and RCC. Error bars represent SEM.

4.3 Towards more selective targeting of T cell subsets

Whilst maximal anti-tumour activity may be achieved through optimisation of immune modulatory mAbs displaying dual activity, toxicity is of major concern to treating clinicians, particularly as combination strategies are increasingly employed (Sharma and Allison, 2015). It therefore becomes equally important to develop agents with reproducible, selective activity against individual T cell subsets. However, this first requires identification of candidate target molecules that consistently display a more restricted expression profile amongst T cell subsets.

In order to identify therapeutic targets that might allow more selective depletion of Treg cells, the expression profile of molecules previously demonstrated to be expressed at high levels on Treg cells, as well as targets largely abandoned in the therapeutic setting (e.g. CD25) were re-visited (Figure 16).

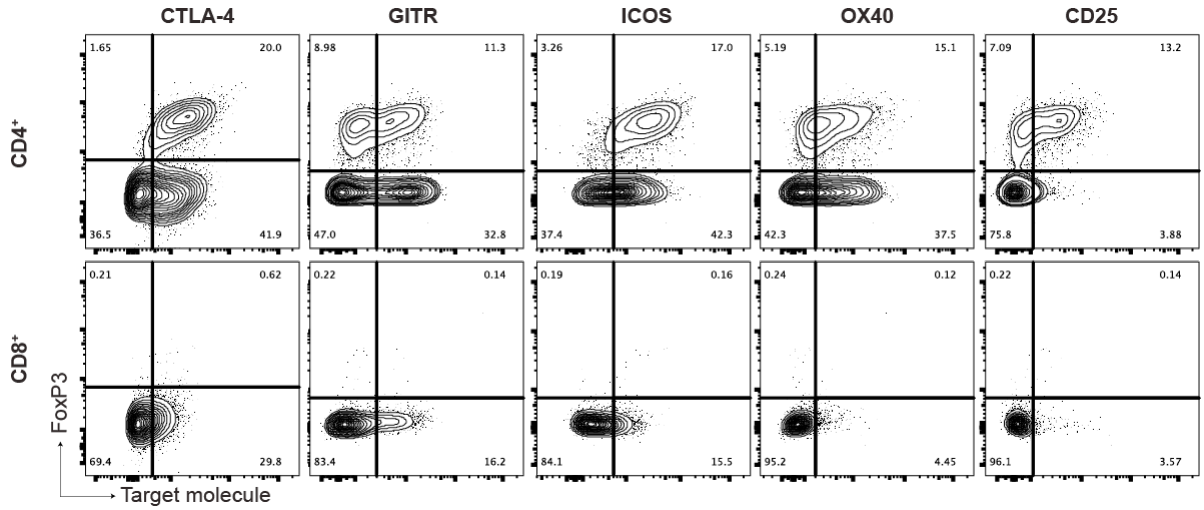

Figure 16: Flow-based screening of candidate molecules for selective targeting of Treg cells Tumour-infiltrating T cell subsets were analysed by multi-parametric flow cytometry. Following identification of live, $CD3^+CD4^+$ (upper panel) or $CD3^+CD8^+$ (lower panel) subsets, FoxP3 (y axis) was plotted against candidate target molecules (x axis) as annotated above each plot. A representative example from a primary NSCLC tumour is displayed. Percentages are displayed in each quadrant gate.

Although CTLA-4, GITR, ICOS and OX40 were expressed at high levels (based on MFI) on tumour-infiltrating $CD4^+FoxP3^+$ Treg cells, a significant fraction of $CD4^+FoxP3^-$ effectors and to a lesser extent $CD8^+$ T cells also expressed these molecules. The concern in this context is not potential elimination of $CD4^+FoxP3^-$ or $CD8^+$ cell subsets expressing relevant target molecules, since preferential depletion of only the highest expressers has been demonstrated in vivo (Simpson et al., 2013). Rather, that mAb-induced enhancement of effector function might precipitate off target toxicity. In contrast, CD25 expression was observed to be largely restricted to $CD4^+FoxP3^+$ Treg cells on which it was expressed at highest levels. CD25 therefore appeared a promising therapeutic target to take forward for more comprehensive evaluation.

4.4 CD25 expression profiles in mouse models and human cancers validate its use as a target for therapeutic Treg cell depletion

To validate the potential translational value of CD25 as a selective target for Treg cell depletion, the expression of CD25 on PBMCs and TILs in a larger cohort of patients with advanced melanoma, early-stage NSCLC and RCC was evaluated by flow cytometry (Figure 17).

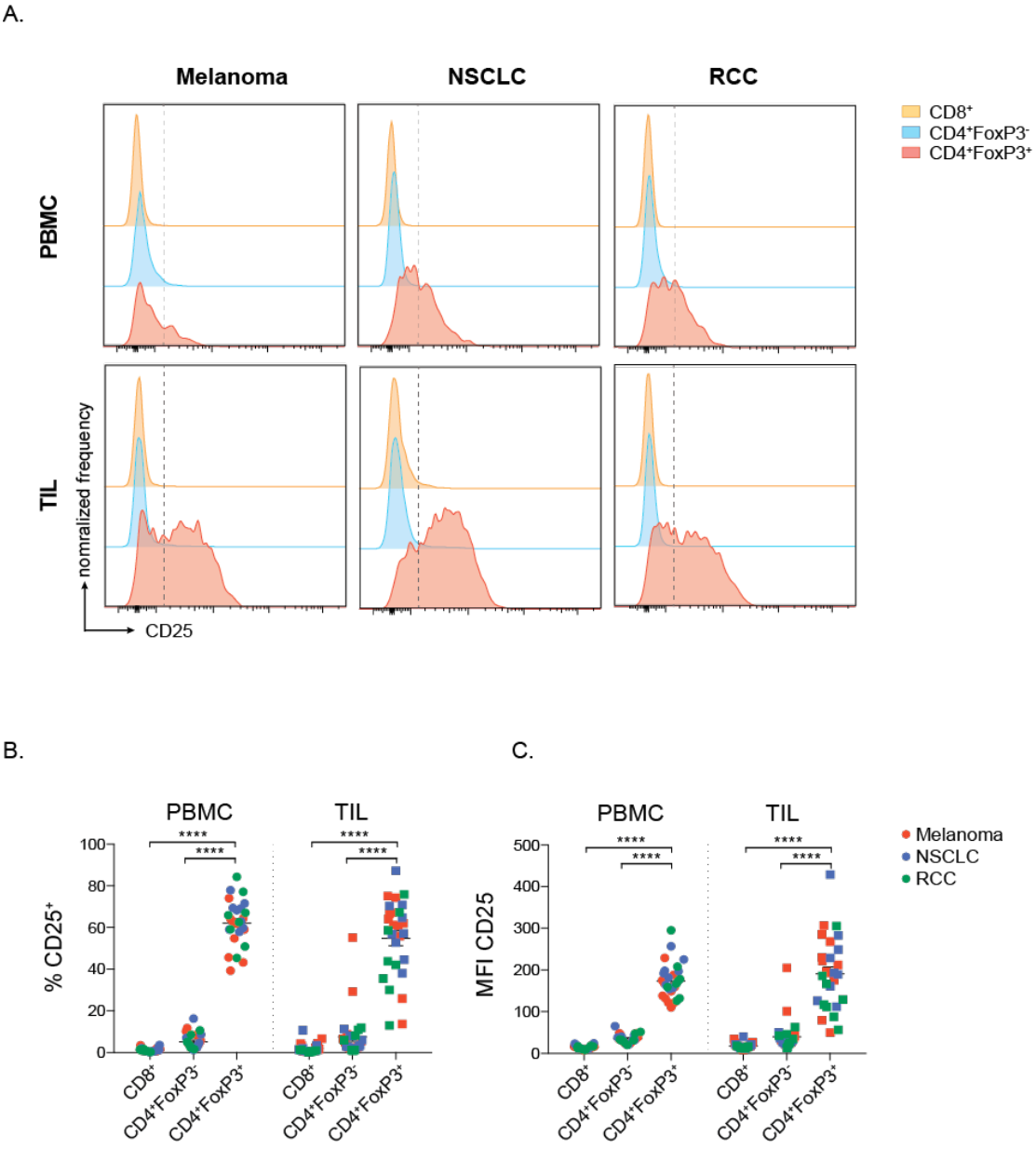

Figure 17: CD25 expression is largely restricted to Treg cells in human tumours (A) Histograms demonstrating relative expression of CD25 on $CD8^+$, $CD4^+FoxP3^-$ and $CD4^+FoxP3^+$ cell subsets in blood and tumour. A representative example of NSCLC is displayed. Grey dotted lines indicate gating. (B) Percentage expression of CD25 on $CD8^+$, $CD4^+FoxP3^-$ and $CD4^+FoxP3^+$ cell subsets in blood (PBMC) and tumour in patents with advanced melanoma (n=8), NSCLC (n=8) and RCC (n=8). (C) MFI of CD25 expression on individual cell subsets in blood and tumour within the same cohort. Error bars represent SEM.

CD25 expression appeared largely restricted to $CD4^+FoxP3^+$ Treg cells (mean % $CD25^+$=54.8% of $CD4^+FoxP3^+$, 7.5% of $CD4^+FoxP3^-$ and 1.9% of $CD8^+$; $p<0.0001$) (Figure 17A and B). Further, the level of CD25 expression, as assessed by MFI, was significantly higher on $CD4^+FoxP3^+$ Treg cells relative to $CD4^+FoxP3^-$ and $CD8^+$ T cells within all studied tumour subtypes (mean MFI $CD4^+FoxP3^+$=190.0, $CD4^+FoxP3^-$=34.5 and $CD8^+$=17.9; $p<0.0001$) (Figure 17C). These findings were remarkably consistent, despite potential variability in immunogenicity of individual tumours and significant heterogeneity in the clinical characteristics of the studied patient population (Chapter 2.4.3.1, Materials and Methods) and were further supported by data derived from multiple models of transplantable tumour cell lines of variable immunogenicity including MCA205 sarcoma, MC38 colon adenocarcinoma, B16 melanoma and CT26 colorectal carcinoma (Figure 18).

Consistently, in multiple mouse models of cancer, in contrast to reports from in vitro studies (reviewed in Boyman and Sprent, 2012), minimal expression of CD25 on the Teff cell compartment ($CD4^+FoxP3^-$ and $CD8^+$ subsets) was observed in vivo and the percentage of CD25-expressing Teff cells ($CD8^+$=3.08-8.35%, $CD4^+FoxP3^-$=14.11-26.87%) was significantly lower than on Treg cells (83.66-90.23%) ($p<0.001$) (Figure 18A and B). CD25 expression was also observed on Treg cells present in draining lymph nodes and blood. However, the level of expression, based on mean fluorescence intensity (MFI) was significantly lower than that observed on tumour-infiltrating Treg cells (Figure 18C).

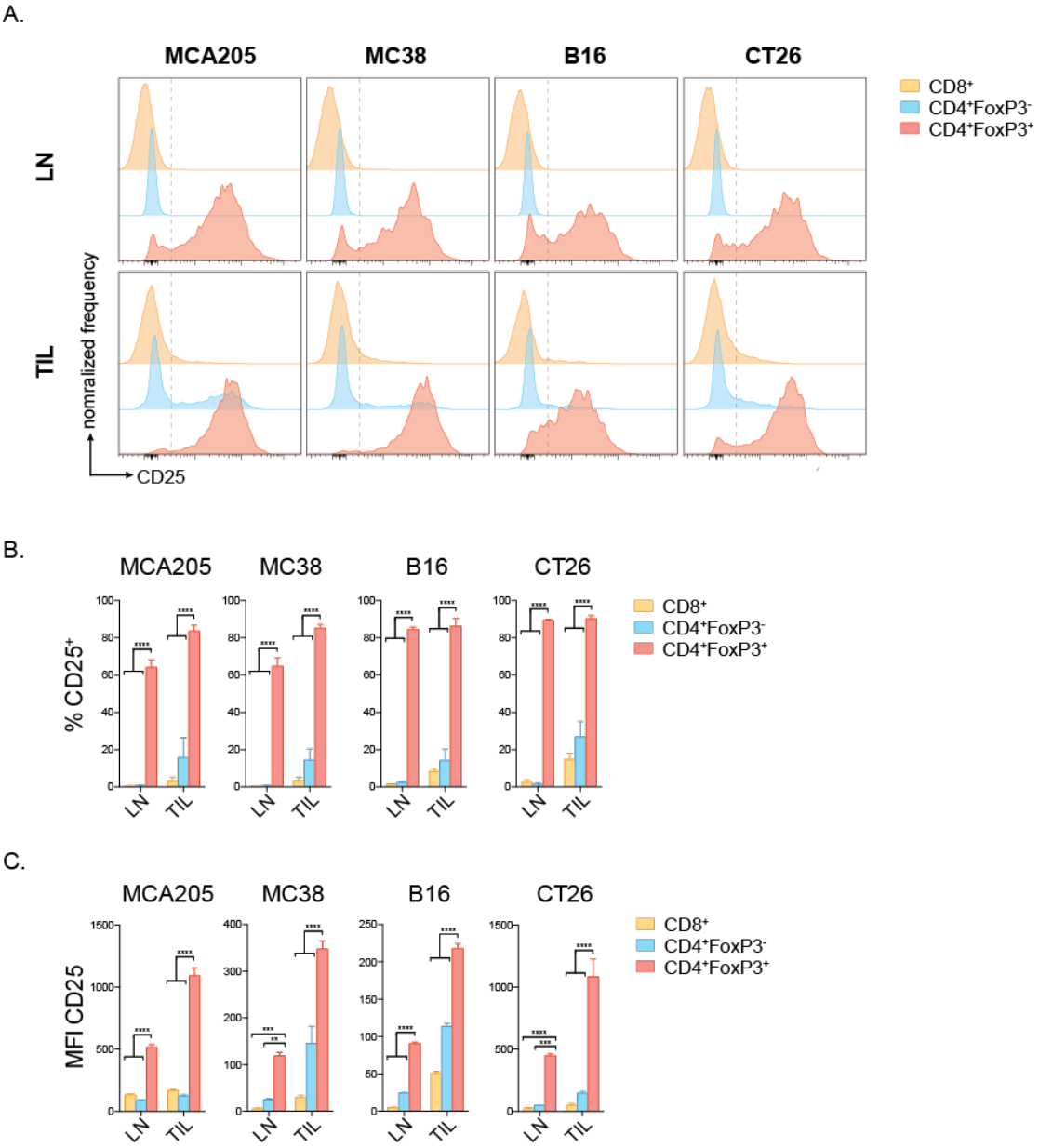

Figure 18: CD25 expression is largely restricted to tumour-infiltrating Treg cells in mouse models of cancer

(A-C) Mice were injected subcutaneously (s.c.) in the flank with MCA205 ($5x10^5$ cells, C57BL/6 mice, n=10), MC38 ($5x10^5$ cells, C57BL/6 mice, n=5), B16 ($2.5x10^5$ cells, C7BL/6 mice (n=3) or CT26 ($5x10^5$ cells, BALB/c mice, n=3) cells. LNs and TILs were processed 10 days after tumour challenge and analysed by flow cytometry. (A) Representative histograms demonstrating expression of CD25 on T cell subsets in LNs and TILs. Dotted lines represent gating of $CD25^+$ cells. (B) Percentage and (C) MFI of CD25 in each T cell subpopulation. Error bars represent standard error of the mean (SEM). The experiment was repeated three times.

Taken together these data suggested that CD25 is a largely selective target for Treg cells in mouse models and human cancers and that the lack of anti-tumour activity observed in pre-clinical mouse models is unlikely to relate to depletion of CD25-expressing effector T cell populations. Further in vivo study was therefore required to decipher the activity of the most extensively studied anti-CD25 mAb (clone PC61, rat IgG1, λ), here labelled αCD25-r1, which had previously displayed limited activity against established tumours in pre-clinical studies (Golgher et al., 2002; Jones et al., 2002; Onizuka et al., 1999; Quezada et al., 2008; Shimizu et al., 1999).

4.5 Anti-CD25-r1-mediated depletion of Treg cells is confined to lymph node and blood

Consistent with existing pre-clinical data (Onizuka et al., 1999; Setiady et al., 2010), administration of 200μg of αCD25-r1 on day 5 after tumour challenge resulted in a reduced frequency of $CD25^{+}FoxP3^{+}$ cells (detected with an anti-CD25 antibody binding to a different epitope to the therapeutic mAb) in PBMCs and LN. However, αCD25-r1 failed to deplete tumour-infiltrating Treg cells, which demonstrated a $CD4^{+}FoxP3^{+}$, but $CD25^{-}$ phenotype following therapy (Figure 19A and B). Their frequency remained comparable to that of untreated mice, potentially explaining the lack of efficacy observed against established tumours in previous studies, despite an apparent reduction in $CD25^{+}$ T cells within the tumour (Golgher et al., 2002; Jones et al., 2002; Onizuka et al., 1999; Quezada et al., 2008; Shimizu et al., 1999).

Previous analysis of the tumour microenvironment in mouse models and human melanoma metastases highlighted the importance of activatory and inhibitory FcγRs in influencing the ADCC activity of therapeutic mAbs. In both mouse and human tumours, upregulation of the inhibitory FcγR CD32b was observed. In acknowledgement of this as a potential explanation for the lack of intra-tumoural ADCC activity observed with αCD25-r1, the impact of an anti-CD25 mAb optimised for ADCC activity was determined. The constant region of the original anti-CD25 mAb obtained from clone PC61 was replaced with murine IgG2a and κ constant regions (αCD25-m2a) (performed by Fred

Arce Vargas), the classical mouse isotype associated with ADCC. Thereafter, its in vivo activity was compared to both αCD25-r1 and, as a control, the anti-CTLA-4 mAb (clone 9H10), previously described mediate effective depletion of intra-tumoural Treg (Simpson et al., 2013).

Both anti-CD25 antibody variants resulted in reduced expression of CD25 on T cells and a reduction in the number of Treg cells in blood and LN, but only αCD25-m2a resulted in depletion of tumour-infiltrating Treg cells to levels comparable to those observed with anti-CTLA-4 mAb. The observed loss of CD25 expression with the PC61 variant likely related to downregulation of the receptor or mAb-induced capping (Figure 19A and B). In keeping with these observations, both anti-CD25 isotypes resulted in an increased Teff/Treg cell ratio in blood and LN, but only αCD25-m2a increased the intra-tumoural ratio in a similar manner to anti-CTLA-4 (Figure 19C).

A.

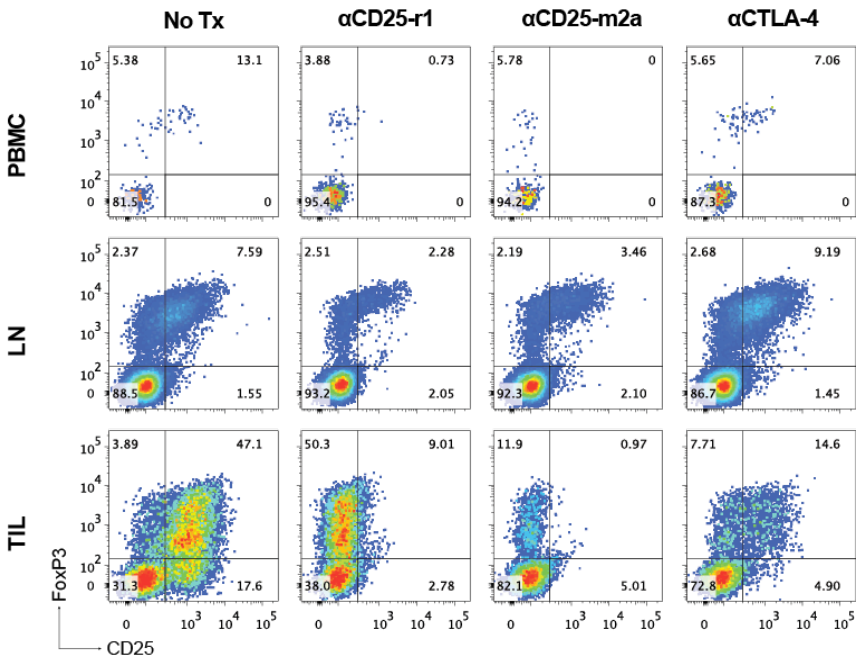

B.

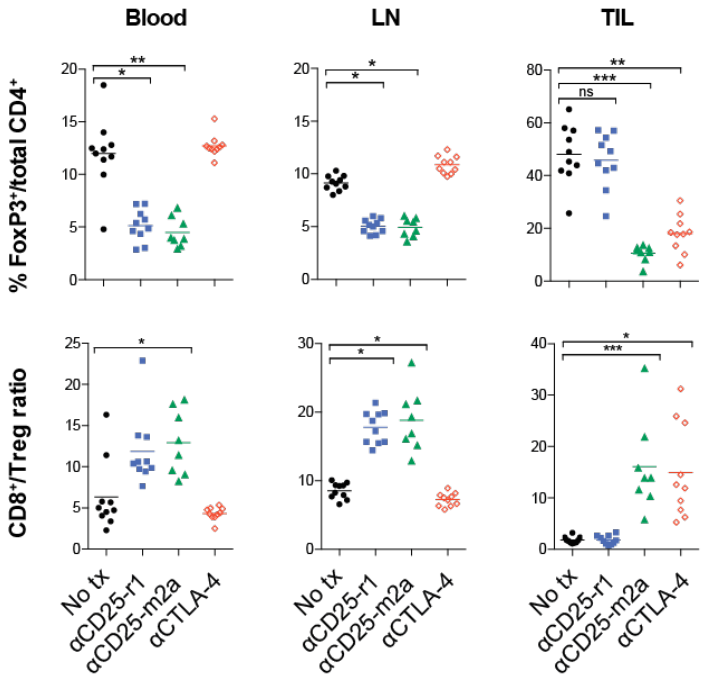

C.

Figure 19: **Anti-CD25-r1 fails to deplete tumour-infiltrating Treg cells**

Tumour-bearing mice were injected with 200µg of anti-CD25-r1 (αCD25-r1), anti-CD25-m2a (αCD25-m2a) or anti-CTLA-4 (αCTLA-4) on days 5 and 7 after s.c. inoculation with $5x10^5$ MCA205 cells. Peripheral blood mononuclear cells (PBMC), lymph nodes (LN) and tumours (TIL) were harvested on day 9, processed and stained for flow cytometry analysis. (A) Expression of CD25 (detected with antibody clone 7D4) and FoxP3 on $CD4^+$ T cells. (B) Percentage of $FoxP3^+$ cells from total $CD4^+$ T cells. (C) $CD8^+$/Treg ratios in PBMC, LN and TIL.

In contrast to CTLA-4, CD25 is expressed at high levels in blood and tumour. However, ADCC of Treg cells with αCD25-r1 was only observed in PBMC and LN suggesting a tumour-specific mechanism of inhibition. This did not appear to relate to a lack of intra-tumoural T cell infiltration which had been identified previously (Quezada et al., 2008). Based on previous observations, the expression of activatory and inhibitory FcγRs on individual leukocyte subpopulations in the blood, spleen, LN and tumour was determined. Further, the binding affinity of the two anti-CD25 Fc variants to activatory and inhibitory FcγRs was evaluated in attempt to shed light on the dissociation in activity of αCD25-r1 mAb observed between blood, LN and tumour.

4.6 Fc gamma receptor IIb and variable A:I binding profiles influence the depleting activity of anti-CD25 antibodies

Expression of activatory and inhibitory FcγRs appeared higher on tumour-infiltrating myeloid cells (granulocytic cells, dendritic cells and monocyte/macrophages) relative to all other studied organs (Figure 20A). Given the impact of antibody isotype in determining affinity for FcγRs, the binding affinity of the two Fc variants of anti-CD25 to FcγRs was evaluated by surface plasmon resonance (SPR) (performed by the Ravetch laboratory) (Figure 20B). Consistent with previous descriptions (Nimmerjahn and Ravetch, 2005), the mIgG2a isoform was observed to bind to all FcγR subtypes with a high activatory to inhibitory ratio. In contrast, αCD25-r1 (rat IgG1) was observed to bind to only a single activatory FcγR, FcγRIII, as well as the inhibitory FcγRIIb. However, in contrast to the mIgG2a isoform, the binding affinity to FcγRIII and FcγRIIb appeared similar, resulting in a low A/I ratio (<1) (Figure 20B).

A.

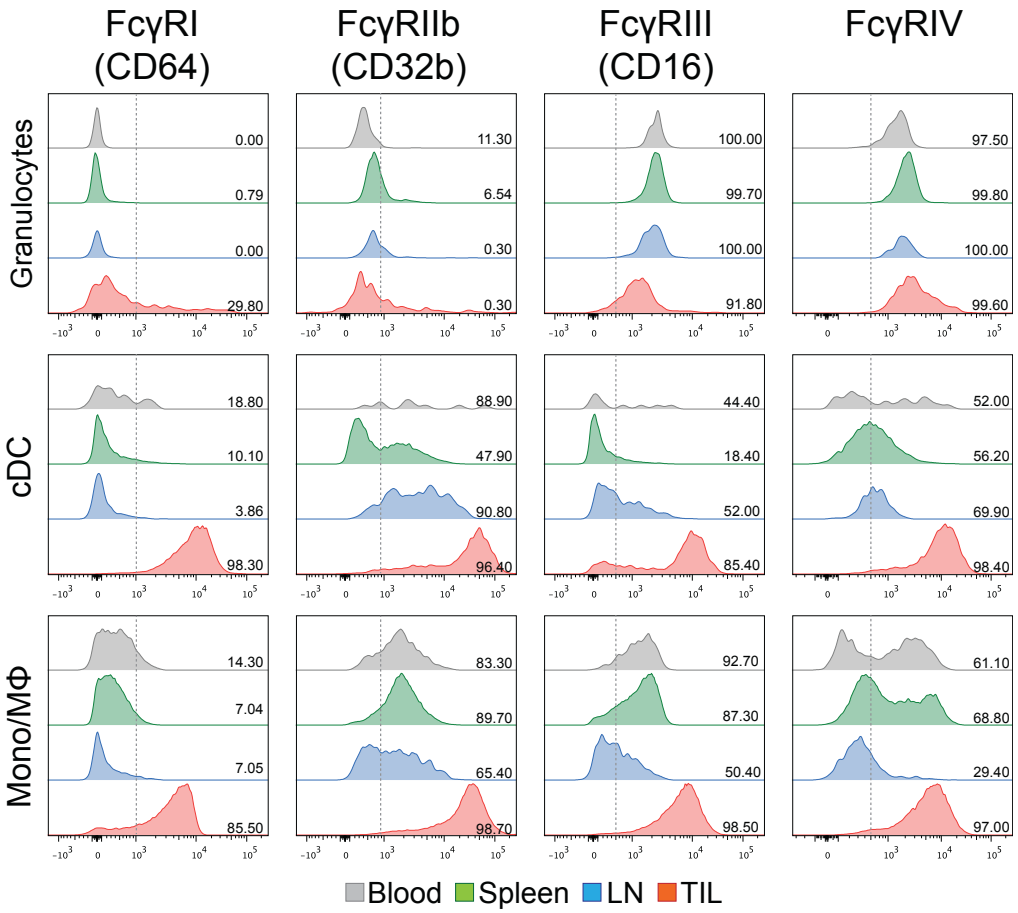

B.

Binding affinity (M^{-1})

	rIgG1	mIgG2a
FcγRI	n.b.	1.1×10^{-8}
FcγRIIb	2.6×10^{-6}	4.2×10^{-6}
FcγRIII	2.5×10^{-6}	4.5×10^{-6}
FcγRIV	n.b.	2.2×10^{-7}

Figure 20: Intra-tumoural Fc gamma receptor expression and binding affinity of anti-CD25 Fc variants (A-B) Expression of FcγRs was assessed by flow cytometry in blood, spleen, LN and s.c. MCA205 tumours (TIL) 10 days after tumour challenge. (A) Representative histograms demonstrating expression of FcγRs on granulocytes ($CD11b^+$ $Ly6G^+$), conventional dendritic cells (cDC) ($CD11c^{high}$ $MHC\text{-}II^+$) and monocyte/macrophages (Mono/Mϕ) ($CD11b^+$ $Ly6G^-$ $NK1.1^-$ $CD11c^{low/neg}$). Grey dotted lines indicate gating. (B) The binding affinity of rat IgG1 and mouse IgG2a isotypes to murine FcγRs as determined by surface plasmon resonance.

In order to determine which specific FcγRs were involved in anti-CD25-mediated Treg cell depletion, the number of tumour-infiltrating Treg cells in mice lacking expression of individual FcγRs was evaluated (Figure 21).

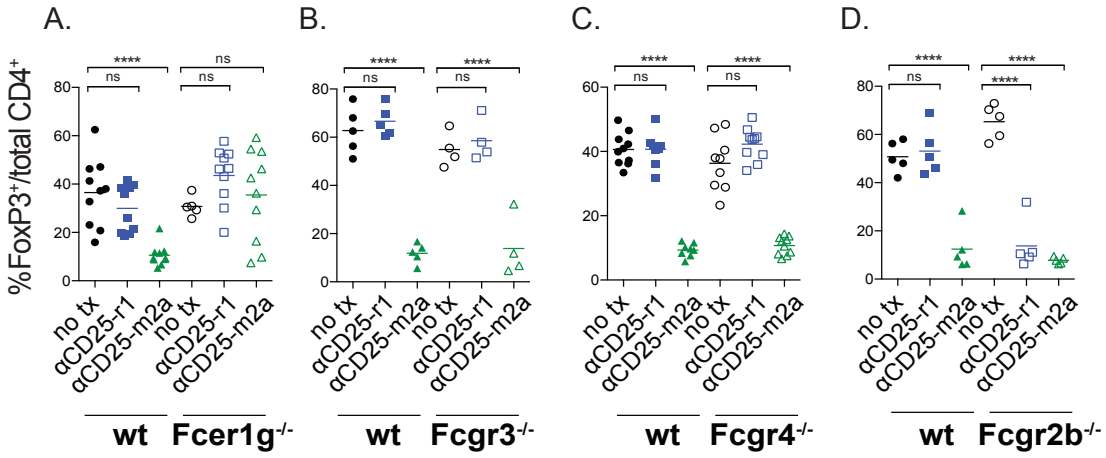

Figure 21: FcγRIIb inhibits αCD25-r1-mediated Treg cell depletion in tumours

(A-D) Wild-type (wt), *Fcer1g*$^{-/-}$, *Fcgr3*$^{-/-}$, *Fcgr4*$^{-/-}$ or *Fcgr2b*$^{-/-}$ mice were injected with 5x10^5 MCA205 cells s.c. and treated with 200µg of αCD25 Fc variants on days 5 and 7. Tissues were harvested and processed for flow cytometry analysis on day 9. Treg (CD4$^+$FoxP3$^+$) as a percentage of total tumour-infiltrating CD4$^+$ T cells is displayed.

Analysis of *Fcer1g*$^{-/-}$ mice, which lack expression of activating FcγRs (I, III and IV), demonstrated a complete absence of Treg cell depletion. These data confirmed that Treg cell elimination by αCD25-r1 in the periphery, and Treg cell elimination by αCD25-m2a in the periphery and tumour, is mediated by FcγR-dependent ADCC and is not the result of blocking IL-2 binding to CD25 (Figure 21A). Intra-tumoural Treg cell depletion by αCD25-m2a was not dependent on any individual activatory FcγR, with Treg cell elimination observed in both *Fcgr3-/-* and *Fcgr4-/-* mice (Figure 21B and C). However, critically, in mice lacking expression of the inhibitory receptor FcγRIIb, intra-tumoural Treg cell depletion by αCD25-r1 was effectively restored and comparable between αCD25-r1 and αCD25-m2a (Figure 21D). The lack of Treg cell depletion by αCD25-r1 in the tumour is therefore explained by its low A/I binding ratio and high intra-tumoural expression of FcγRIIb.

In order to cement the translational value of these findings and demonstrate a context in which anti-CD25 mAbs may have therapeutic value, longitudinal assessment of CD25 expression on TIL subsets was evaluated in patients undergoing immune checkpoint modulation. The particular relevance of this was to ensure, similar to pre-clinical findings, that CD25 expression remains restricted to Treg cells, even in the context of an inflamed human tumour microenvironment.

4.7 CD25 expression remains consistent on TIL subsets in patients undergoing immune checkpoint modulation

Core biopsies were performed on the same tumour lesion at baseline and following 4 cycles of either nivolumab (3mg/kg Q2W) or 2 cycles of pembrolizumab (200mg Q3W) in patients with advanced kidney cancer and melanoma respectively (Figure 22). Despite systemic immune modulation, CD25 expression remained restricted to $FoxP3^+$ Treg cells, even in areas of dense $CD8^+$ T cell infiltrate evaluated by multiplex IHC (Figure 22A and quantified in Figure 22B). These findings confirmed the translational value of the described pre-clinical data and lend further support to the concept of selective therapeutic targeting of Treg cells via CD25 in human cancers.

A.

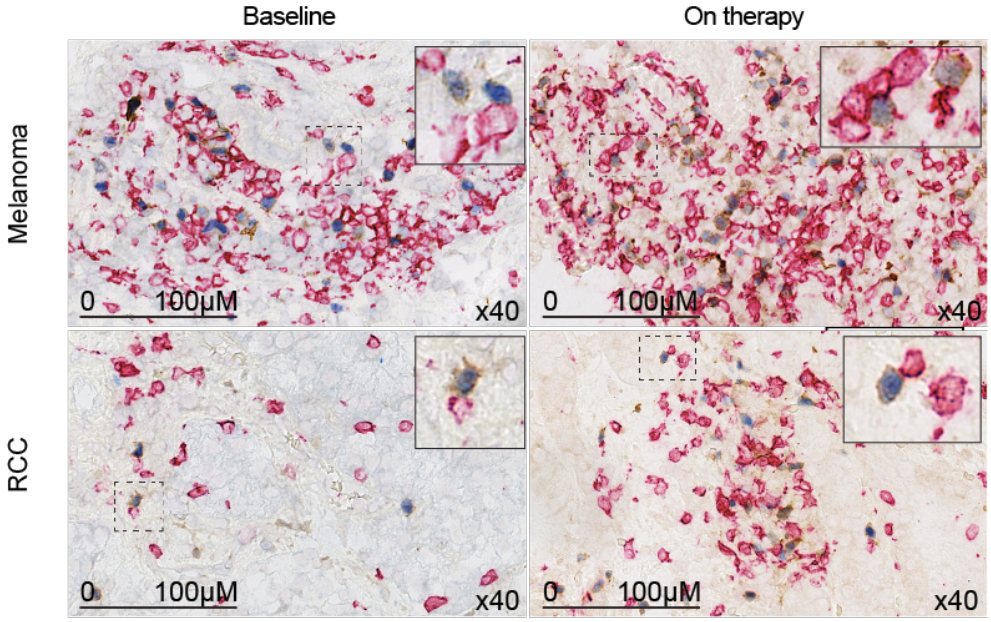

B.

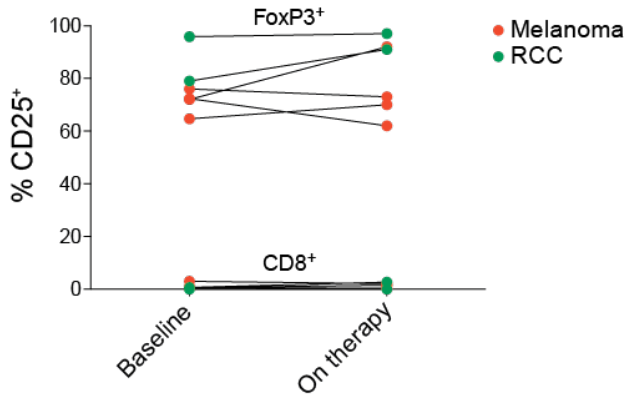

Figure 22: CD25 expression on TIL subsets in patients undergoing PD-1 blockade

(A) Longitudinal analysis of CD25 expression in human melanoma (n=4) and RCC (n=2) lesions prior to ('Baseline') and during PD-1 blockade ('On therapy'). CD8 staining is displayed in red, FoxP3 in blue and CD25 in brown. (B) Quantification of CD25 expression (%) of tumour-infiltrating $CD8^+$ and $FoxP3^+$ T cells at baseline and during PD-1 blockade. Plotted values derive from analysis of 10 x40 high power fields (HPF) per patient at each sampling time point.

4.8 Discussion and Conclusions

CD25 appeared an attractive target for Treg cell depletion owing to its restricted expression profile in both mouse models and human cancers. Contrary to in vitro studies, minimal expression of CD25 was observed on effector T cells in vivo in mouse models or in human subjects undergoing immune checkpoint blockade.

The efficacy of anti-CD25 as an anti-tumour therapy appears to depend upon effective Treg cell depletion in the tumour microenvironment, which can only be achieved by using an antibody isotype optimised for engagement of activating FcγRs. These data suggest that the limited activity observed in pre-clinical studies evaluating the anti-CD25 PC61 mAb is likely explained ineffective or suboptimal intra-tumoural Treg cell depletion, a consequence of its low A:I binding ratio and high intra-tumoural expression of inhibitory FcγRIIb.

High intra-tumoural expression of CD32b might also explain the modest results observed in early clinical trials of the anti-human CD25 antibody daclizumab. However, the impact of anti-human CD25 antibodies of varied IgG subclass remains to be evaluated and further, data presented above in the context of patients treated with anti-human CTLA-4 mAbs, suggest that Treg cell depletion strategies may only be relevant in the context of T cell inflamed tumours.

Treg cell depletion may be achieved by targeting other highly expressed molecules such as CTLA-4, GITR and OX40 (Bulliard et al., 2013, 2014; Coe et al., 2010; Selby et al., 2013; Simpson et al., 2013). However, in contrast to CD25, these molecules are simultaneously expressed by Teff cells. Although immune modulatory mAbs armed with dual activity may display enhanced activity as monotherapy, a concern is that simultaneous expansion of the effector cell compartment could precipitate off target toxicity, particularly when used in combination. Anti-CD25 mAbs lack the additional cell-intrinsic immune modulatory activity of anti-CTLA-4 antibodies and may therefore be more attractive as a candidate combination partner in clinical trials.

5 Results 3: Neoantigen heterogeneity shapes anti-tumour immunity

5.1 Introduction

The majority of current immunotherapeutic approaches are only relevant in the context of tumours with an abundant T cell infiltrate. Paucity of immune infiltration is not uncommon and well recognised amongst those studying the immune tumour microenvironment of human tumours, although rarely acknowledged in the literature (Melero et al., 2014). It follows that identifying underlying drivers of T cell infiltration or indeed methods of promoting T cell infiltration is an area of high scientific priority.

Tumour-specific mutations have recently been recognised to serve as neoantigens, eliciting T cell reactivity and impacting on survival (Brown et al., 2014) and response to immune checkpoint blockade (Rizvi et al., 2015; Snyder et al., 2014; Van Allen et al., 2015). Whilst circulating T cells have been demonstrated to recognise tumour-specific neoantigens in vitro (Rizvi et al., 2015; Snyder et al., 2014), tumour-infiltrating neoantigen-reactive T cells (NARTs) and the pathways acting to regulate their activity are poorly described. The final objective of this study was to identify and characterise these subsets in primary NSCLC, a tumour subtype recognised to harbour a high burden of somatic mutations and therefore potential neoantigens (Alexandrov et al., 2013; Schumacher and Schreiber, 2015)

Bioinformatics analyses were performed by Nicholas McGranahan and Rachel Rosenthal and interpreted together with Andrew Furness. Immunological analysis of human samples was performed independently by Andrew Furness and in collaboration with the Hadrup laboratory.

5.2 Clonal architecture of somatic mutations in primary NSCLC

Initial analyses focused on two patients, L011 and L012. Multi-regional sampling of primary tumours was performed, isolating matched tumour regions for paired genomic and immunological analyses. Individual tumour regions were subjected to whole exome sequencing (WES) and identified somatic mutations plotted as phylogenetic trees (Figure 23). Intra-tumour heteroegeneity in primary NSCLC is well described (de Bruin et al., 2014; Jamal-Hanjani et al., 2017). In keeping with this, despite a comparable smoking history, the clonal architecture of somatic mutations in L011 and L012 varied considerably, with L011 displaying a relatively small subclonal fraction (4%) relative to L012 (44%).

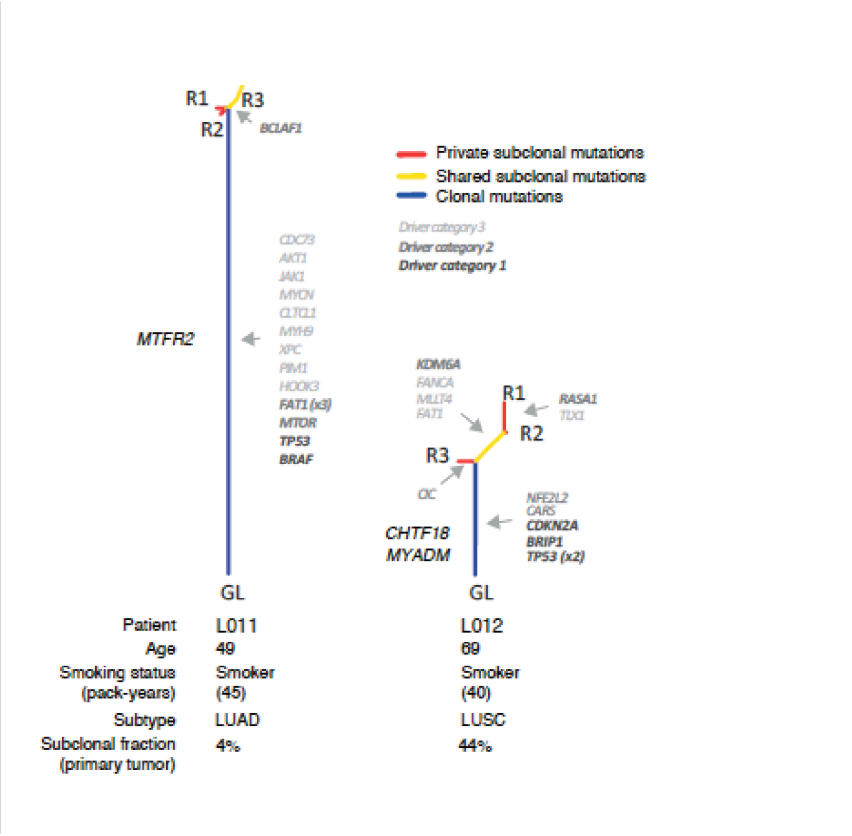

Figure 23: Clonal evolution of primary NSCLC

Phylogenetic trees depict clonal and subclonal mutations for patient L011 (left) and L012 (right). Somatic alterations shared by all tumour cells (clonal) occur early in tumourigenesis (blue trunk). Alterations shared by tumour cells present some regions of the tumour but not all (shared subclonal) occur later in tumourigenesis (yellow branches) and alterations present in only one region of the tumour (private subclonal) also occur later in tumourigenesis (red branches). Additional patient demographics and tumour characteristics are displayed below including tumour subtype, where LUAD = lung adenocarcinoma, LUSC = lung squamous cell carcinoma, GL = germ line and R = region.

5.3 In-silico prediction of putative neoantigens

With use of an established bioinformatics pipeline, putative neoantigens were shortlisted based on predicted binding affinity (<500nM) to the patient's human leucocyte antigen (HLA) (performed by McGranahan and Rosenthal). A total of 313 neoantigens were predicted from the mutations within the primary tumour of L011, 88% of which were clonal, identified in every region of the primary tumour. Conversely, L012, a squamous cell carcinoma, exhibited a relatively low mutational burden and extensive intra-tumoural heterogeneity (ITH), with 75% of the predicted neoantigens deriving from subclonal mutations, present only in a subset of cancer cells.

Mutant peptides were synthesised in vitro, based on the sequence of putative neoantigens (outsourced to Pepscan, Chapter 2.6, Materials and Methods). Simultaneously, tumour-infiltrating lymphocytes from individual tumour regions were expanded to large numbers in vitro. With use of fluorescent-labelled MHC (major histocompatibility complex) multimers bearing putative neoantigens, TILs were screened for reactivity in vitro (Figure 24). 288 and 354 putative neoantigen-loaded MHC multimers were first used to screen in vitro expanded $CD8^+$ T cells derived from individual tumour and normal tissue regions from patients L011 and L012 respectively, using a previously described high-throughput method (Figure 24A-D) (Hadrup et al., 2009).

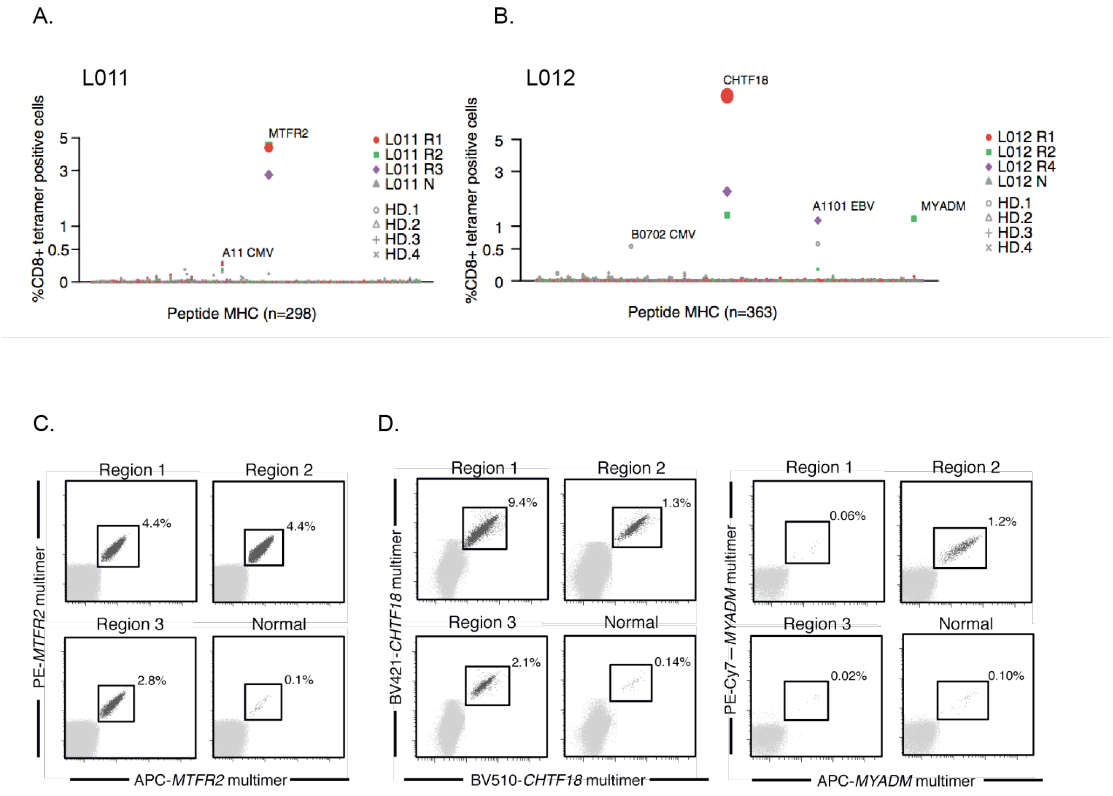

Figure 24: High-throughput screening of in-vitro expanded NSCLC TILs

(A-B) Screening of expanded, region-specific, tumour-infiltrating $CD8^+$ T lymphocytes and control healthy donor (HD) $CD8^+$ PBMCs with MHC multimers bearing candidate neoantigens and control HLA-matched viral peptides. The frequency (%) of $CD8^+$ MHC multimer positive cells out of total $CD3^+CD8^+$ TILs is displayed. (C) Flow plots depicting $CD8^+$ T cell responses against MHC multimers bearing mutant MTFR2 in tumour regions (1-3) and adjacent normal tissue in patient L011 (D) Flow plots depicting $CD8^+$ T cell responses against MHC multimers bearing mutant CHTF18 and mutant MYADM in tumour regions (1-3) and adjacent normal tissue in patient L012.

In patient L011, in-vitro expanded tumour-infiltrating $CD8^+$ T cells appeared reactive to an HLA-B3501-multimer bearing mutant $MFTR2^{D326Y}$ (FAFQE***Y***DSF) (Figure 24A). In L012, two distinct $CD8^+$ T cell populations appeared reactive to an HLA-A1101-multimer bearing mutant $CHTF18^{L769V}$ (LLDI***V***APK) and an HLA-B0702-multimer bearing mutant $MYADM^{R30W}$ (SPMIVGSP***W***) (Figure 24B). Whilst occasional responses against viral peptides were observed, confirming the functionality of the employed MHC-multimer technology, no non-specific reactivity against healthy donor (HD) PBMCs was identified. $CD8^+$ T cell responses were identified in all tumour

regions (2.8-4.4%) and at a low frequency in adjacent normal lung tissue (0.1%) in L011 (Figure 24C). Whilst in L012, responses were detected in all tumour regions against mutant CHTF18 and in a single tumour region against mutant MYADM (Figure 24D).

High HLA binding affinity (<50nM) was predicted for MFTR2^{D326Y} and CHTF18^{L769V} in both wild type and mutant forms (Figure 25A), but only mutant peptides were observed to elicit a T cell response. Higher binding affinity to mutant (<50nM) versus wild type (>1000nM) peptide was also predicted for MYADM (Figure 25B), however reactivity was observed against both. This relates to the position of the MYADM^{R30W} peptide in the anchor residue. Here, it primarily affects HLA-binding but not T cell recognition. In the absence of artificial stabilisation provided in vitro by an MHC multimer system, the low predicted affinity of the wild type peptide to HLA would be expected to prevent adequate presentation in vivo.

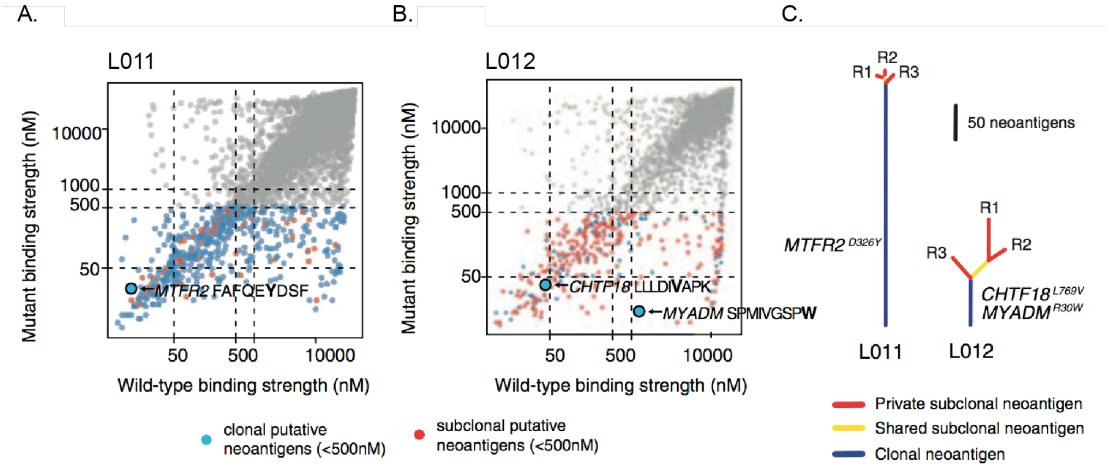

Figure 25: Predicted HLA binding affinity to and clonality of identified neoantigens
(A-B) Putative neoantigens predicted for all missense mutations in L011 and L012. Predicted clonal neoantigens are displayed in blue, subclonal in red. MFTR2^{D326Y}, CHTF18^{L769V} and MYADM^{R30W} neoantigens are highlighted within relevant plots. (C) Evolutionary trees for L011 and L012 based on predicted neoantigens.

Analysis of the clonal architecture of confirmed neoantigens demonstrated all to be clonal, present on every tumour cell (Figure 25C). This was particularly unexpected for L012, given the majority of predicted neoantigens were

subclonal. These observations raised the possibility that given their presence on every tumour cell, clonal neoantigens may be more effective in eliciting T cell responses than subclonal neoantigens.

5.4 Impact of neoantigen clonal architecture on survival in NSCLC

In order to test this hypothesis, a cohort of 106 stage I/II, 43 stage III/IV and one unknown stage lung adenocarcinoma (LUAD) case from The Cancer Genome Atlas (TCGA) were subjected to neoantigen and clonality analysis (Figure 26).

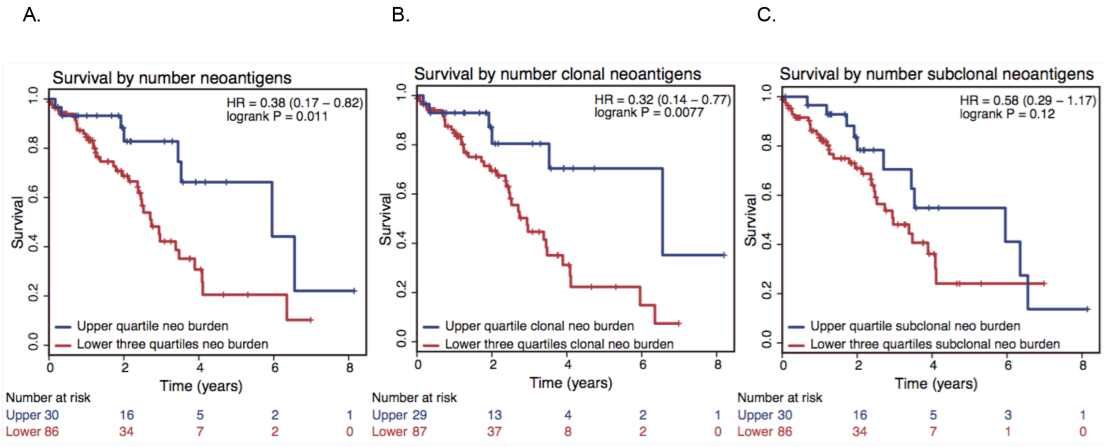

Figure 26: Impact of neoantigen clonality on overall survival in NSCLC

(A) Overall survival in TCGA LUAD cohort amongst tumours harbouring high (upper quartile of neoantigen burden) versus low (remainder of the cohort) total neoantigen burden (B) high (upper quartile of clonal neoantigen burden) versus low (remainder of the cohort) clonal neoantigen burden and (C) high (upper quartile of subclonal neoantigen burden) versus low (remainder of the cohort) subclonal neoantigen burden. Hazard ratios (HR) and logrank p values are displayed within each plot.

In support of the previously described prognostic relevance of tumour neoantigens (Brown et al., 2014), a high neoantigen load (defined as the upper quartile of the number of neoantigens predicted in the cohort) was associated with longer overall survival compared to tumours in the remaining quartiles (Figure 26A, p=0.011). However, tumours harbouring a high number of predicted clonal neoantigens (defined as the upper quartile of the cohort) were associated with significantly improved survival relative to all other

tumours in the cohort (Figure 26B, p=0.0077). Conversely, the number of predicted subclonal neoantigens was not significantly associated with overall survival (Figure 26C, p=0.12). Taken together, these data suggested that beyond total neoantigen burden, the clonal status of neoantigens might be relevant to immune surveillance/response.

5.5 High clonal neoantigen burden is associated with an inflamed tumour microenvironment

In support of this as a hypothesis, within the same TCGA LUAD cohort, differential expression of immune-related genes was evaluated, comparing tumours in the upper quartile of clonal neoantigen burden with those in the lower three quartiles (Figure 27).

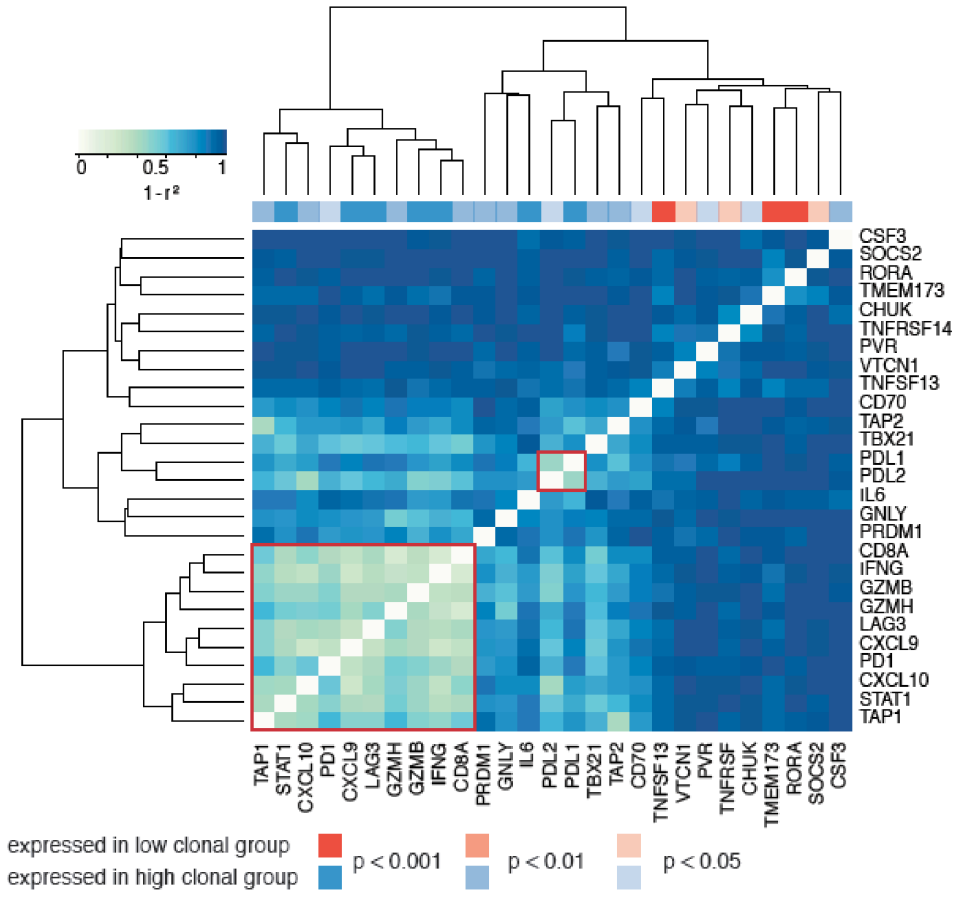

Figure 27: Differential expression of immune-related genes in TCGA LUAD cohort Heatmap demonstrating differential expression of immune-related genes between TCGA LUAD tumours with high and low clonal neoantigen burden, clustered on co-expression. Significance values are displayed above and the associated colour key below. Red boxes indicate clustering/co-expression.

Differential expression of 27 immune-related genes was observed (Figure 27). These included CD8A, genes associated with antigen presentation (TAP-1, TAP-2), T cell migration (CXCL-10 and CXCL-9), effector T cell function (STAT-1, IFN-γ), T cell regulation (PD-1, LAG-3, PD-L1, PD-L2) and cytolytic enzymes (granzyme B, H, and A]. All appeared upregulated in tumours with high clonal neoantigen burden and were observed to cluster, indicating co-expression.

These data suggested that high clonal neoantigen burden in LUAD is associated with an inflamed tumour microenvironment (IFN-γ, GzmB) enriched with activated effector T cells (CD8A), regulated by inhibitory immune checkpoint molecules including PD-1, LAG-3 and inhibitory ligands PD-L1 and PD-L2. However, these data derived from in-silico analysis alone. Earlier in vitro analysis of L011 and L012 had identified expanded, tumour-infiltrating $CD8^+$ T cells reactive to clonal neoantigens. Since in-vitro expansion methods impact upon both phenotypic and functional T cell markers, non-expanded, region-specific $CD8^+$ TILS from L011 and L012 were screened and characterised in attempt to determine the validity of the described immune-related gene expression data.

5.6 Identification of neoantigen-reactive tumour-infiltrating $CD8^+$ T cells in primary NSCLC

MHC multimers bearing mutant MFTR2, CHTF18 and MYADM were used to screen lymphocytes isolated directly from tumour regions and normal lung tissue of L011 and L012 respectively (Figure 28). These tumour digests had not undergone any form of expansion prior to analysis. Individual T cell subsets were identified by multi-parametric flow cytometry as described previously.

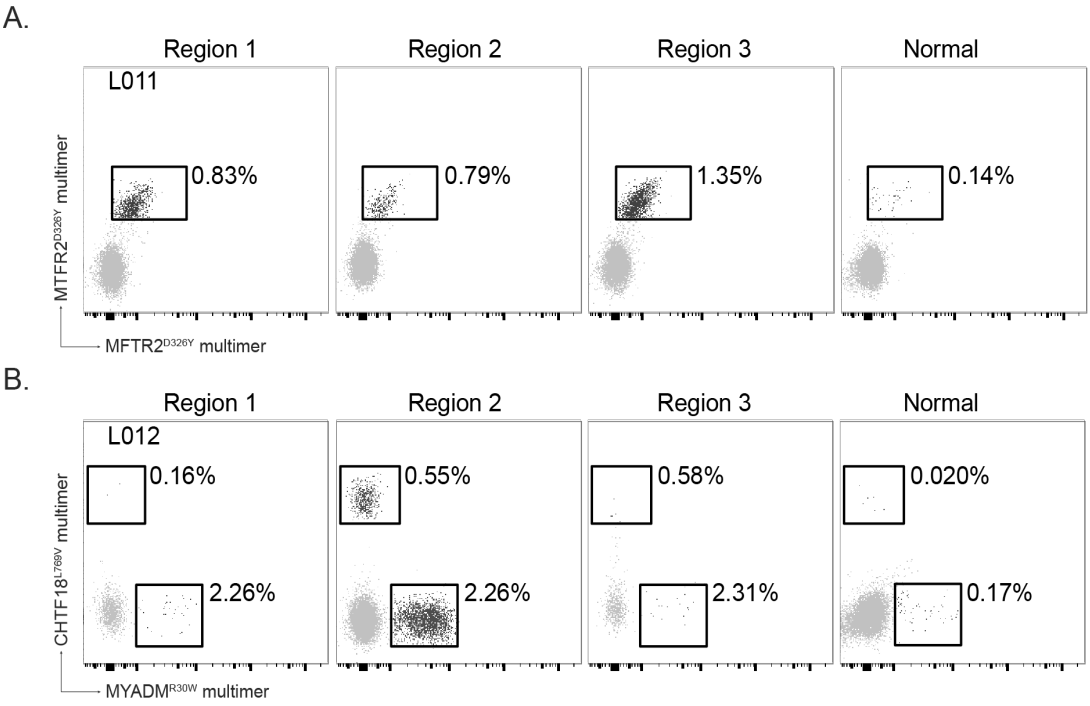

Figure 28: MHC multimer analysis of non-expanded tumour-infiltrating CD8$^+$ T cells
Flow plots demonstrating reactivity to MHC multimers bearing depicted neoantigens in tumour regions 1-3 and adjacent normal tissue for (A) L011 and (B) L012. Displayed percentages are of total tumour-infiltrating CD8$^+$ T cells.

In L011, CD8$^+$ MTFR2-reactive T cells were reliably identified in all tumour regions (R1-R3, 0.79-1.35% of total CD8$^+$ cells) and at very low frequency in adjacent normal lung tissue (0.14% of total CD8$^+$ cells). In L012, CHTF18 and MYDAM-reactive CD8$^+$ T cell populations were identified in tumour region 2 where they represented 2.26% and 0.55% of total CD8$^+$ cells respectively. Tumour regions 1 and 2 appeared more poorly infiltrated by CD8$^+$ T cells, both CHTF18 and MYADM-reactive CD8$^+$ cells were identified, but at much lower frequency. Similar to L011, neoantigen-reactive T cells could also be identified in adjacent normal lung tissue, but at a lower frequency than in tumour regions.

5.7 Characterisation of neoantigen-reactive tumour-infiltrating CD8$^+$ T cells in primary NSCLC

Analysis of immune-related gene expression in the TCGA LUAD cohort suggested that primary NSCLC tumours with high clonal neoantigen burden

display an inflamed phenotype. Although reactivity of $CD8^+$ T cells towards tumour-specific neoantigens has been demonstrated previously (Rizvi et al., 2015; Snyder et al., 2014), such analyses have only ever incorporated T cells derived from peripheral blood; little is known regarding the phenotype of tumour-infiltrating $CD8^+$ neoantigen-reactive T cells (NARTs).

Identified tumour-infiltrating $CD8^+$ NARTs reactive to clonal neoantigens in L011 and L012, were therefore subjected to multi-parametric flow cytometry analysis. Expression of co-inhibitory and co-stimulatory immune checkpoint molecules and functional markers was determined and compared to tumour-infiltrating $CD4^+$ and $CD8^+NART^-$ T cell subsets (Figure 29).

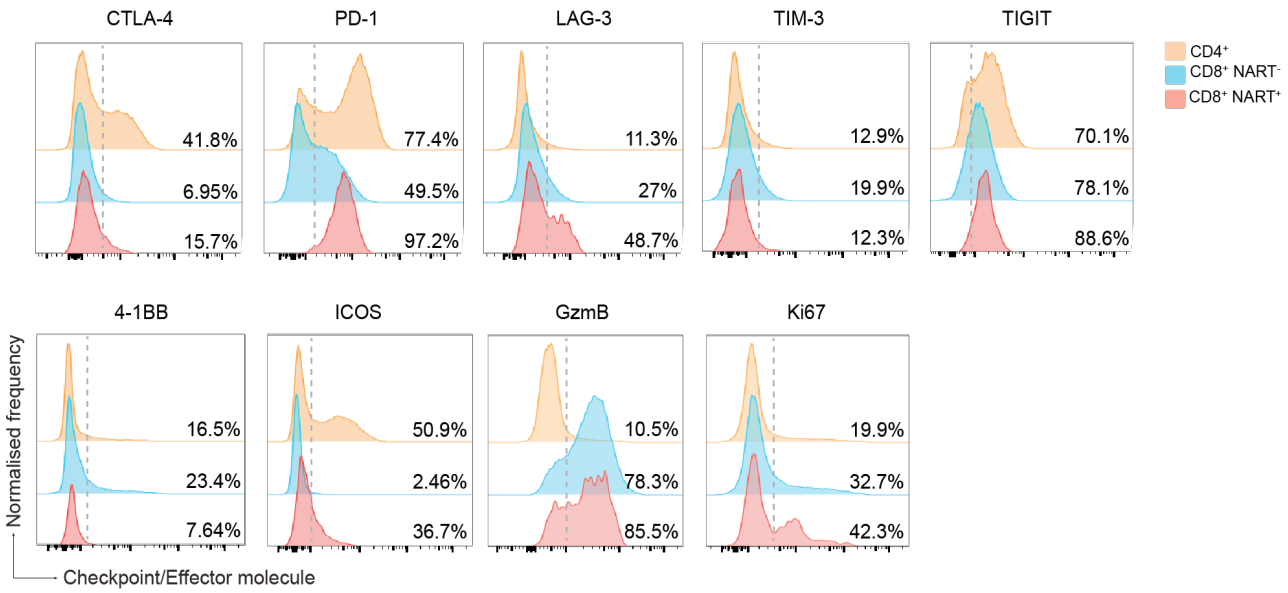

Figure 29: Multi-parametric analysis of tumour-infiltrating $CD8^+$ neoantigen-reactive T cells

Following identification of $CD3^+CD4^+$, $CD3^+CD8^+NART^-$ and $CD3^+CD8^+NART^+$ T cell populations, relative expression of co-inhibitory (upper panel) and co-stimulatory (lower panel, 4-1BB and ICOS) immune checkpoint molecules as well as functional markers (lower panel, GzmB and Ki67) was evaluated. Grey dotted lines indicate gating. Percentages represent fraction of cells within each subset positive for the displayed markers. Representative data is displayed for patient L011.

Consistent with previous analyses, CTLA-4 expression was largely restricted to the $CD4^+$ T cell compartment, although a small fraction of $CD8^+NART^-$

(6.95%) and $CD8^+NART^+$ (15.7%) cells appeared CTLA-4^+. In contrast, PD-1 was expressed by almost all $CD8^+$NARTs (97.2%) and LAG-3 by a large fraction (48.7%), in keeping with the gene expression data derived from the TCGA LUAD cohort. TIM-3 was consistently expressed by a modest fraction of T cells across all studied subsets (12.3-19.9%), whilst TIGIT was expressed by a majority of cells across all studied subsets excluding a small fraction of $CD4^+$ T cells (29.9%).

4-1BB has previously been described as a reliable marker of tumour-reactive $CD8^+$ T cells (Ye et al., 2014), however interestingly only a small fraction of $CD8^+$NARTs appeared 4-$1BB^+$ (7.64%). There are multiple possible explanations for this, including the kinetics of 4-1BB upregulation, however this will be important to elucidate further in a larger population, as this may allow useful differentiation between neoantigen-specific and tumour-associated antigen-specific T cell subsets. ICOS, another co-stimulatory immune checkpoint molecule, displayed a similar expression profile to CTLA-4, although a larger fraction of $CD8^+$NARTs appeared $ICOS^+$ (36.7%).

Analysis of functional markers demonstrated granzyme B (GzmB) to be largely restricted to $CD8^+$ T cell subsets with comparable expression between $NART^-$ and $NART^+$ subsets. Finally, based on Ki67, the greatest fraction of proliferating cells was observed amongst the $CD8^+$NARTs (42.3%) relative to $CD8^+NART^-$ (32.9%) and $CD4^+$ subsets (19.9%).

These data supported the TCGA LUAD gene expression findings, confirming PD-1 and LAG-3 as attractive targets for antibody-based blockade and ICOS as a target for agonistic mAbs. However, beyond this, given the observed prognostic value of clonal neoantigen burden in primary NSCLC and the demonstration that $CD8^+$NARTs reactive to clonal neoantigens are almost universally PD-1^+, the possibility that neoantigen clonal architecture might influence sensitivity to PD-1 blockade was raised.

5.8 Neoantigen heterogeneity influences sensitivity to PD-1 blockade

Rizvi and colleagues previously demonstrated that mutational and putative neoantigen burden influences response to PD-1 blockade in patients with advanced NSCLC (Rizvi et al., 2015), however the clonal architecture of mutations was not considered in this context. The same dataset was analysed with use of the developed bioinformatics pipeline and the clonal architecture of putative neoantigens determined (Figure 30A).

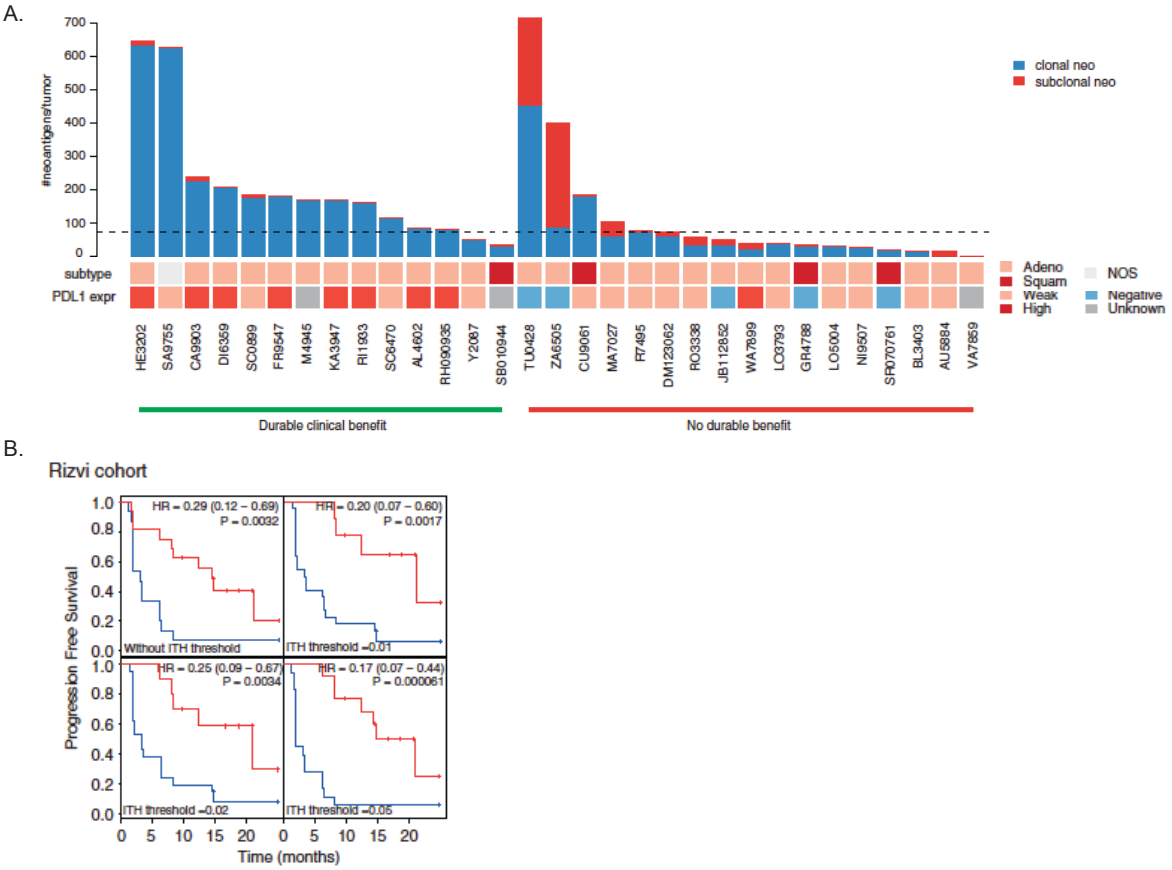

Figure 30: Clonal neoantigen burden and ITH influences response to PD-1 blockade

(A) Samples are grouped according to clinical benefit, with durable clinical benefit on the left (green underscore) and no durable benefit on the right (red underscore). Bar plot depicts clonal neoantigens in blue and subclonal neoantigens in red. Histological subtype and expression of PD-L1 are shown below. (B) Progression-free survival in the same cohort of tumours displaying high clonal neoantigen burden (≥70) without an ITH threshold (HR = 0.29 (0.12−0.69), log rank P=0.0032] or with an ITH threshold of 0.01 (HR=0.20(0.07−0.60), log-rank P = 0.0017), 0.02 (HR = 0.25 (0.09−0.67), log-rank P=0.0034), or 0.05 (HR = 0.17 (0.07−0.44), log rank P=0.000061).

These data yielded an unexpected finding. Tumours associated with durable clinical benefit (DCB, defined as in (Rizvi et al., 2015), partial response or stable disease lasting > 6 months) to PD-1 blockade consistently displayed a high burden of clonal neoantigens (≥70). However, response to PD-1 blockade also appeared contingent upon the relative fraction of subclonal neoantigens. Almost every tumour (12/13) that exhibited a low neoantigen subclonal fraction (<5%) and high neoantigen burden (≥70), demonstrated durable clinical benefit with pembrolizumab. In contrast, only 2 out of 18 tumours with a high subclonal neoantigen fraction (>5%) or low clonal neoantigen burden benefited from pembrolizumab. Even in the context of high overall putative neoantigen burden, resistance to PD-1 blockade was observed in tumours with a high subclonal fraction (e.g. TU0428, ZA6505).

Tumours with both a high clonal neoantigen burden and low neoantigen heterogeneity were associated with significantly longer progression free survival and this relationship remained robust to the choice of ITH threshold, with lower hazard ratios observed compared to using neoantigen burden alone (Figure 30B). Further, in keeping the immune-related gene expression data and recent clinical data (Reck et al., 2016), strong PD-L1 staining (>50% membranous staining) appeared enriched in these patients.

5.9 Discussion and Conclusions

Neoantigen burden has been demonstrated to influence prognosis (Brown et al., 2014) and sensitivity to immune checkpoint blockade in advanced NSCLC and melanoma (Rizvi et al., 2015; Snyder et al., 2014; Van Allen et al., 2015). However, the impact of ITH in the neoantigen landscape on this relationship has not been determined. These data are limited by cohort size and single-site biopsy data, which can overestimate the fraction of clonal mutations. Nevertheless, clonal and subclonal neoantigens do not appear equivalent in driving anti-tumour immunity.

The gene expression data derived from the TCGA LUAD cohort are supported by protein level findings of NART characterisation. It follows that clonal neoantigen burden might be of predictive value in determining response to

PD-1 blockade. However, the influence of neoantigen ITH was not anticipated. It is curious that despite screening more than 250 peptides against putative subclonal neoantigens, only T cells recognising clonal neoantigens were detected. Perhaps all can be explained by a unifying hypothesis whereby lower antigen dosage secondary to high neoantigen ITH is less effective in driving T cell responses with impact on prognosis, response to PD-1 blockade and the feasibility of detecting tumour-infiltrating T cells reactive to subclonal neoantigens. However, these data should not be over-interpreted given the number of evaluated patients (n=2) and the possibility that other variables, including methods of in-vitro expansion could have impacted upon detection of NARTs.

The demonstration that PD-L1 expression appeared enriched in patients with high clonal neoantigen burden in TCGA LUAD and Rizvi cohorts is pleasing, suggesting this may be a useful surrogate for clonal neoantigen burden and neoantigen ITH. NSCLC is the most common cause of cancer death worldwide (Cancer Research UK, 2015) and clinically applicable biomarkers are much needed, particularly in low- and middle-income countries. Whilst the limitations of PD-L1 as a biomarker are recognised given its inducible/dynamic nature, it was recently used successfully to stratify NSCLC patients to anti-PD-1 therapy versus chemotherapy (Reck et al., 2016).

Perhaps the most important finding amongst these data was also that least anticipated. ITH within solid tumours and their metastases is well recognised (de Bruin et al., 2014; Gerlinger et al., 2012, 2014; Jamal-Hanjani et al., 2017; Jiménez-Sánchez et al., 2017). However, clonal neoantigens represent a therapeutic target present on all tumour cells, regardless of subsequent evolution. To this end, adoptive cell-based approaches, of particular relevance to poorly infiltrated tumours, and/or vaccination strategies, both targeting clonal neoantigens, in combination with immune checkpoint modulation may hold promise in overcoming the significant challenge posed by ITH.

6 Final discussion and conclusions

Dissecting the in vivo activity of anti-CTLA-4 mAbs highlights the importance of comprehensively profiling the expression of a candidate target molecule and considering the implications of this in the design of a therapy with the potential for additional Fc-dependent effector activity. Further, whether in the context of malignancy, arthritis, transplant medicine or beyond, these data also emphasize the importance of recognising the impact of the local microenvironment in determining the activity of a given therapy (Furness et al., 2014), a concept perhaps not always considered enough in the pre-clinical design of antibody-based therapies.

Within pre-clinical models and human tumours, it will be important to expand this work and determine whether innate effector cell infiltration and FcγR expression profiles vary across individual tumour subtypes and anatomical disease sites. If tissue-resident cell subsets are implicated, this is highly plausible. Another important consideration will be the impact of the cytokine milieu within the TME on FcγR expression. Tumour-associated macrophages are well recognised to display varied activation states within a spectrum of two opposing poles: M1 and M2 (Biswas and Mantovani, 2010). These are associated with anti- and pro-tumoural activity respectively and are a result of the local cytokine milieu; in vitro data suggest cytokines can impact significantly upon on FcγR expression on cell lines (Grattage et al., 1992).

Where discrepancy in activity is observed between mouse models and the clinic, further investigation, rather than replacement with the next active compound is paramount. This is particularly relevant in the setting of immune-modulatory therapies where the potential benefits for responding patients are unparalleled. Anti-CTLA-4 antibodies are an example of this, where the impressive activity in mouse models was not recapitulated in the modest response rates observed in the clinical setting (Schadendorf et al., 2015). However, this is rarely acknowledged, perhaps because ipilimumab was the first drug to prolong survival in advanced melanoma (Hodi et al., 2010; Robert et al., 2011) and led to the current renaissance of tumour immunotherapy.

Having focused efforts on projects evaluating the tumour microenvironment in mouse models and human cancers in parallel, it is apparent that a majority of models used in this setting (when administered s.c. and excluding B16 melanoma) are most reflective of an inflamed human tumour microenvironment. As such, they are useful for determining the mechanisms of immune-based therapies which rely upon an existing inflamed tumour microenvironment and potentially also mechanisms of acquired resistance in this setting, but are of limited value in understanding intrinsic resistance.

Consistent with this as a potential explanation for the modest response rates observed with ipilimumab relative to mouse models (Leach et al., 1996; Schadendorf et al., 2015; Simpson et al., 2013), FcγR polymorphisms only appear to influence survival in patients with melanoma treated with ipilimumab in the context of high mutational or neoantigen burden. When considering the clinical development of Treg cell directed strategies, including those targeting CD25, this is of potential relevance and stratification may be required to identify those most likely to derive benefit. The presented pre-clinical data deciphering the in vivo activity of anti-CD25 mAbs also highlight once again the importance of considering the microenvironment in which the mAb is desired to have activity and potential inhibitory mechanisms that might be unique to or enriched within it.

Even in the context of combination immunotherapeutic approaches, a majority of patients fail to derive benefit (Gerlinger et al., 2012; Hellmann et al., 2018; Melero et al., 2014; Motzer et al., 2018). Paucity of T and NK cell infiltration represents a key barrier to the successful clinical application of immune checkpoint modulation (Melero et al., 2014). The presented immuno-genomic data provides novel insight into underlying drivers of T cell infiltration. A number of strategies are in clinical development which aim to promote T cell infiltration including oncolytic virotherapies (Ribas et al., 2017), however it remains unclear whether promoting T cell infiltration in this manner will overcome the challenge posed by intra-tumoural heterogeneity. Debulking strategies such as radiotherapy are potentially relevant in this context

(Twyman-Saint Victor et al., 2015), although these do not overcome the potential requirement for a bottleneck of clonal neoantigens to drive an effective immune response. A possible method of overcoming all such challenges is the adoptive transfer of T cells reactive to clonal neoantigens, however significant challenges are also posed herein including the source of T cells, their differentiation status, the ability to successfully infiltrate tumours and overcoming the regulatory mechanisms common to any activated T cell.

Recent data suggest that loss of MHC class I expression is not uncommon in advanced melanoma, representing an important mechanism of primary resistance to checkpoint blockade, but also with implications for adoptive therapeutic approaches (Rodig et al., 2018). Despite the focus of this thesis, such observations emphasize the importance of looking beyond T cells. Myeloid and stromal cells constitute a significant fraction of intra-tumoural cell subsets and have capacity to transform the TME (Gentles et al., 2015). Indeed, cancer-associated fibroblast-derived transforming growth factor beta (TGFβ) was recently demonstrated to play a key role in mediating T cell exclusion from tumours, influencing spatial patterns that had been observed for many years, yet remained unexplained (Mariathasan et al., 2018)

Within this thesis, the reciprocal exchange of pre-clinical and clinical data has been fundamental in driving clinically meaningful discoveries. Wherever possible, strategies should be in place for the integration of basic and clinical science, in this context collaboration is paramount and the work presented in this thesis strives to be reflective of such an approach.

7 Appendix

7.1 List of research papers and abstracts published during this PhD fellowship

7.1.1 Primary research articles (*denotes equal contribution)

Samson et al. Intravenous delivery of oncolytic reovirus to brain tumours in patients to immunologically prime for sequential checkpoint blockade. ***In Press, Science Translational Medicine*** (October 2017)

Chakravarthy A, **Furness AJS** et al. DNA methylation-based tumour deconvolution identifies immune drivers of survival in head and neck cancer. ***Submitted to Nature Medicine*** (September 2017)

Arce Vargas F*, **Furness AJS*** et al. Manipulation of Fc-FcR interaction influences the anti-tumor activity of human anti-CTLA-4 antibodies. ***Submitted to Immunity*** *(June 2017)*

Linch M et al. Intratumoural evolutionary landscape of high-risk prostate cancer: the PROGENY study of genomic and immune parameters. ***Annals of Oncology*** 28:2472-2480 (2017)

Abbosh C et al. Phylogenetic ctDNA analysis depicts early-stage lung cancer evolution. ***Nature*** 545(7655):446-451 (2017)

Jamal-Hanjani M et al. Tracking the Evolution of Non-Small-Cell Lung Cancer. ***N. Engl. J. Med.*** 376(22):2109-2121 (2017)

Arce Vargas F*, **Furness AJS*** et al. Depletion of tumor-infiltrating regulatory T cells with anti-CD25 requires Fc-optimization and synergizes with PD-1 blockade to eradicate established tumors. ***Immunity*** 46(4):577-586 (2017)

Bentzen A et al. Next-generation detection of antigen-responsive T cells using DNA barcode-labelled MHC-I multimers. ***Nature Biotechnology*** 34(10):1037-1045 (2016)

McGranahan N*, **Furness AJS***, Rosenthal R* et al. Clonal neoantigens elicit T cell immunoreactivity and response to checkpoint blockade. ***Science*** 351(6280):1463-9 (2016)

Wilkins A, **Furness AJS** et al. The melanoma-specific graded prognostic assessment does not adequately discriminate prognosis in a modern population with brain metastases from malignant melanoma. ***British Journal of Cancer*** 113(9):1275-81 (2015)

Martin-Liberal J, Furness AJS, Joshi K, Peggs KS, Quezada SA, Larkin J. Anti-programmed cell death-1 therapy and insulin-dependent diabetes. ***Cancer Immunology Immunotherapy*** 64(6): 765-7 (2015)

Kelderman S et al. Lactate dehydrogenase as a selection criterion for ipilimumab treatment in metastatic melanoma. ***Cancer Immunology Immunotherapy*** 63(5):449-58 (2014)

Gerlinger M, Quezada SA, Peggs KS, **Furness AJS** et al. Ultra-deep T-cell receptor sequencing reveals the complexity and intratumour heterogeneity of T-cell clones in renal cell carcinomas. ***The Journal of Pathology***. 231(4):424-32 (2013)

7.1.2 Review articles

Furness AJS, Quezada SA and Peggs KS. Neoantigen heterogeneity: a key driver of immune response and sensitivity to immune checkpoint blockade? ***Immunotherapy*** 8(7): 763-766 (2016)

Furness AJS, Joshi K, Peggs KS and Quezada SA. Biomarkers of response to immune modulatory therapies in cancer. ***. J Clin Cell Immunol*** 6:347 (2015)

Furness AJS, Arce-Vargas F, Peggs KS and Quezada S. Impact of tumour microenvironment and Fc receptors on the activity of immunomodulatory antibodies. ***Trends in Immunology****, Cell Press* 35(7):290-8 (2014)

7.1.3 Abstracts and presentations

Oral Presentations

Mapping the immune checkpoint landscape in human tumours. Companion Diagnostics Session. ***European Society for Medical Oncology Asia*****,** Singapore, 2016

ACP McElwain Prize Lecture, ***NCRI Cancer Conference*****,** Liverpool, U.K., 2016

Novel Insights into T cell Recognition and Regulation at the Tumour Site, invited speaker - plenary talk, Immunotherapy Session, ***AACR Precision Medicine Series: Targeting the Vulnerabilities of Cancer***, Miami, U.S.A., 2016

Characterisation of immune and tumour-specific neoantigen landscapes informs optimal therapeutic targeting in non-small cell lung cancer. ***CIMT****,* Mainz, Germany, 2016

Defining the genomic and transcriptomic aberrations underpinning spatial heterogeneity of immune infiltrates and its clinical impact in breast cancer. ***IMPAKT Breast Cancer Conference,*** Brussels, Belgium, 2016

Clonal neoantigens elicit T cell immunoreactivity and sensitivity to immune checkpoint blockade. Sylvia Lawler prize meeting, ***The Royal Society of Medicine***, London, U.K., 2016

Innovations in Cancer Research – Melanoma, ***The Royal Marsden NHS Foundation Trust***, London, U.K., 2016

'Immunotherapy', Cancer Research at UCL/UCLH - Public Open Day, Oral presentation, ***University College London***, London U.K. 2016

Targeting Cancer's Achilles Heel. ***UCL Clinical Trials Centre***, London, U.K., 2015

Poster Presentations

Pembrolizumab-induced subacute sensory ataxia, ***Submitted to British Thoracic Oncology Group Meeting*****,** Dublin, Ireland, 2018

Urine-derived lymphocytes (UDLs) as a non-invasive surrogate marker of tumour-infiltrating lymphocytes (TILs) in patients with muscle-invasive bladder cancer. ***European Cancer Congress (ESMO-ECCO)*****,** Madrid, Spain 2017

Identification and evaluation of immune recognition towards mutation-derived epitopes in NSCLC ***Cancer Immunology and Immunotherapy Keystone Symposium*****,** British Columbia, Canada, 2017

Immune cell profiling in bone marrow of myeloma patients post autologous stem cell transplantation reveals presence of cytotoxic CD4 and CD8 cells with prominent expression of LAG-3 and other checkpoint proteins. ***European Hematology Association Congress*****,** Madrid, Spain, 2017

ADAPTeR: A phase II study of anti-PD-1 (nivolumab) therapy as pre- and post-operative therapy in metastatic renal cell carcinoma, Poster presentation, ***American Society of Clinical Oncology - Annual Meeting***, Chicago, U.S.A., 2016

Defining the mechanisms of response and resistance to anti-PD-1 therapy: an exploratory phase II study of pembrolizumab in advanced melanoma (ADAPTeM), Poster presentation, ***American Society of Clinical Oncology - Annual Meeting***, Chicago, U.S.A., 2016

Heterogeneity in immune checkpoint molecule expression between T lymphocyte subsets in non-small cell lung cancer. ***CRUK Lung Cancer Centre of Excellence conference*****,** Manchester, U.K., 2015

Identification and characterisation of neoantigen-reactive tumour-infiltrating $CD8^+$ T lymphocytes in non-small cell lung cancer. ***CRUK Lung Cancer Centre of Excellence conference*****,** Manchester, U.K., 2015

Profiling of the immune tumour microenvironment generates a roadmap for checkpoint modulation in advanced melanoma. ***European Cancer Congress (ESMO-ECCO)*****,** Vienna, Austria, 2015

Enhancing intra-tumoural Treg depletion through antibody engineering and analysis of checkpoint landscape in cancer. ***CRI-CIMT-AACR- The Inaugural International Cancer Immunotherapy Conference: Translating Science into Survival*****,** New York, U.S.A., 2015

Exploring and exploiting the immunogenomic landscape for therapeutic gain in non-small cell lung cancer. ***CRUK Student/Post Doc Summer Conference*****,** York, U.K., July 2015

Serum Lactate dehydrogenase (LDH) as a prognostic selection criterion for ipilimumab treatment in metastatic melanoma. ***American Society of Clinical Oncology - Annual Meeting***, Chicago, U.S.A., 2013

Reference List

Alexandrov, L.B., Nik-Zainal, S., Wedge, D.C., Aparicio, S.A.J.R., Behjati, S., Biankin, A.V., Bignell, G.R., Bolli, N., Borg, A., Børresen-Dale, A.-L., et al. (2013). Signatures of mutational processes in human cancer. Nature *500*, 415–421.

Andersen, R.S., Kvistborg, P., Frøsig, T.M., Pedersen, N.W., Lyngaa, R., Bakker, A.H., Shu, C.J., Straten, P. thor, Schumacher, T.N., and Hadrup, S.R. (2012). Parallel detection of antigen-specific T cell responses by combinatorial encoding of MHC multimers. Nat. Protoc. *7*, 891–902.

Attia, P., Maker, A.V., Haworth, L.R., Rogers-Freezer, L., and Rosenberg, S.A. (2005). Inability of a fusion protein of IL-2 and diphtheria toxin (Denileukin Diftitox, DAB389IL-2, ONTAK) to eliminate regulatory T lymphocytes in patients with melanoma. J. Immunother. Hagerstown Md 1997 *28*, 582–592.

Bakker, A.H., Hoppes, R., Linnemann, C., Toebes, M., Rodenko, B., Berkers, C.R., Hadrup, S.R., van Esch, W.J.E., Heemskerk, M.H.M., Ovaa, H., et al. (2008). Conditional MHC class I ligands and peptide exchange technology for the human MHC gene products HLA-A1, -A3, -A11, and -B7. Proc. Natl. Acad. Sci. *105*, 3825–3830.

Barok, M., Isola, J., Pályi-Krekk, Z., Nagy, P., Juhász, I., Vereb, G., Kauraniemi, P., Kapanen, A., Tanner, M., Vereb, G., et al. (2007). Trastuzumab causes antibody-dependent cellular cytotoxicity-mediated growth inhibition of submacroscopic JIMT-1 breast cancer xenografts despite intrinsic drug resistance. Mol. Cancer Ther. *6*, 2065–2072.

Biswas, S.K., and Mantovani, A. (2010). Macrophage plasticity and interaction with lymphocyte subsets: cancer as a paradigm. Nat. Immunol. *11*, 889–896.

Bolland, S., Pearse, R.N., Kurosaki, T., and Ravetch, J.V. (1998). SHIP modulates immune receptor responses by regulating membrane association of Btk. Immunity *8*, 509–516.

Boyman, O., and Sprent, J. (2012). The role of interleukin-2 during homeostasis and activation of the immune system. Nat. Rev. Immunol. *12*, 180–190.

Brichard, V., Van Pel, A., Wölfel, T., Wölfel, C., De Plaen, E., Lethé, B., Coulie, P., and Boon, T. (1993). The tyrosinase gene codes for an antigen recognized by autologous cytolytic T lymphocytes on HLA-A2 melanomas. J. Exp. Med. *178*, 489–495.

Brown, S.D., Warren, R.L., Gibb, E.A., Martin, S.D., Spinelli, J.J., Nelson, B.H., and Holt, R.A. (2014). Neo-antigens predicted by tumor genome meta-analysis correlate with increased patient survival. Genome Res. *24*, 743–750.

van der Bruggen, P., Traversari, C., Chomez, P., Lurquin, C., De Plaen, E., Van den Eynde, B., Knuth, A., and Boon, T. (1991). A gene encoding an antigen recognized by cytolytic T lymphocytes on a human melanoma. Science *254*, 1643–1647.

Bruhns, P. (2012). Properties of mouse and human IgG receptors and their contribution to disease models. Blood *119*, 5640–5649.

Bruhns, P., Iannascoli, B., England, P., Mancardi, D.A., Fernandez, N., Jorieux, S., and Daëron, M. (2009). Specificity and affinity of human Fcγ receptors and their polymorphic variants for human IgG subclasses. Blood *113*, 3716–3725.

de Bruin, E.C., McGranahan, N., Mitter, R., Salm, M., Wedge, D.C., Yates, L., Jamal-Hanjani, M., Shafi, S., Murugaesu, N., Rowan, A.J., et al. (2014). Spatial and temporal diversity in genomic instability processes defines lung cancer evolution. Science *346*, 251–256.

Brunet, J.F., Denizot, F., Luciani, M.F., Roux-Dosseto, M., Suzan, M., Mattei, M.G., and Golstein, P. (1987). A new member of the immunoglobulin superfamily--CTLA-4. Nature *328*, 267–270.

Bulliard, Y., Jolicoeur, R., Windman, M., Rue, S.M., Ettenberg, S., Knee, D.A., Wilson, N.S., Dranoff, G., and Brogdon, J.L. (2013). Activating Fc γ receptors contribute to the antitumor activities of immunoregulatory receptor-targeting antibodies. J. Exp. Med. *210*, 1685–1693.

Bulliard, Y., Jolicoeur, R., Zhang, J., Dranoff, G., Wilson, N.S., and Brogdon, J.L. (2014). OX40 engagement depletes intratumoral Tregs via activating FcγRs, leading to antitumor efficacy. Immunol. Cell Biol. *92*, 475–480.

Cartron, G., Dacheux, L., Salles, G., Solal-Celigny, P., Bardos, P., Colombat, P., and Watier, H. (2002). Therapeutic activity of humanized anti-CD20 monoclonal antibody and polymorphism in IgG Fc receptor FcgammaRIIIa gene. Blood *99*, 754–758.

Castle, J.C., Kreiter, S., Diekmann, J., Löwer, M., van de Roemer, N., de Graaf, J., Selmi, A., Diken, M., Boegel, S., Paret, C., et al. (2012). Exploiting the mutanome for tumor vaccination. Cancer Res. *72*, 1081–1091.

Chang, C.X.L., Tan, A.T., Or, M.Y., Toh, K.Y., Lim, P.Y., Chia, A.S.E., Froesig, T.M., Nadua, K.D., Oh, H.-L.J., Leong, H.N., et al. (2013). Conditional ligands for Asian HLA variants facilitate the definition of $CD8^+$ T-cell responses in acute and chronic viral diseases: New technology. Eur. J. Immunol. *43*, 1109–1120.

Chen, H., Liakou, C.I., Kamat, A., Pettaway, C., Ward, J.F., Tang, D.N., Sun, J., Jungbluth, A.A., Troncoso, P., Logothetis, C., et al. (2009). Anti-CTLA-4 therapy results in higher CD4+ICOShi T cell frequency and IFN-gamma levels in both nonmalignant and malignant prostate tissues. Proc. Natl. Acad. Sci. U. S. A. *106*, 2729–2734.

Clynes, R.A., Towers, T.L., Presta, L.G., and Ravetch, J.V. (2000). Inhibitory Fc receptors modulate in vivo cytotoxicity against tumor targets. Nat. Med. *6*, 443–446.

Coe, D., Begom, S., Addey, C., White, M., Dyson, J., and Chai, J.-G. (2010). Depletion of regulatory T cells by anti-GITR mAb as a novel mechanism for cancer immunotherapy. Cancer Immunol. Immunother. CII *59*, 1367–1377.

Collins, A.V., Brodie, D.W., Gilbert, R.J.C., Iaboni, A., Manso-Sancho, R., Walse, B., Stuart, D.I., van der Merwe, P.A., and Davis, S.J. (2002). The interaction properties of costimulatory molecules revisited. Immunity *17*, 201–210.

Comin-Anduix, B., Escuin-Ordinas, H., and Ibarrondo, F.J. (2016). Tremelimumab: research and clinical development. OncoTargets Ther. *9*, 1767–1776.

Coulie, P.G., Brichard, V., Van Pel, A., Wölfel, T., Schneider, J., Traversari, C., Mattei, S., De Plaen, E., Lurquin, C., Szikora, J.P., et al. (1994). A new gene coding for a differentiation antigen recognized by autologous cytolytic T lymphocytes on HLA-A2 melanomas. J. Exp. Med. *180*, 35–42.

Curran, M.A., and Allison, J.P. (2009). Tumor vaccines expressing flt3 ligand synergize with ctla-4 blockade to reject preimplanted tumors. Cancer Res. *69*, 7747–7755.

Dahan, R., Sega, E., Engelhardt, J., Selby, M., Korman, A.J., and Ravetch, J.V. (2015). FcγRs Modulate the Anti-tumor Activity of Antibodies Targeting the PD-1/PD-L1 Axis. Cancer Cell *28*, 285–295.

D'Ambrosio, D., Hippen, K.L., Minskoff, S.A., Mellman, I., Pani, G., Siminovitch, K.A., and Cambier, J.C. (1995). Recruitment and activation of PTP1C in negative regulation of antigen receptor signaling by Fc gamma RIIB1. Science *268*, 293–297.

Damen, J.E., Liu, L., Rosten, P., Humphries, R.K., Jefferson, A.B., Majerus, P.W., and Krystal, G. (1996). The 145-kDa protein induced to associate with Shc by multiple cytokines is an inositol tetraphosphate and phosphatidylinositol 3,4,5-triphosphate 5-phosphatase. Proc. Natl. Acad. Sci. U. S. A. *93*, 1689–1693.

Dannull, J. (2005). Enhancement of vaccine-mediated antitumor immunity in cancer patients after depletion of regulatory T cells. J. Clin. Invest. *115*, 3623–3633.

De Simone, M., Arrigoni, A., Rossetti, G., Gruarin, P., Ranzani, V., Politano, C., Bonnal, R.J.P., Provasi, E., Sarnicola, M.L., Panzeri, I., et al. (2016). Transcriptional Landscape of Human Tissue Lymphocytes Unveils Uniqueness of Tumor-Infiltrating T Regulatory Cells. Immunity *45*, 1135–1147.

Duncan, A.R., Woof, J.M., Partridge, L.J., Burton, D.R., and Winter, G. (1988). Localization of the binding site for the human high-affinity Fc receptor on IgG. Nature *332*, 563–564.

van Elsas, A., Hurwitz, A.A., and Allison, J.P. (1999). Combination immunotherapy of B16 melanoma using anti-cytotoxic T lymphocyte-associated antigen 4 (CTLA-4) and granulocyte/macrophage colony-stimulating factor (GM-CSF)-producing vaccines induces rejection of subcutaneous and metastatic tumors accompanied by autoimmune depigmentation. J. Exp. Med. *190*, 355–366.

van Elsas, A., Sutmuller, R.P., Hurwitz, A.A., Ziskin, J., Villasenor, J., Medema, J.P., Overwijk, W.W., Restifo, N.P., Melief, C.J., Offringa, R., et al. (2001). Elucidating the autoimmune and antitumor effector mechanisms of a treatment based on cytotoxic T lymphocyte antigen-4 blockade in combination with a B16 melanoma vaccine: comparison of prophylaxis and therapy. J. Exp. Med. *194*, 481–489.

Fluckiger, A.C., Li, Z., Kato, R.M., Wahl, M.I., Ochs, H.D., Longnecker, R., Kinet, J.P., Witte, O.N., Scharenberg, A.M., and Rawlings, D.J. (1998). Btk/Tec kinases regulate sustained increases in intracellular Ca2+ following B-cell receptor activation. EMBO J. *17*, 1973–1985.

Frøsig, T.M., Yap, J., Seremet, T., Lyngaa, R., Svane, I.M., Thor Straten, P., Heemskerk, M.H.M., Grotenbreg, G.M., and Hadrup, S.R. (2015). Design and validation of conditional ligands for HLA-B*08:01, HLA-B*15:01, HLA-B*35:01, and HLA-B*44:05: Development of New Conditional Ligands. Cytometry A *87*, 967–975.

Furness, A.J.S., Vargas, F.A., Peggs, K.S., and Quezada, S.A. (2014). Impact of tumour microenvironment and Fc receptors on the activity of immunomodulatory antibodies. Trends Immunol. *35*, 290–298.

Gentles, A.J., Newman, A.M., Liu, C.L., Bratman, S.V., Feng, W., Kim, D., Nair, V.S., Xu, Y., Khuong, A., Hoang, C.D., et al. (2015). The prognostic landscape of genes and infiltrating immune cells across human cancers. Nat. Med. *21*, 938–945.

Gerlinger, M., Rowan, A.J., Horswell, S., Larkin, J., Endesfelder, D., Gronroos, E., Martinez, P., Matthews, N., Stewart, A., Tarpey, P., et al. (2012). Intratumor heterogeneity and branched evolution revealed by multiregion sequencing. N. Engl. J. Med. *366*, 883–892.

Gerlinger, M., Horswell, S., Larkin, J., Rowan, A.J., Salm, M.P., Varela, I., Fisher, R., McGranahan, N., Matthews, N., Santos, C.R., et al. (2014). Genomic architecture and evolution of clear cell renal cell carcinomas defined by multiregion sequencing. Nat. Genet. *46*, 225–233.

Ghazizadeh, S., Bolen, J.B., and Fleit, H.B. (1994). Physical and functional association of Src-related protein tyrosine kinases with Fc gamma RII in monocytic THP-1 cells. J. Biol. Chem. *269*, 8878–8884.

Gilboa, E. (1999). The makings of a tumor rejection antigen. Immunity *11*, 263–270.

Golay, J., Cortiana, C., Manganini, M., Cazzaniga, G., Salvi, A., Spinelli, O., Bassan, R., Barbui, T., Biondi, A., Rambaldi, A., et al. (2006). The sensitivity of acute lymphoblastic leukemia cells carrying the t(12;21) translocation to campath-1H-mediated cell lysis. Haematologica *91*, 322–330.

Golgher, D., Jones, E., Powrie, F., Elliott, T., and Gallimore, A. (2002). Depletion of CD25+ regulatory cells uncovers immune responses to shared murine tumor rejection antigens. Eur. J. Immunol. *32*, 3267–3275.

Grattage, L.P., McKenzie, I.F., and Hogarth, P.M. (1992). Effects of PMA, cytokines and dexamethasone on the expression of cell surface Fc receptors and mRNA in U937 cells. Immunol. Cell Biol. *70 (Pt 2)*, 97–105.

Gros, A., Robbins, P.F., Yao, X., Li, Y.F., Turcotte, S., Tran, E., Wunderlich, J.R., Mixon, A., Farid, S., Dudley, M.E., et al. (2014). PD-1 identifies the patient-specific CD8+ tumor-reactive repertoire infiltrating human tumors. J. Clin. Invest. *124*, 2246–2259.

Grugan, K.D., McCabe, F.L., Kinder, M., Greenplate, A.R., Harman, B.C., Ekert, J.E., van Rooijen, N., Anderson, G.M., Nemeth, J.A., Strohl, W.R., et al. (2012). Tumor-associated macrophages promote invasion while retaining Fc-dependent anti-tumor function. J. Immunol. Baltim. Md 1950 *189*, 5457–5466.

Guilliams, M., Bruhns, P., Saeys, Y., Hammad, H., and Lambrecht, B.N. (2014). The function of Fcγ receptors in dendritic cells and macrophages. Nat. Rev. Immunol. *14*, 94–108.

Hadrup, S.R., Bakker, A.H., Shu, C.J., Andersen, R.S., van Veluw, J., Hombrink, P., Castermans, E., Thor Straten, P., Blank, C., Haanen, J.B., et al. (2009). Parallel detection of antigen-specific T-cell responses by multidimensional encoding of MHC multimers. Nat. Methods *6*, 520–526.

de Haij, S., Jansen, J.H.M., Boross, P., Beurskens, F.J., Bakema, J.E., Bos, D.L., Martens, A., Verbeek, J.S., Parren, P.W.H.I., van de Winkel, J.G.J., et al. (2010). In vivo cytotoxicity of type I CD20 antibodies critically depends on Fc receptor ITAM signaling. Cancer Res. *70*, 3209–3217.

Hamaguchi, Y., Xiu, Y., Komura, K., Nimmerjahn, F., and Tedder, T.F. (2006). Antibody isotype-specific engagement of Fcγ receptors regulates B lymphocyte depletion during CD20 immunotherapy. J. Exp. Med. *203*, 743–753.

Hanson, D.C., Canniff, P.C., Primiano, M.J., Donovan, C.B., Gardner, J.P., Natoli, E.J., Morgan, R.W., Mather, R.J., Singleton, D.H., Hermes, P.A., et al. (2004). Preclinical in vitro characterization of anti-CTLA4 therapeutic antibody CP-675,206. Cancer Res. *64*, 877–877.

Hara, M., Nakanishi, H., Tsujimura, K., Matsui, M., Yatabe, Y., Manabe, T., and Tatematsu, M. (2008). Interleukin-2 potentiation of cetuximab antitumor

activity for epidermal growth factor receptor-overexpressing gastric cancer xenografts through antibody-dependent cellular cytotoxicity. Cancer Sci. *99*, 1471–1478.

Hellmann, M.D., Ciuleanu, T.-E., Pluzanski, A., Lee, J.S., Otterson, G.A., Audigier-Valette, C., Minenza, E., Linardou, H., Burgers, S., Salman, P., et al. (2018). Nivolumab plus Ipilimumab in Lung Cancer with a High Tumor Mutational Burden. N. Engl. J. Med.

Hodi, F.S., Butler, M., Oble, D.A., Seiden, M.V., Haluska, F.G., Kruse, A., Macrae, S., Nelson, M., Canning, C., Lowy, I., et al. (2008). Immunologic and clinical effects of antibody blockade of cytotoxic T lymphocyte-associated antigen 4 in previously vaccinated cancer patients. Proc. Natl. Acad. Sci. U. S. A. *105*, 3005–3010.

Hodi, F.S., O'Day, S.J., McDermott, D.F., Weber, R.W., Sosman, J.A., Haanen, J.B., Gonzalez, R., Robert, C., Schadendorf, D., Hassel, J.C., et al. (2010). Improved survival with ipilimumab in patients with metastatic melanoma. N. Engl. J. Med. *363*, 711–723.

Hom, S.S., Schwartzentruber, D.J., Rosenberg, S.A., and Topalian, S.L. (1993). Specific release of cytokines by lymphocytes infiltrating human melanomas in response to shared melanoma antigens. J. Immunother. Emphas. Tumor Immunol. Off. J. Soc. Biol. Ther. *13*, 18–30.

Hoof, I., Peters, B., Sidney, J., Pedersen, L.E., Sette, A., Lund, O., Buus, S., and Nielsen, M. (2009). NetMHCpan, a method for MHC class I binding prediction beyond humans. Immunogenetics *61*, 1–13.

Huang, A.C., Postow, M.A., Orlowski, R.J., Mick, R., Bengsch, B., Manne, S., Xu, W., Harmon, S., Giles, J.R., Wenz, B., et al. (2017). T-cell invigoration to tumour burden ratio associated with anti-PD-1 response. Nature *545*, 60–65.

Hurwitz, A.A., Foster, B.A., Kwon, E.D., Truong, T., Choi, E.M., Greenberg, N.M., Burg, M.B., and Allison, J.P. (2000). Combination immunotherapy of primary prostate cancer in a transgenic mouse model using CTLA-4 blockade. Cancer Res. *60*, 2444–2448.

Iwama, S., De Remigis, A., Callahan, M.K., Slovin, S.F., Wolchok, J.D., and Caturegli, P. (2014). Pituitary expression of CTLA-4 mediates hypophysitis secondary to administration of CTLA-4 blocking antibody. Sci. Transl. Med. *6*, 230ra45.

Jacobs, J.F.M., Punt, C.J.A., Lesterhuis, W.J., Sutmuller, R.P.M., Brouwer, H.M. -l. H., Scharenborg, N.M., Klasen, I.S., Hilbrands, L.B., Figdor, C.G., de Vries, I.J.M., et al. (2010). Dendritic Cell Vaccination in Combination with Anti-CD25 Monoclonal Antibody Treatment: A Phase I/II Study in Metastatic Melanoma Patients. Clin. Cancer Res. *16*, 5067–5078.

Jamal-Hanjani, M., Wilson, G.A., McGranahan, N., Birkbak, N.J., Watkins, T.B.K., Veeriah, S., Shafi, S., Johnson, D.H., Mitter, R., Rosenthal, R., et al.

(2017). Tracking the Evolution of Non–Small-Cell Lung Cancer. N. Engl. J. Med. *376*, 2109–2121.

Janik, J.E., Morris, J.C., O'Mahony, D., Pittaluga, S., Jaffe, E.S., Redon, C.E., Bonner, W.M., Brechbiel, M.W., Paik, C.H., Whatley, M., et al. (2015). ^{90} Y-daclizumab, an anti-CD25 monoclonal antibody, provided responses in 50% of patients with relapsed Hodgkin's lymphoma. Proc. Natl. Acad. Sci. *112*, 13045–13050.

Ji, R.-R., Chasalow, S.D., Wang, L., Hamid, O., Schmidt, H., Cogswell, J., Alaparthy, S., Berman, D., Jure-Kunkel, M., Siemers, N.O., et al. (2012). An immune-active tumor microenvironment favors clinical response to ipilimumab. Cancer Immunol. Immunother. CII *61*, 1019–1031.

Jie, H.-B., Schuler, P.J., Lee, S.C., Srivastava, R.M., Argiris, A., Ferrone, S., Whiteside, T.L., and Ferris, R.L. (2015). CTLA-4^{+} Regulatory T Cells Increased in Cetuximab-Treated Head and Neck Cancer Patients Suppress NK Cell Cytotoxicity and Correlate with Poor Prognosis. Cancer Res. *75*, 2200–2210.

Jiménez-Sánchez, A., Memon, D., Pourpe, S., Veeraraghavan, H., Li, Y., Vargas, H.A., Gill, M.B., Park, K.J., Zivanovic, O., Konner, J., et al. (2017). Heterogeneous Tumor-Immune Microenvironments among Differentially Growing Metastases in an Ovarian Cancer Patient. Cell *170*, 927–938.e20.

Johnson, P., and Glennie, M. (2003). The mechanisms of action of rituximab in the elimination of tumor cells. Semin. Oncol. *30*, 3–8.

Johnson, D.B., Balko, J.M., Compton, M.L., Chalkias, S., Gorham, J., Xu, Y., Hicks, M., Puzanov, I., Alexander, M.R., Bloomer, T.L., et al. (2016). Fulminant Myocarditis with Combination Immune Checkpoint Blockade. N. Engl. J. Med. *375*, 1749–1755.

Jones, E., Dahm-Vicker, M., Simon, A.K., Green, A., Powrie, F., Cerundolo, V., and Gallimore, A. (2002). Depletion of CD25+ regulatory cells results in suppression of melanoma growth and induction of autoreactivity in mice. Cancer Immun. *2*, 1.

June, C.H. (2007). Adoptive T cell therapy for cancer in the clinic. J. Clin. Invest. *117*, 1466–1476.

Kalergis, A.M., and Ravetch, J.V. (2002). Inducing tumor immunity through the selective engagement of activating Fcgamma receptors on dendritic cells. J. Exp. Med. *195*, 1653–1659.

Kavanagh, B., O'Brien, S., Lee, D., Hou, Y., Weinberg, V., Rini, B., Allison, J.P., Small, E.J., and Fong, L. (2008). CTLA4 blockade expands FoxP3+ regulatory and activated effector CD4+ T cells in a dose-dependent fashion. Blood *112*, 1175–1183.

Kawakami, Y., Zakut, R., Topalian, S.L., Stötter, H., and Rosenberg, S.A. (1992). Shared human melanoma antigens. Recognition by tumor-infiltrating

lymphocytes in HLA-A2.1-transfected melanomas. J. Immunol. Baltim. Md 1950 *148*, 638–643.

Kawakami, Y., Eliyahu, S., Delgado, C.H., Robbins, P.F., Sakaguchi, K., Appella, E., Yannelli, J.R., Adema, G.J., Miki, T., and Rosenberg, S.A. (1994). Identification of a human melanoma antigen recognized by tumor-infiltrating lymphocytes associated with in vivo tumor rejection. Proc. Natl. Acad. Sci. U. S. A. *91*, 6458–6462.

Kim, J.M., Rasmussen, J.P., and Rudensky, A.Y. (2007). Regulatory T cells prevent catastrophic autoimmunity throughout the lifespan of mice. Nat. Immunol. *8*, 191–197.

Koene, H.R., Kleijer, M., Algra, J., Roos, D., von dem Borne, A.E., and de Haas, M. (1997). Fc gammaRIIIa-158V/F polymorphism influences the binding of IgG by natural killer cell Fc gammaRIIIa, independently of the Fc gammaRIIIa-48L/R/H phenotype. Blood *90*, 1109–1114.

Krummel, M.F., and Allison, J.P. (1996). CTLA-4 engagement inhibits IL-2 accumulation and cell cycle progression upon activation of resting T cells. J. Exp. Med. *183*, 2533–2540.

Larkin, J., Chiarion-Sileni, V., Gonzalez, R., Grob, J.J., Cowey, C.L., Lao, C.D., Schadendorf, D., Dummer, R., Smylie, M., Rutkowski, P., et al. (2015). Combined Nivolumab and Ipilimumab or Monotherapy in Untreated Melanoma. N. Engl. J. Med. *373*, 23–34.

Lawrence, M.S., Stojanov, P., Mermel, C.H., Robinson, J.T., Garraway, L.A., Golub, T.R., Meyerson, M., Gabriel, S.B., Lander, E.S., and Getz, G. (2014). Discovery and saturation analysis of cancer genes across 21 tumour types. Nature *505*, 495–501.

Lazar, G.A., Dang, W., Karki, S., Vafa, O., Peng, J.S., Hyun, L., Chan, C., Chung, H.S., Eivazi, A., Yoder, S.C., et al. (2006). Engineered antibody Fc variants with enhanced effector function. Proc. Natl. Acad. Sci. U. S. A. *103*, 4005–4010.

Leach, D.R., Krummel, M.F., and Allison, J.P. (1996). Enhancement of antitumor immunity by CTLA-4 blockade. Science *271*, 1734–1736.

Li, S., Schmitz, K.R., Jeffrey, P.D., Wiltzius, J.J.W., Kussie, P., and Ferguson, K.M. (2005). Structural basis for inhibition of the epidermal growth factor receptor by cetuximab. Cancer Cell *7*, 301–311.

Li, X., Gibson, A.W., and Kimberly, R.P. (2014). Human FcR Polymorphism and Disease. In Fc Receptors, M. Daeron, and F. Nimmerjahn, eds. (Cham: Springer International Publishing), pp. 275–302.

Liakou, C.I., Kamat, A., Tang, D.N., Chen, H., Sun, J., Troncoso, P., Logothetis, C., and Sharma, P. (2008). CTLA-4 blockade increases IFNgamma-producing CD4+ICOShi cells to shift the ratio of effector to

regulatory T cells in cancer patients. Proc. Natl. Acad. Sci. U. S. A. *105*, 14987–14992.

Liu, Q., Oliveira-Dos-Santos, A.J., Mariathasan, S., Bouchard, D., Jones, J., Sarao, R., Kozieradzki, I., Ohashi, P.S., Penninger, J.M., and Dumont, D.J. (1998). The inositol polyphosphate 5-phosphatase ship is a crucial negative regulator of B cell antigen receptor signaling. J. Exp. Med. *188*, 1333–1342.

Long, G.V., Atkinson, V., Cebon, J.S., Jameson, M.B., Fitzharris, B.M., McNeil, C.M., Hill, A.G., Ribas, A., Atkins, M.B., Thompson, J.A., et al. (2017). Standard-dose pembrolizumab in combination with reduced-dose ipilimumab for patients with advanced melanoma (KEYNOTE-029): an open-label, phase 1b trial. Lancet Oncol.

Lu, Y.-C., Yao, X., Li, Y.F., El-Gamil, M., Dudley, M.E., Yang, J.C., Almeida, J.R., Douek, D.C., Samuels, Y., Rosenberg, S.A., et al. (2013). Mutated PPP1R3B is recognized by T cells used to treat a melanoma patient who experienced a durable complete tumor regression. J. Immunol. Baltim. Md 1950 *190*, 6034–6042.

Luke, J.J., Zha, Y., Matijevich, K., and Gajewski, T.F. (2016). Single dose denileukin diftitox does not enhance vaccine-induced T cell responses or effectively deplete Tregs in advanced melanoma: immune monitoring and clinical results of a randomized phase II trial. J. Immunother. Cancer *4*.

Lute, K.D., May, K.F., Lu, P., Zhang, H., Kocak, E., Mosinger, B., Wolford, C., Phillips, G., Caligiuri, M.A., Zheng, P., et al. (2005). Human CTLA4 knock-in mice unravel the quantitative link between tumor immunity and autoimmunity induced by anti-CTLA-4 antibodies. Blood *106*, 3127–3133.

Mahnke, K., Schönfeld, K., Fondel, S., Ring, S., Karakhanova, S., Wiedemeyer, K., Bedke, T., Johnson, T.S., Storn, V., Schallenberg, S., et al. (2007). Depletion of CD4+CD25+ human regulatory T cellsin vivo: Kinetics of Treg depletion and alterations in immune functionsin vivo andin vitro. Int. J. Cancer *120*, 2723–2733.

Mariathasan, S., Turley, S.J., Nickles, D., Castiglioni, A., Yuen, K., Wang, Y., Kadel, E.E., Koeppen, H., Astarita, J.L., Cubas, R., et al. (2018). TGFβ attenuates tumour response to PD-L1 blockade by contributing to exclusion of T cells. Nature *554*, 544–548.

Matsushita, H., Vesely, M.D., Koboldt, D.C., Rickert, C.G., Uppaluri, R., Magrini, V.J., Arthur, C.D., White, J.M., Chen, Y.-S., Shea, L.K., et al. (2012). Cancer exome analysis reveals a T-cell-dependent mechanism of cancer immunoediting. Nature *482*, 400–404.

McGranahan, N., Furness, A.J.S., Rosenthal, R., Ramskov, S., Lyngaa, R., Saini, S.K., Jamal-Hanjani, M., Wilson, G.A., Birkbak, N.J., Hiley, C.T., et al. (2016). Clonal neoantigens elicit T cell immunoreactivity and sensitivity to immune checkpoint blockade. Science.

Melero, I., Rouzaut, A., Motz, G.T., and Coukos, G. (2014). T-Cell and NK-Cell Infiltration into Solid Tumors: A Key Limiting Factor for Efficacious Cancer Immunotherapy. Cancer Discov. *4*, 522–526.

Mellor, J.D., Brown, M.P., Irving, H.R., Zalcberg, J.R., and Dobrovic, A. (2013). A critical review of the role of Fc gamma receptor polymorphisms in the response to monoclonal antibodies in cancer. J. Hematol. Oncol.J Hematol Oncol *6*, 1.

Mendez, S., Reckling, S.K., Piccirillo, C.A., Sacks, D., and Belkaid, Y. (2004). Role for $CD4^+$ $CD25^+$ Regulatory T Cells in Reactivation of Persistent Leishmaniasis and Control of Concomitant Immunity. J. Exp. Med. *200*, 201–210.

Motzer, R.J., Tannir, N.M., McDermott, D.F., Arén Frontera, O., Melichar, B., Choueiri, T.K., Plimack, E.R., Barthélémy, P., Porta, C., George, S., et al. (2018). Nivolumab plus Ipilimumab versus Sunitinib in Advanced Renal-Cell Carcinoma. N. Engl. J. Med. *378*, 1277–1290.

Musolino, A., Naldi, N., Bortesi, B., Pezzuolo, D., Capelletti, M., Missale, G., Laccabue, D., Zerbini, A., Camisa, R., Bisagni, G., et al. (2008). Immunoglobulin G fragment C receptor polymorphisms and clinical efficacy of trastuzumab-based therapy in patients with HER-2/neu-positive metastatic breast cancer. J. Clin. Oncol. Off. J. Am. Soc. Clin. Oncol. *26*, 1789–1796.

Muta, T., Kurosaki, T., Misulovin, Z., Sanchez, M., Nussenzweig, M.C., and Ravetch, J.V. (1994). A 13-amino-acid motif in the cytoplasmic domain of Fc gamma RIIB modulates B-cell receptor signalling. Nature *369*, 340.

Nathanson, T., Ahuja, A., Rubinsteyn, A., Aksoy, B.A., Hellmann, M.D., Miao, D.D., Allen, E.V., Merghoub, T., Wolchok, J.D., Snyder, A., et al. (2016). Somatic Mutations and Neoepitope Homology in Melanomas Treated with CTLA-4 Blockade. Cancer Immunol. Res. canimm.0019.2016.

Nielsen, M., Lundegaard, C., Blicher, T., Lamberth, K., Harndahl, M., Justesen, S., Røder, G., Peters, B., Sette, A., Lund, O., et al. (2007). NetMHCpan, a Method for Quantitative Predictions of Peptide Binding to Any HLA-A and -B Locus Protein of Known Sequence. PLoS ONE *2*, e796.

Nimmerjahn, F., and Ravetch, J.V. (2005). Divergent immunoglobulin g subclass activity through selective Fc receptor binding. Science *310*, 1510–1512.

Nimmerjahn, F., and Ravetch, J.V. (2007). Antibodies, Fc receptors and cancer. Curr. Opin. Immunol. *19*, 239–245.

Nimmerjahn, F., Bruhns, P., Horiuchi, K., and Ravetch, J.V. (2005). FcgammaRIV: a novel FcR with distinct IgG subclass specificity. Immunity *23*, 41–51.

Onizuka, S., Tawara, I., Shimizu, J., Sakaguchi, S., Fujita, T., and Nakayama, E. (1999). Tumor Rejection by in Vivo Administration of Anti-CD25 (Interleukin-2 Receptor α) Monoclonal Antibody. Cancer Res. *59*, 3128–3133.

Ono, M., Bolland, S., Tempst, P., and Ravetch, J.V. (1996). Role of the inositol phosphatase SHIP in negative regulation of the immune system by the receptor Fc(gamma)RIIB. Nature *383*, 263–266.

Parren, P.W., Warmerdam, P.A., Boeije, L.C., Arts, J., Westerdaal, N.A., Vlug, A., Capel, P.J., Aarden, L.A., and van de Winkel, J.G. (1992). On the interaction of IgG subclasses with the low affinity Fc gamma RIIa (CD32) on human monocytes, neutrophils, and platelets. Analysis of a functional polymorphism to human IgG2. J. Clin. Invest. *90*, 1537–1546.

Peggs, K.S., Quezada, S.A., Chambers, C.A., Korman, A.J., and Allison, J.P. (2009). Blockade of CTLA-4 on both effector and regulatory T cell compartments contributes to the antitumor activity of anti-CTLA-4 antibodies. J. Exp. Med. *206*, 1717–1725.

Pentcheva-Hoang, T., Egen, J.G., Wojnoonski, K., and Allison, J.P. (2004). B7-1 and B7-2 selectively recruit CTLA-4 and CD28 to the immunological synapse. Immunity *21*, 401–413.

Plitas, G., Konopacki, C., Wu, K., Bos, P.D., Morrow, M., Putintseva, E.V., Chudakov, D.M., and Rudensky, A.Y. (2016). Regulatory T Cells Exhibit Distinct Features in Human Breast Cancer. Immunity *45*, 1122–1134.

Quezada, S.A., Peggs, K.S., Curran, M.A., and Allison, J.P. (2006). CTLA4 blockade and GM-CSF combination immunotherapy alters the intratumor balance of effector and regulatory T cells. J. Clin. Invest. *116*, 1935–1945.

Quezada, S.A., Peggs, K.S., Simpson, T.R., Shen, Y., Littman, D.R., and Allison, J.P. (2008). Limited tumor infiltration by activated T effector cells restricts the therapeutic activity of regulatory T cell depletion against established melanoma. J. Exp. Med. *205*, 2125–2138.

Rasku, M., Clem, A.L., Telang, S., Taft, B., Gettings, K., Gragg, H., Cramer, D., Lear, S.C., McMasters, K.M., Miller, D.M., et al. (2008). Transient T cell depletion causes regression of melanoma metastases. J. Transl. Med. *6*, 12.

Ravetch, J.V., and Lanier, L.L. (2000). Immune inhibitory receptors. Science *290*, 84–89.

Read, S., Malmström, V., and Powrie, F. (2000). Cytotoxic T lymphocyte-associated antigen 4 plays an essential role in the function of CD25(+)CD4(+) regulatory cells that control intestinal inflammation. J. Exp. Med. *192*, 295–302.

Read, S., Greenwald, R., Izcue, A., Robinson, N., Mandelbrot, D., Francisco, L., Sharpe, A.H., and Powrie, F. (2006). Blockade of CTLA-4 on CD4+CD25+ regulatory T cells abrogates their function in vivo. J. Immunol. Baltim. Md 1950 *177*, 4376–4383.

Rech, A.J., Mick, R., Martin, S., Recio, A., Aqui, N.A., Powell, D.J., Colligon, T.A., Trosko, J.A., Leinbach, L.I., Pletcher, C.H., et al. (2012). CD25 Blockade Depletes and Selectively Reprograms Regulatory T Cells in Concert with Immunotherapy in Cancer Patients. Sci. Transl. Med. *4*, 134ra62-134ra62.

Reck, M., Rodríguez-Abreu, D., Robinson, A.G., Hui, R., Csőszi, T., Fülöp, A., Gottfried, M., Peled, N., Tafreshi, A., Cuffe, S., et al. (2016). Pembrolizumab versus Chemotherapy for PD-L1–Positive Non–Small-Cell Lung Cancer. N. Engl. J. Med. *375*, 1823–1833.

Redpath, S., Michaelsen, T.E., Sandlie, I., and Clark, M.R. (1998). The influence of the hinge region length in binding of human IgG to human Fcgamma receptors. Hum. Immunol. *59*, 720–727.

Ribas, A., Kefford, R., Marshall, M.A., Punt, C.J.A., Haanen, J.B., Marmol, M., Garbe, C., Gogas, H., Schachter, J., Linette, G., et al. (2013). Phase III Randomized Clinical Trial Comparing Tremelimumab With Standard-of-Care Chemotherapy in Patients With Advanced Melanoma. J. Clin. Oncol. JCO.2012.44.6112.

Ribas, A., Dummer, R., Puzanov, I., VanderWalde, A., Andtbacka, R.H.I., Michielin, O., Olszanski, A.J., Malvehy, J., Cebon, J., Fernandez, E., et al. (2017). Oncolytic Virotherapy Promotes Intratumoral T Cell Infiltration and Improves Anti-PD-1 Immunotherapy. Cell *170*, 1109–1119.e10.

Rizvi, N.A., Hellmann, M.D., Snyder, A., Kvistborg, P., Makarov, V., Havel, J.J., Lee, W., Yuan, J., Wong, P., Ho, T.S., et al. (2015). Cancer immunology. Mutational landscape determines sensitivity to PD-1 blockade in non-small cell lung cancer. Science *348*, 124–128.

Robbins, P.F., Lu, Y.-C., El-Gamil, M., Li, Y.F., Gross, C., Gartner, J., Lin, J.C., Teer, J.K., Cliften, P., Tycksen, E., et al. (2013). Mining exomic sequencing data to identify mutated antigens recognized by adoptively transferred tumor-reactive T cells. Nat. Med. *19*, 747–752.

Robert, C., Thomas, L., Bondarenko, I., O'Day, S., M D, J.W., Garbe, C., Lebbe, C., Baurain, J.-F., Testori, A., Grob, J.-J., et al. (2011). Ipilimumab plus dacarbazine for previously untreated metastatic melanoma. N. Engl. J. Med. *364*, 2517–2526.

Rodig, S.J., Gusenleitner, D., Jackson, D.G., Gjini, E., Giobbie-Hurder, A., Jin, C., Chang, H., Lovitch, S.B., Horak, C., Weber, J.S., et al. (2018). MHC proteins confer differential sensitivity to CTLA-4 and PD-1 blockade in untreated metastatic melanoma. Sci. Transl. Med. *10*.

Romano, E., Kusio-Kobialka, M., Foukas, P.G., Baumgaertner, P., Meyer, C., Ballabeni, P., Michielin, O., Weide, B., Romero, P., and Speiser, D.E. (2015). Ipilimumab-dependent cell-mediated cytotoxicity of regulatory T cells ex vivo by nonclassical monocytes in melanoma patients. Proc. Natl. Acad. Sci. U. S. A. *112*, 6140–6145.

van Rooij, N., van Buuren, M.M., Philips, D., Velds, A., Toebes, M., Heemskerk, B., van Dijk, L.J.A., Behjati, S., Hilkmann, H., El Atmioui, D., et al. (2013). Tumor exome analysis reveals neoantigen-specific T-cell reactivity in an ipilimumab-responsive melanoma. J. Clin. Oncol. Off. J. Am. Soc. Clin. Oncol. *31*, e439-442.

Rooney, M.S., Shukla, S.A., Wu, C.J., Getz, G., and Hacohen, N. (2015). Molecular and genetic properties of tumors associated with local immune cytolytic activity. Cell *160*, 48–61.

Rosenberg, S.A., Packard, B.S., Aebersold, P.M., Solomon, D., Topalian, S.L., Toy, S.T., Simon, P., Lotze, M.T., Yang, J.C., and Seipp, C.A. (1988). Use of tumor-infiltrating lymphocytes and interleukin-2 in the immunotherapy of patients with metastatic melanoma. A preliminary report. N. Engl. J. Med. *319*, 1676–1680.

Sakaguchi, S., Sakaguchi, N., Asano, M., Itoh, M., and Toda, M. (1995). Immunologic self-tolerance maintained by activated T cells expressing IL-2 receptor alpha-chains (CD25). Breakdown of a single mechanism of self-tolerance causes various autoimmune diseases. J. Immunol. Baltim. Md 1950 *155*, 1151–1164.

Sakaguchi, S., Sakaguchi, N., Shimizu, J., Yamazaki, S., Sakihama, T., Itoh, M., Kuniyasu, Y., Nomura, T., Toda, M., and Takahashi, T. (2001). Immunologic tolerance maintained by CD25+ CD4+ regulatory T cells: their common role in controlling autoimmunity, tumor immunity, and transplantation tolerance. Immunol. Rev. *182*, 18–32.

Salmon, J.E., Edberg, J.C., Brogle, N.L., and Kimberly, R.P. (1992). Allelic polymorphisms of human Fc gamma receptor IIA and Fc gamma receptor IIIB. Independent mechanisms for differences in human phagocyte function. J. Clin. Invest. *89*, 1274–1281.

Salomon, B., Lenschow, D.J., Rhee, L., Ashourian, N., Singh, B., Sharpe, A., and Bluestone, J.A. (2000). B7/CD28 Costimulation Is Essential for the Homeostasis of the CD4+CD25+ Immunoregulatory T Cells that Control Autoimmune Diabetes. Immunity *12*, 431–440.

Sampson, J.H., Schmittling, R.J., Archer, G.E., Congdon, K.L., Nair, S.K., Reap, E.A., Desjardins, A., Friedman, A.H., Friedman, H.S., Herndon, J.E., et al. (2012). A Pilot Study of IL-2Rα Blockade during Lymphopenia Depletes Regulatory T-cells and Correlates with Enhanced Immunity in Patients with Glioblastoma. PLoS ONE *7*, e31046.

Sarmay, G., Lund, J., Rozsnyay, Z., Gergely, J., and Jefferis, R. (1992). Mapping and comparison of the interaction sites on the Fc region of IgG responsible for triggering antibody dependent cellular cytotoxicity (ADCC) through different types of human Fc gamma receptor. Mol. Immunol. *29*, 633–639.

Schadendorf, D., Hodi, F.S., Robert, C., Weber, J.S., Margolin, K., Hamid, O., Patt, D., Chen, T.-T., Berman, D.M., and Wolchok, J.D. (2015). Pooled Analysis of Long-Term Survival Data From Phase II and Phase III Trials of Ipilimumab in Unresectable or Metastatic Melanoma. J. Clin. Oncol. Off. J. Am. Soc. Clin. Oncol. *33*, 1889–1894.

Scharenberg, A.M., El-Hillal, O., Fruman, D.A., Beitz, L.O., Li, Z., Lin, S., Gout, I., Cantley, L.C., Rawlings, D.J., and Kinet, J.P. (1998). Phosphatidylinositol-3,4,5-trisphosphate (PtdIns-3,4,5-P3)/Tec kinase-dependent calcium signaling pathway: a target for SHIP-mediated inhibitory signals. EMBO J. *17*, 1961–1972.

Schmidt, E.M., Wang, C.J., Ryan, G.A., Clough, L.E., Qureshi, O.S., Goodall, M., Abbas, A.K., Sharpe, A.H., Sansom, D.M., and Walker, L.S.K. (2009). Ctla-4 controls regulatory T cell peripheral homeostasis and is required for suppression of pancreatic islet autoimmunity. J. Immunol. Baltim. Md 1950 *182*, 274–282.

Schneider-Merck, T., Lammerts van Bueren, J.J., Berger, S., Rossen, K., van Berkel, P.H.C., Derer, S., Beyer, T., Lohse, S., Bleeker, W.K., Peipp, M., et al. (2010). Human IgG2 antibodies against epidermal growth factor receptor effectively trigger antibody-dependent cellular cytotoxicity but, in contrast to IgG1, only by cells of myeloid lineage. J. Immunol. Baltim. Md 1950 *184*, 512–520.

Schumacher, T.N., and Schreiber, R.D. (2015). Neoantigens in cancer immunotherapy. Science *348*, 69–74.

Schwab, I., and Nimmerjahn, F. (2013). Intravenous immunoglobulin therapy: how does IgG modulate the immune system? Nat. Rev. Immunol. *13*, 176–189.

Schwartz, J.C., Zhang, X., Fedorov, A.A., Nathenson, S.G., and Almo, S.C. (2001). Structural basis for co-stimulation by the human CTLA-4/B7-2 complex. Nature *410*, 604–608.

Segal, N.H., Parsons, D.W., Peggs, K.S., Velculescu, V., Kinzler, K.W., Vogelstein, B., and Allison, J.P. (2008). Epitope landscape in breast and colorectal cancer. Cancer Res. *68*, 889–892.

Selby, M.J., Engelhardt, J.J., Quigley, M., Henning, K.A., Chen, T., Srinivasan, M., and Korman, A.J. (2013). Anti-CTLA-4 Antibodies of IgG2a Isotype Enhance Antitumor Activity through Reduction of Intratumoral Regulatory T Cells. Cancer Immunol. Res. *1*, 32–42.

Setiady, Y.Y., Coccia, J.A., and Park, P.U. (2010). *In vivo* depletion of $CD4^+$ $FOXP3^+$ Treg cells by the PC61 anti-CD25 monoclonal antibody is mediated by $Fc\gamma RIII^+$ phagocytes. Eur. J. Immunol. *40*, 780–786.

Sharma, P., and Allison, J.P. (2015). Immune Checkpoint Targeting in Cancer Therapy: Toward Combination Strategies with Curative Potential. Cell *161*, 205–214.

Shields, R.L., Namenuk, A.K., Hong, K., Meng, Y.G., Rae, J., Briggs, J., Xie, D., Lai, J., Stadlen, A., Li, B., et al. (2001). High resolution mapping of the binding site on human IgG1 for Fc gamma RI, Fc gamma RII, Fc gamma RIII, and FcRn and design of IgG1 variants with improved binding to the Fc gamma R. J. Biol. Chem. *276*, 6591–6604.

Shields, R.L., Lai, J., Keck, R., O'Connell, L.Y., Hong, K., Meng, Y.G., Weikert, S.H.A., and Presta, L.G. (2002). Lack of fucose on human IgG1 N-linked oligosaccharide improves binding to human Fcgamma RIII and antibody-dependent cellular toxicity. J. Biol. Chem. *277*, 26733–26740.

Shimizu, J., Yamazaki, S., and Sakaguchi, S. (1999). Induction of tumor immunity by removing CD25+CD4+ T cells: a common basis between tumor immunity and autoimmunity. J. Immunol. Baltim. Md 1950 *163*, 5211–5218.

Shrikant, P., Khoruts, A., and Mescher, M.F. (1999). CTLA-4 blockade reverses CD8+ T cell tolerance to tumor by a CD4+ T cell- and IL-2-dependent mechanism. Immunity *11*, 483–493.

Shukla, S.A., Rooney, M.S., Rajasagi, M., Tiao, G., Dixon, P.M., Lawrence, M.S., Stevens, J., Lane, W.J., Dellagatta, J.L., Steelman, S., et al. (2015). Comprehensive analysis of cancer-associated somatic mutations in class I HLA genes. Nat. Biotechnol. *33*, 1152–1158.

Simpson, T.R., Li, F., Montalvo-Ortiz, W., Sepulveda, M.A., Bergerhoff, K., Arce, F., Roddie, C., Henry, J.Y., Yagita, H., Wolchok, J.D., et al. (2013). Fc-dependent depletion of tumor-infiltrating regulatory T cells co-defines the efficacy of anti-CTLA-4 therapy against melanoma. J. Exp. Med. *210*, 1695–1710.

Smith, P., DiLillo, D.J., Bournazos, S., Li, F., and Ravetch, J.V. (2012). Mouse model recapitulating human Fcγ receptor structural and functional diversity. Proc. Natl. Acad. Sci. U. S. A. *109*, 6181–6186.

Snyder, A., Makarov, V., Merghoub, T., Yuan, J., Zaretsky, J.M., Desrichard, A., Walsh, L.A., Postow, M.A., Wong, P., Ho, T.S., et al. (2014). Genetic basis for clinical response to CTLA-4 blockade in melanoma. N. Engl. J. Med. *371*, 2189–2199.

Stamper, C.C., Zhang, Y., Tobin, J.F., Erbe, D.V., Ikemizu, S., Davis, S.J., Stahl, M.L., Seehra, J., Somers, W.S., and Mosyak, L. (2001). Crystal structure of the B7-1/CTLA-4 complex that inhibits human immune responses. Nature *410*, 608–611.

Stephens, L.A., and Mason, D. (2000). CD25 is a marker for CD4+ thymocytes that prevent autoimmune diabetes in rats, but peripheral T cells

with this function are found in both CD25+ and CD25- subpopulations. J. Immunol. Baltim. Md 1950 *165*, 3105–3110.

Suri-Payer, E., Amar, A.Z., Thornton, A.M., and Shevach, E.M. (1998). CD4+CD25+ T cells inhibit both the induction and effector function of autoreactive T cells and represent a unique lineage of immunoregulatory cells. J. Immunol. Baltim. Md 1950 *160*, 1212–1218.

Szolek, A., Schubert, B., Mohr, C., Sturm, M., Feldhahn, M., and Kohlbacher, O. (2014). OptiType: precision HLA typing from next-generation sequencing data. Bioinformatics *30*, 3310–3316.

Takai, T. (2002). Roles of Fc receptors in autoimmunity. Nat. Rev. Immunol. *2*, 580–592.

Tamir, I., Stolpa, J.C., Helgason, C.D., Nakamura, K., Bruhns, P., Daeron, M., and Cambier, J.C. (2000). The RasGAP-binding protein p62dok is a mediator of inhibitory FcgammaRIIB signals in B cells. Immunity *12*, 347–358.

Tarhini, A.A., Edington, H., Butterfield, L.H., Lin, Y., Shuai, Y., Tawbi, H., Sander, C., Yin, Y., Holtzman, M., Johnson, J., et al. (2014). Immune monitoring of the circulation and the tumor microenvironment in patients with regionally advanced melanoma receiving neoadjuvant ipilimumab. PloS One *9*, e87705.

Telang, S., Rasku, M.A., Clem, A.L., Carter, K., Klarer, A.C., Badger, W.R., Milam, R.A., Rai, S.N., Pan, J., Gragg, H., et al. (2011). Phase II trial of the regulatory T cell-depleting agent, denileukin diftitox, in patients with unresectable stage IV melanoma. BMC Cancer *11*.

Thompson, C.B., and Allison, J.P. (1997). The emerging role of CTLA-4 as an immune attenuator. Immunity *7*, 445–450.

Toebes, M., Coccoris, M., Bins, A., Rodenko, B., Gomez, R., Nieuwkoop, N.J., van de Kasteele, W., Rimmelzwaan, G.F., Haanen, J.B.A.G., Ovaa, H., et al. (2006). Design and use of conditional MHC class I ligands. Nat. Med. *12*, 246–251.

Tran, E., Robbins, P.F., Lu, Y.-C., Prickett, T.D., Gartner, J.J., Jia, L., Pasetto, A., Zheng, Z., Ray, S., Groh, E.M., et al. (2016). T-Cell Transfer Therapy Targeting Mutant KRAS in Cancer. N. Engl. J. Med. *375*, 2255–2262.

Tridandapani, S., Chacko, G.W., Van Brocklyn, J.R., and Coggeshall, K.M. (1997a). Negative signaling in B cells causes reduced Ras activity by reducing Shc-Grb2 interactions. J. Immunol. Baltim. Md 1950 *158*, 1125–1132.

Tridandapani, S., Kelley, T., Pradhan, M., Cooney, D., Justement, L.B., and Coggeshall, K.M. (1997b). Recruitment and phosphorylation of SH2-containing inositol phosphatase and Shc to the B-cell Fc gamma immunoreceptor tyrosine-based inhibition motif peptide motif. Mol. Cell. Biol. *17*, 4305–4311.

Tumeh, P.C., Harview, C.L., Yearley, J.H., Shintaku, I.P., Taylor, E.J.M., Robert, L., Chmielowski, B., Spasic, M., Henry, G., Ciobanu, V., et al. (2014). PD-1 blockade induces responses by inhibiting adaptive immune resistance. Nature *515*, 568–571.

Turk, M.J., Guevara-Patiño, J.A., Rizzuto, G.A., Engelhorn, M.E., and Houghton, A.N. (2004). Concomitant Tumor Immunity to a Poorly Immunogenic Melanoma Is Prevented by Regulatory T Cells. J. Exp. Med. *200*, 771–782.

Twyman-Saint Victor, C., Rech, A.J., Maity, A., Rengan, R., Pauken, K.E., Stelekati, E., Benci, J.L., Xu, B., Dada, H., Odorizzi, P.M., et al. (2015). Radiation and dual checkpoint blockade activate non-redundant immune mechanisms in cancer. Nature *520*, 373–377.

Van Allen, E.M., Miao, D., Schilling, B., Shukla, S.A., Blank, C., Zimmer, L., Sucker, A., Hillen, U., Foppen, M.H.G., Goldinger, S.M., et al. (2015). Genomic correlates of response to CTLA-4 blockade in metastatic melanoma. Science *350*, 207–211.

Waitz, R., Solomon, S.B., Petre, E.N., Trumble, A.E., Fassò, M., Norton, L., and Allison, J.P. (2012). Potent induction of tumor immunity by combining tumor cryoablation with anti-CTLA-4 therapy. Cancer Res. *72*, 430–439.

Walker, L.S.K., and Sansom, D.M. (2011). The emerging role of CTLA4 as a cell-extrinsic regulator of T cell responses. Nat. Rev. Immunol. *11*, 852–863.

Wang, A.V., Scholl, P.R., and Geha, R.S. (1994). Physical and functional association of the high affinity immunoglobulin G receptor (Fc gamma RI) with the kinases Hck and Lyn. J. Exp. Med. *180*, 1165–1170.

Warmerdam, P.A., van de Winkel, J.G., Vlug, A., Westerdaal, N.A., and Capel, P.J. (1991). A single amino acid in the second Ig-like domain of the human Fc gamma receptor II is critical for human IgG2 binding. J. Immunol. Baltim. Md 1950 *147*, 1338–1343.

Weng, W.-K., and Levy, R. (2003). Two immunoglobulin G fragment C receptor polymorphisms independently predict response to rituximab in patients with follicular lymphoma. J. Clin. Oncol. Off. J. Am. Soc. Clin. Oncol. *21*, 3940–3947.

Wing, K., Onishi, Y., Prieto-Martin, P., Yamaguchi, T., Miyara, M., Fehervari, Z., Nomura, T., and Sakaguchi, S. (2008). CTLA-4 control over Foxp3+ regulatory T cell function. Science *322*, 271–275.

Wu, J., Edberg, J.C., Redecha, P.B., Bansal, V., Guyre, P.M., Coleman, K., Salmon, J.E., and Kimberly, R.P. (1997). A novel polymorphism of FcgammaRIIIa (CD16) alters receptor function and predisposes to autoimmune disease. J. Clin. Invest. *100*, 1059–1070.

Yao, S., Zhu, Y., and Chen, L. (2013). Advances in targeting cell surface signalling molecules for immune modulation. Nat. Rev. Drug Discov. *12*, 130–146.

Ye, Q., Song, D.-G., Poussin, M., Yamamoto, T., Best, A., Li, C., Coukos, G., and Powell, D.J. (2014). CD137 Accurately Identifies and Enriches for Naturally Occurring Tumor-Reactive T Cells in Tumor. Clin. Cancer Res. *20*, 44–55.

Yokosuka, T., Kobayashi, W., Takamatsu, M., Sakata-Sogawa, K., Zeng, H., Hashimoto-Tane, A., Yagita, H., Tokunaga, M., and Saito, T. (2010). Spatiotemporal basis of CTLA-4 costimulatory molecule-mediated negative regulation of T cell activation. Immunity *33*, 326–339.

Zhang, W., Gordon, M., Schultheis, A.M., Yang, D.Y., Nagashima, F., Azuma, M., Chang, H.-M., Borucka, E., Lurje, G., Sherrod, A.E., et al. (2007). FCGR2A and FCGR3A polymorphisms associated with clinical outcome of epidermal growth factor receptor expressing metastatic colorectal cancer patients treated with single-agent cetuximab. J. Clin. Oncol. Off. J. Am. Soc. Clin. Oncol. *25*, 3712–3718.